

UUC FILE COPY

AD A059945

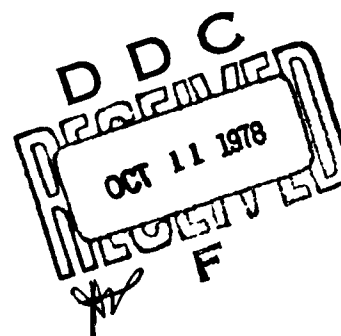
AFFDL-TR-78-79

LEVEL

2

REPAIR OF BONDED PRIMARY STRUCTURE

BOEING COMMERCIAL AIRPLANE COMPANY
P.O. BOX 3707
SEATTLE, WASHINGTON 98124



June 1978

Final Report for Period September 1976 - ~~April~~ 1978

Approved for public release; distribution unlimited

AIR FORCE FLIGHT DYNAMICS
AIR FORCE WRIGHT AERONAUTICAL LABORATORY
AIR FORCE SYSTEMS COMMAND
WRIGHT-PATTERSON AIR FORCE BASE, OHIO 45433

78 10 10 095

NOTICE

When Government drawings, specifications, or other data are used for any purpose other than in connection with a definitely related Government procurement operation, the United States Government thereby incurs no responsibility nor any obligation whatsoever; and the fact that the government may have formulated, furnished, or in any way supplied the said drawings, specifications, or other data, is not to be regarded by implication or otherwise as in any manner licensing the holder or any other person or corporation, or conveying any rights or permission to manufacture, use, or sell any patented invention that may in any way be related thereto.

This report has been reviewed by the Information Office (IO) and is releasable to the National Technical Information Service (NTIS). At NTIS, it will be available to the general public, including foreign nations.

This technical report has been reviewed and is approved for publication.



Harold C. Croop
Project Engineer
AFFDL/FBS



Larry G. Kelly, Acting Chief
Structural Concepts Branch
Structural Mechanics Division

FOR THE COMMANDER



RALPH L. KUSTER, Jr., Colonel, USAF
Chief, Structural Mechanics Division

Copies of this report should not be returned unless return is required by security considerations, contractual obligations, or notice on a specific document.

UNCLASSIFIED

SECURITY CLASSIFICATION OF THIS PAGE (When Data Entered)

19 REPORT DOCUMENTATION PAGE		READ INSTRUCTIONS BEFORE COMPLETING FORM	
1. REPORT NUMBER AFFDLTR-78-79	2. GOVT ACCESSION NO.	3. RECIPIENT'S CATALOG NUMBER	
4. TITLE (and Subtitle) REPAIR OF BONDED PRIMARY STRUCTURE.		5. TYPE OF REPORT & PERIOD COVERED Final Report. Sep 1976 - May 1978	
7. AUTHOR(s) J. E. McCarty, R. E. Horton, M. C. Hooke, R. Z. Mayberry, M. L. Satterthwait		6. PERFORMING ORG. REPORT NUMBER	
8. PERFORMING ORGANIZATION NAME AND ADDRESS Boeing Commercial Airplane Company P.O. Box 3707 Seattle, Washington 98124		9. CONTRACT OR GRANT NUMBER(s) F33615-76-C-3137	
10. PROGRAM ELEMENT, PROJECT, TASK AREA & WORK UNIT NUMBERS 62201F 2401/G3/08		11. REPORT DATE Jun 1978	
12. CONTROLLING OFFICE NAME AND ADDRESS Air Force Flight Dynamics Laboratory Air Force Systems Command Wright-Patterson AFB, Ohio 45433		13. NUMBER OF PAGES 110	
14. MONITORING AGENCY NAME & ADDRESS (if different from Controlling Office) 117p.		15. SECURITY CLASS. (of this report) Unclassified	
15a. DECLASSIFICATION/DOWNGRADING SCHEDULE			
16. DISTRIBUTION STATEMENT (of this Report) Approved for public release; distribution unlimited			
17. DISTRIBUTION STATEMENT (of the abstract entered in Block 20, if different from Report)			
18. SUPPLEMENTARY NOTES			
19. KEY WORDS (Continue on reverse side if necessary and identify by block number) Adhesive Bonding Primary Bonded Structure Metal Bonding Bonded Aerospace Structure Aircraft Repair Repair			
20. ABSTRACT (Continue on reverse side if necessary and identify by block number) This report describes a program to develop durable, cost-effective repair methods for adhesive bonded primary structure. Tasks included the evaluation and selection of adhesive systems, the design, analysis and demonstration of repair methods and the performance of cost and flow time studies. Facilities and equipment required at the repair depots to accomplish these repairs were identified.			

DD FORM 1 JAN 73 1473 EDITION OF NOV 65 IS OBSOLETE

UNCLASSIFIED

SECURITY CLASSIFICATION OF THIS PAGE (When Data Entered)

390 145

LB

PREFACE

This final technical report covers the work accomplished during the five phases of contract F33615-76-C-3137, "Repair of Bonded Primary Structure," by the Boeing Commercial Airplane Company, P.O. Box 3707, Seattle, Washington.

The work was accomplished under the sponsorship of the Air Force Flight Dynamics Laboratory (Project 2401 Task 03). Mr. C. Beck and Mr. H. Croop of the Flight Dynamics Laboratory (AFFDL/FBS) were the Air Force project engineers.

Mr. J. E. McCarty was the Boeing program manager, and Mr. R. E. Horton, the deputy manager. Other Boeing personnel who made technical contributions to the program and their areas of activity are as follows: M. C. Locke and R. Z. Mayberry, Materials; M. L. Satterthwait, Manufacturing; B. Parashar, Quality Control. This work was performed in the period from 1 September 1976 through 31 March 1978.

ACCOMPLISH for	
1.08	Write Section <input checked="" type="checkbox"/>
1.09	Edit Section <input type="checkbox"/>
1.10 <input type="checkbox"/>	
1.11 <input type="checkbox"/>	
1.12 <input type="checkbox"/>	
1.13 <input type="checkbox"/>	
1.14 <input type="checkbox"/>	
1.15 <input type="checkbox"/>	
1.16 <input type="checkbox"/>	
1.17 <input type="checkbox"/>	
1.18 <input type="checkbox"/>	
1.19 <input type="checkbox"/>	
1.20 <input type="checkbox"/>	
1.21 <input type="checkbox"/>	
1.22 <input type="checkbox"/>	
1.23 <input type="checkbox"/>	
1.24 <input type="checkbox"/>	
1.25 <input type="checkbox"/>	
1.26 <input type="checkbox"/>	
1.27 <input type="checkbox"/>	
1.28 <input type="checkbox"/>	
1.29 <input type="checkbox"/>	
1.30 <input type="checkbox"/>	
1.31 <input type="checkbox"/>	
1.32 <input type="checkbox"/>	
1.33 <input type="checkbox"/>	
1.34 <input type="checkbox"/>	
1.35 <input type="checkbox"/>	
1.36 <input type="checkbox"/>	
1.37 <input type="checkbox"/>	
1.38 <input type="checkbox"/>	
1.39 <input type="checkbox"/>	
1.40 <input type="checkbox"/>	
1.41 <input type="checkbox"/>	
1.42 <input type="checkbox"/>	
1.43 <input type="checkbox"/>	
1.44 <input type="checkbox"/>	
1.45 <input type="checkbox"/>	
1.46 <input type="checkbox"/>	
1.47 <input type="checkbox"/>	
1.48 <input type="checkbox"/>	
1.49 <input type="checkbox"/>	
1.50 <input type="checkbox"/>	
1.51 <input type="checkbox"/>	
1.52 <input type="checkbox"/>	
1.53 <input type="checkbox"/>	
1.54 <input type="checkbox"/>	
1.55 <input type="checkbox"/>	
1.56 <input type="checkbox"/>	
1.57 <input type="checkbox"/>	
1.58 <input type="checkbox"/>	
1.59 <input type="checkbox"/>	
1.60 <input type="checkbox"/>	
1.61 <input type="checkbox"/>	
1.62 <input type="checkbox"/>	
1.63 <input type="checkbox"/>	
1.64 <input type="checkbox"/>	
1.65 <input type="checkbox"/>	
1.66 <input type="checkbox"/>	
1.67 <input type="checkbox"/>	
1.68 <input type="checkbox"/>	
1.69 <input type="checkbox"/>	
1.70 <input type="checkbox"/>	
1.71 <input type="checkbox"/>	
1.72 <input type="checkbox"/>	
1.73 <input type="checkbox"/>	
1.74 <input type="checkbox"/>	
1.75 <input type="checkbox"/>	
1.76 <input type="checkbox"/>	
1.77 <input type="checkbox"/>	
1.78 <input type="checkbox"/>	
1.79 <input type="checkbox"/>	
1.80 <input type="checkbox"/>	
1.81 <input type="checkbox"/>	
1.82 <input type="checkbox"/>	
1.83 <input type="checkbox"/>	
1.84 <input type="checkbox"/>	
1.85 <input type="checkbox"/>	
1.86 <input type="checkbox"/>	
1.87 <input type="checkbox"/>	
1.88 <input type="checkbox"/>	
1.89 <input type="checkbox"/>	
1.90 <input type="checkbox"/>	
1.91 <input type="checkbox"/>	
1.92 <input type="checkbox"/>	
1.93 <input type="checkbox"/>	
1.94 <input type="checkbox"/>	
1.95 <input type="checkbox"/>	
1.96 <input type="checkbox"/>	
1.97 <input type="checkbox"/>	
1.98 <input type="checkbox"/>	
1.99 <input type="checkbox"/>	
2.00 <input type="checkbox"/>	
2.01 <input type="checkbox"/>	
2.02 <input type="checkbox"/>	
2.03 <input type="checkbox"/>	
2.04 <input type="checkbox"/>	
2.05 <input type="checkbox"/>	
2.06 <input type="checkbox"/>	
2.07 <input type="checkbox"/>	
2.08 <input type="checkbox"/>	
2.09 <input type="checkbox"/>	
2.10 <input type="checkbox"/>	
2.11 <input type="checkbox"/>	
2.12 <input type="checkbox"/>	
2.13 <input type="checkbox"/>	
2.14 <input type="checkbox"/>	
2.15 <input type="checkbox"/>	
2.16 <input type="checkbox"/>	
2.17 <input type="checkbox"/>	
2.18 <input type="checkbox"/>	
2.19 <input type="checkbox"/>	
2.20 <input type="checkbox"/>	
2.21 <input type="checkbox"/>	
2.22 <input type="checkbox"/>	
2.23 <input type="checkbox"/>	
2.24 <input type="checkbox"/>	
2.25 <input type="checkbox"/>	
2.26 <input type="checkbox"/>	
2.27 <input type="checkbox"/>	
2.28 <input type="checkbox"/>	
2.29 <input type="checkbox"/>	
2.30 <input type="checkbox"/>	
2.31 <input type="checkbox"/>	
2.32 <input type="checkbox"/>	
2.33 <input type="checkbox"/>	
2.34 <input type="checkbox"/>	
2.35 <input type="checkbox"/>	
2.36 <input type="checkbox"/>	
2.37 <input type="checkbox"/>	
2.38 <input type="checkbox"/>	
2.39 <input type="checkbox"/>	
2.40 <input type="checkbox"/>	
2.41 <input type="checkbox"/>	
2.42 <input type="checkbox"/>	
2.43 <input type="checkbox"/>	
2.44 <input type="checkbox"/>	
2.45 <input type="checkbox"/>	
2.46 <input type="checkbox"/>	
2.47 <input type="checkbox"/>	
2.48 <input type="checkbox"/>	
2.49 <input type="checkbox"/>	
2.50 <input type="checkbox"/>	
2.51 <input type="checkbox"/>	
2.52 <input type="checkbox"/>	
2.53 <input type="checkbox"/>	
2.54 <input type="checkbox"/>	
2.55 <input type="checkbox"/>	
2.56 <input type="checkbox"/>	
2.57 <input type="checkbox"/>	
2.58 <input type="checkbox"/>	
2.59 <input type="checkbox"/>	
2.60 <input type="checkbox"/>	
2.61 <input type="checkbox"/>	
2.62 <input type="checkbox"/>	
2.63 <input type="checkbox"/>	
2.64 <input type="checkbox"/>	
2.65 <input type="checkbox"/>	
2.66 <input type="checkbox"/>	
2.67 <input type="checkbox"/>	
2.68 <input type="checkbox"/>	
2.69 <input type="checkbox"/>	
2.70 <input type="checkbox"/>	
2.71 <input type="checkbox"/>	
2.72 <input type="checkbox"/>	
2.73 <input type="checkbox"/>	
2.74 <input type="checkbox"/>	
2.75 <input type="checkbox"/>	
2.76 <input type="checkbox"/>	
2.77 <input type="checkbox"/>	
2.78 <input type="checkbox"/>	
2.79 <input type="checkbox"/>	
2.80 <input type="checkbox"/>	
2.81 <input type="checkbox"/>	
2.82 <input type="checkbox"/>	
2.83 <input type="checkbox"/>	
2.84 <input type="checkbox"/>	
2.85 <input type="checkbox"/>	
2.86 <input type="checkbox"/>	
2.87 <input type="checkbox"/>	
2.88 <input type="checkbox"/>	
2.89 <input type="checkbox"/>	
2.90 <input type="checkbox"/>	
2.91 <input type="checkbox"/>	
2.92 <input type="checkbox"/>	
2.93 <input type="checkbox"/>	
2.94 <input type="checkbox"/>	
2.95 <input type="checkbox"/>	
2.96 <input type="checkbox"/>	
2.97 <input type="checkbox"/>	
2.98 <input type="checkbox"/>	
2.99 <input type="checkbox"/>	
3.00 <input type="checkbox"/>	
3.01 <input type="checkbox"/>	
3.02 <input type="checkbox"/>	
3.03 <input type="checkbox"/>	
3.04 <input type="checkbox"/>	
3.05 <input type="checkbox"/>	
3.06 <input type="checkbox"/>	
3.07 <input type="checkbox"/>	
3.08 <input type="checkbox"/>	
3.09 <input type="checkbox"/>	
3.10 <input type="checkbox"/>	
3.11 <input type="checkbox"/>	
3.12 <input type="checkbox"/>	
3.13 <input type="checkbox"/>	
3.14 <input type="checkbox"/>	
3.15 <input type="checkbox"/>	
3.16 <input type="checkbox"/>	
3.17 <input type="checkbox"/>	
3.18 <input type="checkbox"/>	
3.19 <input type="checkbox"/>	
3.20 <input type="checkbox"/>	
3.21 <input type="checkbox"/>	
3.22 <input type="checkbox"/>	
3.23 <input type="checkbox"/>	
3.24 <input type="checkbox"/>	
3.25 <input type="checkbox"/>	
3.26 <input type="checkbox"/>	
3.27 <input type="checkbox"/>	
3.28 <input type="checkbox"/>	
3.29 <input type="checkbox"/>	
3.30 <input type="checkbox"/>	
3.31 <input type="checkbox"/>	
3.32 <input type="checkbox"/>	
3.33 <input type="checkbox"/>	
3.34 <input type="checkbox"/>	
3.35 <input type="checkbox"/>	
3.36 <input type="checkbox"/>	
3.37 <input type="checkbox"/>	
3.38 <input type="checkbox"/>	
3.39 <input type="checkbox"/>	
3.40 <input type="checkbox"/>	
3.41 <input type="checkbox"/>	
3.42 <input type="checkbox"/>	
3.43 <input type="checkbox"/>	
3.44 <input type="checkbox"/>	
3.45 <input type="checkbox"/>	
3.46 <input type="checkbox"/>	
3.47 <input type="checkbox"/>	
3.48 <input type="checkbox"/>	
3.49 <input type="checkbox"/>	
3.50 <input type="checkbox"/>	
3.51 <input type="checkbox"/>	
3.52 <input type="checkbox"/>	
3.53 <input type="checkbox"/>	
3.54 <input type="checkbox"/>	
3.55 <input type="checkbox"/>	
3.56 <input type="checkbox"/>	
3.57 <input type="checkbox"/>	
3.58 <input type="checkbox"/>	
3.59 <input type="checkbox"/>	
3.60 <input type="checkbox"/>	
3.61 <input type="checkbox"/>	
3.62 <input type="checkbox"/>	
3.63 <input type="checkbox"/>	
3.64 <input type="checkbox"/>	
3.65 <input type="checkbox"/>	
3.66 <input type="checkbox"/>	
3.67 <input type="checkbox"/>	
3.68 <input type="checkbox"/>	
3.69 <input type="checkbox"/>	
3.70 <input type="checkbox"/>	
3.71 <input type="checkbox"/>	
3.72 <input type="checkbox"/>	
3.73 <input type="checkbox"/>	
3.74 <input type="checkbox"/>	
3.75 <input type="checkbox"/>	
3.76 <input type="checkbox"/>	
3.77 <input type="checkbox"/>	
3.78 <input type="checkbox"/>	
3.79 <input type="checkbox"/>	
3.80 <input type="checkbox"/>	
3.81 <input type="checkbox"/>	
3.82 <input type="checkbox"/>	
3.83 <input type="checkbox"/>	
3.84 <input type="checkbox"/>	
3.85 <input type="checkbox"/>	
3.86 <input type="checkbox"/>	
3.87 <input type="checkbox"/>	
3.88 <input type="checkbox"/>	
3.89 <input type="checkbox"/>	
3.90 <input type="checkbox"/>	
3.91 <input type="checkbox"/>	
3.92 <input type="checkbox"/>	
3.93 <input type="checkbox"/>	
3.94 <input type="checkbox"/>	
3.95 <input type="checkbox"/>	
3.96 <input type="checkbox"/>	
3.97 <input type="checkbox"/>	
3.98 <input type="checkbox"/>	
3.99 <input type="checkbox"/>	
4.00 <input type="checkbox"/>	
4.01 <input type="checkbox"/>	
4.02 <input type="checkbox"/>	
4.03 <input type="checkbox"/>	
4.04 <input type="checkbox"/>	
4.05 <input type="checkbox"/>	
4.06 <input type="checkbox"/>	
4.07 <input type="checkbox"/>	
4.08 <input type="checkbox"/>	
4.09 <input type="checkbox"/>	
4.10 <input type="checkbox"/>	
4.11 <input type="checkbox"/>	
4.12 <input type="checkbox"/>	
4.13 <input type="checkbox"/>	
4.14 <input type="checkbox"/>	
4.15 <input type="checkbox"/>	
4.16 <input type="checkbox"/>	
4.17 <input type="checkbox"/>	
4.18 <input type="checkbox"/>	
4.19 <input type="checkbox"/>	
4.20 <input type="checkbox"/>	
4.21 <input type="checkbox"/>	
4.22 <input type="checkbox"/>	
4.23 <input type="checkbox"/>	
4.24 <input type="checkbox"/>	
4.25 <input type="checkbox"/>	
4.26 <input type="checkbox"/>	
4.27 <input type="checkbox"/>	
4.28 <input type="checkbox"/>	
4.29 <input type="checkbox"/>	
4.30 <input type="checkbox"/>	
4.31 <input type="checkbox"/>	
4.32 <input type="checkbox"/>	
4.33 <input type="checkbox"/>	
4.34 <input type="checkbox"/>	
4.35 <input type="checkbox"/>	
4.36 <input type="checkbox"/>	
4.37 <input type="checkbox"/>	
4.38 <input type="checkbox"/>	
4.39 <input type="checkbox"/>	
4.40 <input type="checkbox"/>	
4.41 <input type="checkbox"/>	
4.42 <input type="checkbox"/>	
4.43 <input type="checkbox"/>	
4.44 <input type="checkbox"/>	
4.45 <input type="checkbox"/>	
4.46 <input type="checkbox"/>	
4.47 <input type="checkbox"/>	
4.48 <input type="checkbox"/>	
4.49 <input type="checkbox"/>	
4.50 <input type="checkbox"/>	
4.51 <input type="checkbox"/>	
4.52 <input type="checkbox"/>	
4.53 <input type="checkbox"/>	
4.54 <input type="checkbox"/>	
4.55 <input type="checkbox"/>	
4.56 <input type="checkbox"/>	
4.57 <input type="checkbox"/>	
4.58 <input type="checkbox"/>	
4.59 <input type="checkbox"/>	
4.60 <input type="checkbox"/>	
4.61 <input type="checkbox"/>	
4.62 <input type="checkbox"/>	
4.63 <input type="checkbox"/>	
4.64 <input type="checkbox"/>	
4.65 <input type="checkbox"/>	
4.66 <input type="checkbox"/>	
4.67 <input type="checkbox"/>	
4.68 <input type="checkbox"/>	
4.69 <input type="checkbox"/>	
4.70 <input type="checkbox"/>	
4.71 <input type="checkbox"/>	
4.72 <input type="checkbox"/>	
4.73 <input type="checkbox"/>	
4.74 <input type="checkbox"/>	
4.75 <input type="checkbox"/>	
4.76 <input type="checkbox"/>	
4.77 <input type="checkbox"/>	
4.78 <input type="checkbox"/>	
4.79 <input type="checkbox"/>	
4.80 <input type="checkbox"/>	
4.81 <input type="checkbox"/>	
4.82 <input type="checkbox"/>	
4.83 <input type="checkbox"/>	
4.84 <input type="checkbox"/>	
4.85 <input type="checkbox"/>	
4.86 <input type="checkbox"/>	
4.87 <input type="checkbox"/>	
4.88 <input type="checkbox"/>	
4.89 <input type="checkbox"/>	
4.90 <input type="checkbox"/>	
4.91 <input type="checkbox"/>	
4.92 <input type="checkbox"/>	
4.93 <input type="checkbox"/>	
4.94 <input type="checkbox"/>	
4.95 <input type="checkbox"/>	
4.96 <input type="checkbox"/>	
4.97 <input type="checkbox"/>	
4.98 <input type="checkbox"/>	
4.99 <input type="checkbox"/>	
5.00 <input type="checkbox"/>	
5.01 <input type="checkbox"/>	
5.02 <input type="checkbox"/>	
5.03 <input type="checkbox"/>	
5.04 <input type="checkbox"/>	
5.05 <input type="checkbox"/>	
5.06 <input type="checkbox"/>	
5.07 <input type="checkbox"/>	
5.08 <input type="checkbox"/>	
5.09 <input type="checkbox"/>	
5.10 <input type="checkbox"/>	
5.11 <input type="checkbox"/>	
5.12 <input type="checkbox"/>	
5.13 <input type="checkbox"/>	
5.14 <input type="checkbox"/>	
5.15 <input type="checkbox"/>	
5.16 <input type="checkbox"/>	
5.17 <input type="checkbox"/>	
5.18 <input type="checkbox"/>	
5.19 <input type="checkbox"/>	
5.20 <input type="checkbox"/>	
5.21 <input type="checkbox"/>	
5.22 <input type="checkbox"/>	
5.23 <input type="checkbox"/>	
5.24 <input type="checkbox"/>	
5.25 <input type="checkbox"/>	
5.26 <input type="checkbox"/>	
5.27 <input type="checkbox"/>	
5.28 <input type="checkbox"/>	
5.29 <input type="checkbox"/>	
5.30 <input type="checkbox"/>	
5.31 <input type="checkbox"/>	
5.32 <input type="checkbox"/>	
5.33 <input type="checkbox"/>	
5.34 <input type="checkbox"/>	
5.35 <input type="checkbox"/>	
5.36 <input type="checkbox"/>	
5.37 <input type="checkbox"/>	
5.38 <input type="checkbox"/>	
5.39 <input type="checkbox"/>	
5.40 <input type="checkbox"/>	
5.41 <input type="checkbox"/>	
5.42 <input type="checkbox"/>	
5.43 <input type="checkbox"/>	
5.44 <input type="checkbox"/>	
5.45 <input type="checkbox"/>	
5.46 <input type="checkbox"/>	
5.47 <input type="checkbox"/>	
5.48 <input type="checkbox"/>	
5.49 <input type="checkbox"/>	
5.50 <input type="checkbox"/>	
5.51 <input type="checkbox"/>	
5.52 <input type="checkbox"/>	
5.53 <input type="checkbox"/>	
5.54 <input type="checkbox"/>	
5.55 <input type="checkbox"/>	
5.56 <input type="checkbox"/>	
5.57 <input type="checkbox"/>	
5.58 <input type="checkbox"/>	
5.59 <input type="checkbox"/>	
5.60 <input type="checkbox"/>	
5.61 <input type="checkbox"/>	
5.62 <input type="checkbox"/>	
5.63 <input type="checkbox"/>	
5.64 <input type="checkbox"/>	
5.65 <input type="checkbox"/>	
5.66 <input type="checkbox"/>	
5.67 <input type="checkbox"/>	
5.68 <input type="checkbox"/>	
5.69 <input type="checkbox"/>	
5.70 <input type="checkbox"/>	
5.71 <input type="checkbox"/>	
5.72 <input type="checkbox"/>	
5.73 <input type="checkbox"/>	
5.74 <input type="checkbox"/>	
5.75 <input type="checkbox"/>	
5.76 <input type="checkbox"/>	
5.77 <input type="checkbox"/>	
5.78 <input type="checkbox"/>	
5.79 <input type="checkbox"/>	
5.80 <input type="checkbox"/>	
5.81 <input type="checkbox"/>	
5.82 <input type="checkbox"/>	
5.83 <input type="checkbox"/>	
5.84 <input type="checkbox"/>	
5.85 <input type="checkbox"/>	
5.86 <input type="checkbox"/>	
5.87 <input type="checkbox"/>	
5.88 <input type="checkbox"/>	
5.89 <input type="checkbox"/>	
5.90 <input type="checkbox"/>	
5.91 <input type="checkbox"/>	
5.92 <input type="checkbox"/>	
5.93 <input type="checkbox"/>	
5.94 <input type="checkbox"/>	
5.95 <input type="checkbox"/>	
5.96 <input type="checkbox"/>	
5.97 <input type="checkbox"/>	
5.98 <input type="checkbox"/>	
5.99 <input type="checkbox"/>	
6.00 <input type="checkbox"/>	
6.01 <input type="checkbox"/>	
6.02 <input type="checkbox"/>	
6.03 <input type="checkbox"/>	
6.04 <input type="checkbox"/>	
6.05 <input type="checkbox"/>	
6.06 <input type="checkbox"/>	
6.07 <input type="checkbox"/>	
6.08 <input type="checkbox"/>	
6.09 <input type="checkbox"/>	
6.10 <input type="checkbox"/>	
6.11 <input type="checkbox"/>	
6.12 <input type="checkbox"/>	
6.13 <input type="checkbox"/>	
6.14 <input type="checkbox"/>	
6.15 <input type="checkbox"/>	
6.16 <input type="checkbox"/>	
6.17 <input type="checkbox"/>	
6.18 <input type="checkbox"/>	
6.19 <input type="checkbox"/>	
6.20 <input type="checkbox"/>	
6.21 <input type="checkbox"/>	
6.22 <input type="checkbox"/>	
6.23 <input type="checkbox"/>	
6.24 <input type="checkbox"/>	
6.25 <input type="checkbox"/>	
6.26 <input type="checkbox"/>	
6.27 <input type="checkbox"/>	
6.28 <input type="checkbox"/>	
6.29 <input type="checkbox"/>	
6.30 <input type="checkbox"/>	
6.31 <input type="checkbox"/>	
6.32 <input type="checkbox"/>	
6.33 <input type="checkbox"/>	
6.34 <input type="checkbox"/>	
6.35 <input type="checkbox"/>	
6.36 <input type="checkbox"/>	
6.37 <input type="checkbox"/>	
6.38 <input type="checkbox"/>	
6.39 <input type="checkbox"/>	
6.40 <input type="checkbox"/>	
6.41 <input type="checkbox"/>	
6.42 <input type="checkbox"/>	
6.43 <input type="checkbox"/>	
6.44 <input type="checkbox"/>	
6.45 <input type="checkbox"/>	
6.46 <input type="checkbox"/>	
6.47 <input type="checkbox"/>	
6.48 <input type="checkbox"/>	
6.49 <input type="checkbox"/>	
6.50 <input type="checkbox"/>	
6.51 <input type="checkbox"/>	
6.52 <input type="checkbox"/>	
6.53 <input type="checkbox"/>	
6.54 <input type="checkbox"/>	
6.55 <input type="checkbox"/>	
6.56 <input type="checkbox"/>	
6.57 <input type="checkbox"/>	
6.58 <input type="checkbox"/>	
6.59 <input type="checkbox"/>	
6.60 <input type="checkbox"/>	
6.61 <input type="checkbox"/>	
6.62 <input type="checkbox"/>	
6.63 <input type="checkbox"/>	
6.64 <input type="checkbox"/>	
6.65 <input type="checkbox"/>	
6.66 <input type="checkbox"/>	
6.67 <input type="checkbox"/>	
6.68 <input type="checkbox"/>	
6.69 <input type="checkbox"/>	
6.70 <input type="checkbox"/>	
6.71 <input type="checkbox"/>	
6.72 <input type="checkbox"/>	
6.73 <input type="checkbox"/>	
6.74 <input type="checkbox"/>	
6.75 <input type="checkbox"/>	
6.76 <input type="checkbox"/>	
6.77 <input type="checkbox"/>	

TABLE OF CONTENTS

	Page
1.0 INTRODUCTION AND SUMMARY	1
2.0 DAMAGE CAUSES AND SEVERITY	5
3.0 MATERIAL EVALUATION	8
3.1 Selection of Candidate Adhesive Systems	8
3.2 Test Plans	8
3.3 Types of Specimens	12
3.4 Specimen Processing	14
3.5 Test Results	15
3.6 Test Conclusions	19
4.0 EVALUATION OF REPAIRED PANELS	24
4.1 Panel Design	24
4.2 Panel Fabrication	29
4.3 Panel Test and Results	36
4.4 Panel Test Conclusions	41
5.0 DEMONSTRATION OF LARGE REPAIRS	42
5.1 Description of the Baseline Structure	42
5.2 Selection of Repair Demonstration Areas	43
5.3 Repair Requirements and Criteria	47
5.4 Design	47
5.5 Analysis	48
5.6 Fabrication of the Repairs	63
5.6.1 Mechanical Fastened/Bonded Repair	67
5.6.2 Vacuum Bonded Repair - External Longeron	74
5.6.3 Vacuum Bonded Repair - Overhead	81
5.6.4 Post-Repair Evaluation	86
5.7 Cost and Flow Time Studies	99
6.0 DEFINITION OF FACILITY AND EQUIPMENT REQUIREMENTS	104
7.0 CONCLUSIONS	109

MISSING PAGE NOT FILLED
 BLANK

78 10 10 095

LIST OF ILLUSTRATIONS

No.		Page
1	Program Schedule	2
2	Typical Entry Damage for 20-mm HE, Normal Impact	7
3	Slow Rate Environmental Fatigue Cycle	10
4	Slow Cycle Environmental Fatigue Testing Facility	12
5	Standard Adhesive Lap Shear Specimen	12
6	Wedge Test Specimen Configuration	13
7	Shear Load Versus Lap Length EA9628 Adhesive	17
8	Shear Load Versus Lap Length FM73 Adhesive	17
9	Comparison of Cyclic Load/Environmental Exposure Data	23
10	Repair Test Panel Configurations and Loading Modes	25
11	Detail of Skin Splice Repair	26
12	Detail of Frame Tee/Skin Repair	27
13	Detail of Frame Tee	28
14	Design Curve Derivation FM73 Adhesive	29
15	Build-up Provided at End of Shear Panel Frame Tee for Test Loading	30
16	Removal of the "Damaged Area" with a High Speed Router	31
17	Panel with "Damaged Material" and Organic Coating Removed from Surfaces to be Bonded	31
18	Fatigue Control and Repair Test Panel with Details Prior to Bonding	32
19	Applying Phosphoric Acid to Bond Surfaces Prior to Anodizing	33
20	Anodizing Repair Test Panel Prior to Bonding	33
21	Rinsing Panel after Anodizing	34
22	Inspection of Anodized Surface with a Polarized Filter	34
23	Priming Surface with BR127 Primer	35
24	Control and Repaired Shear Panel Prior to Test	35
25	Test Panels and Environmental Load Cycling Fixtures	36
26	Frame Tee Tension Pull-off Test in Progress	37
27	Typical Failure of a Repaired Skin Splice Panel	38
28	Typical Failure of the Frame/Skin Shear Test Panels	39
29	Typical Failure of Frame Tee Tension Pull-off Panels	40
30	Extension of Splice Strap Width to Reduce Peel Stresses at Edge of Frame Tee	40
31	Details of Upper Quadrant Frame/Longeron Intersection- PABST Baseline	44
32	Typical Intermediate Frame Detail- PABST Baseline	45
33	Lower Body Frame/Longeron Detail- PABST Baseline	45
34	Bonded Longitudinal Splice Detail- PABST Baseline	46
35	Areas on PABST Structure for Repair Study	46
36	Checkpoint "B" Repair Internal Longeron	49
37	Checkpoint "D" Repair External Longeron	51
38	Comparison Between Fatigue Quality of Repair and Baseline	54
39	Comparison of Douglas and Boeing Crack Growth Analysis Results	55
40	Geometry Magnification Factor for Flaw/Crack at Edge of Fastener Hole ($t = 0.040$)	57
41	Geometry Magnification Factor for Flaw/Crack at Edge of Fastener Hole ($t = 0.050$)	58

LIST OF ILLUSTRATIONS (CONTINUED)

No.		Page
42	Geometry Magnification Factor for Flaw/Crack at Edge of Fastener Hole ($t = 0.060$)	59
43	Geometry Magnification Factor for Flaw/Crack at Edge of Fastener Hole ($t = 0.071$)	60
44	Comparison of Crack Growth Behavior of Surface Flaw and Flaw at a Hole	61
45	Corner Hole Flaws Comparison	62
46	Skin Crack Growth Behavior Adjacent to and Under Bonded Repair Doubler	64
47	Skin Crack Growth Behavior in Basic Structure and Under Bonded Frame Repair	65
48	Location of Repair Demonstration Areas Pabst Panel	66
49	Laminated Panels to Evaluate Rivets Versus Bolt/Springs for Cure Pressure	67
50	Edge View Showing Porous Edge of Panel Pressurized with Rivets (Top) as Compared with More Dense Bolt/Spring Bonded Panel (Bottom)	68
51	Start of Damage Removal	68
52	Attaching Bar Templates to Guide High-speed Router	69
53	All "Damaged" Material Removed from Panel	69
54	Metal Detail Pieces Used for Repair	70
55	Detail Parts Prefit Prior to Surface Preparation and Bonding	70
56	Organic Removed from Bond Area and Masking Applied Around Periphery	71
57	Anodizing the Surfaces to be Bonded	71
58	Curing BR127 Adhesive Primer with a Portable Compressed Air Heater	72
59	Overall View Showing Compressed Air Heater and Heating Set-up	73
60	Holes Drilled in Repair Details Prior to Installing Pressurizing Bolts and Springs	73
61	Pressurizing Bolts and Springs Installed for Cure of the Bond	74
62	Repair Complete Rivets Installed after Removal of Bolts	75
63	Bonding an External Longeron on Repair Demonstration Panel	75
64	Lay-up of Fiberglass Tool to be Used to Maintain Surface Contour During Subsequent Repair Bonding	76
65	Curing Fiberglass Bond Tool	76
66	Fiberglass Bonding Tool Fabrication Complete	77
67	Removal of Material for Bonded Repair	77
68	Bond Area Ready for Surface Preparation	78
69	Phosphoric Acid Anodizing Aluminum Surface to be Bonded	78
70	Spray Application of BR127 Adhesive Primer	79
71	Curing Adhesive Primer	79
72	First Stage Bond of Skin Patch and Plug	80
73	Inspection of Skin Patch for Bonded Repair with a Fokker Bond Tester	80
74	Completed Repair External Longeron	81
75	Panel Mounted for Making Overhead Repair	82
76	Material Removed for Overhead Repair	82
77	Applying Phosphoric Acid to Gauze on Plate to be Used to Press Against Lower Surface	83
78	Plate Clamped Against Lower Surface and Anodizing Clips Attached	84
79	Curing Adhesive Primer with Portable Compressed Air Heater	84

LIST OF ILLUSTRATIONS (CONCLUDED)

No.		Page
80	Interior View of Completed Repairs	85
81	Exterior View of Completed Repairs	85
82	Inspection of Repairs with Ultrasonic Water Coupled Through Transmission Unit	86
83	Location of Specimens Cut from Internal Longeron Repair	87
84	Location of Specimens Cut from External Longeron Repair	88
85	Failure Surfaces of Wedge Specimens from the Overhead Bonded Repair	89
86	Failure Surfaces of Wedge Specimens From the Mechanical Fastener Bonded Repair	90
87	Failure Surfaces of Wedge Specimens From the External Longeron Repair	90
88	SEM Photos Showing Satisfactory Oxide Layer on the EW-2 Specimen Hand Anodized Surface	95
89	SEM Photos Showing Lack of Oxide Build-up On the EW-3 Specimen Hand Anodized Surface	96
90	SEM Photo Showing Satisfactory Oxide Build-up On the EW-3 Specimen Tank Anodized Surface	97
91	SEM Photo Showing Satisfactory Oxide Build-up on the IW-1 Specimen Hand Anodized Surface	98
92	Comparative Man-hours Required for Repairs Using Bolts/Springs for Pressure Application Versus Use of a Vacuum Bag	100
93	Comparative Flow Time of Repair Methods, Internal Longeron	101
94	Comparative Flow Time of Repair Methods, External Longeron	102
95	Comparative Flow Time of Repair Methods, Overhead--No Longeron	103
96	A Buffalo Roll Being Used to Form a Frame Section to Proper Radius	105
97	Use of a Model M-3 Yoder Progressive Multiple Form Roll with a Special Curve-Forming Attachment	106
98	A Sheridan Model A-15 Stretch-Wrap Forming Machine	106
99	A Portable Compressed Hot Air Heater Used for Bond Curing	107

LIST OF TABLES

No.		Page
1	Tests of Candidate Repair Adhesive Systems Using Hand Phosphoric Acid Anodize	9
2	Small Specimen Slow Cycle Environmental Fatigue Tests	10
3	Lap Shear And Peel Test Results	11
4	Ultimate Load Versus Lap Length Data	15
5	Wedge Specimen Test Results	16
6	Retest of Peel Tests Using Both Tank and Nontank Anodize	18
7	Results of Glass Transition Tests on Adhesives and Primer to Determine Cure Effectivity	19
8	Results of Cyclic Load/Environmental Exposure Testing 900 PSI	20
9	Results of Cyclic Load/Environmental Exposure Testing 1200 PSI	21
10	Results of Cyclic Load/Environmental Exposure Testing 1500 PSI	22
11	Results of Control and Repaired Panel Fatigue Tests	38
12	Results of Tests on Specimens Cut From Bolt/Spring Bonded Repair Internal Longerons	91
13	Results of Tests on Specimens Cut From Vacuum Bag Bonded Repair External Longerons	92
14	Results of Tests on Specimens Cut From Overhead Vacuum Bonded Repair	93

1.0 INTRODUCTION AND SUMMARY

The use of adhesive bonding as a joining method in aircraft construction is an accepted means of attaining high structural efficiency and improved fatigue life. Extensive use of this type of construction has been made in aircraft secondary structure. The technology has now matured to the point where adhesive bonding has high potential for providing very attractive cost and weight savings for primary structural applications. The technology advancements that have recently made this possible have occurred in several areas. These include the development of a new generation of 250°F curing adhesive systems with considerably higher strength. More importantly, when combined with the use of recently developed surface preparation methods and corrosion inhibiting primers, they provide vastly improved environmental durability.

The Air Force, in recognition of these advances, is currently supporting an aggressive developmental program to provide the technology and confidence necessary to permit bonding to expand to wide use in primary structure. The most significant of these programs is the Primary Adhesively Bonded Structure Technology (PABST) program, F33615-75-C-3016, being performed by the Douglas Aircraft Company. This program is specifically directed to develop the additional technology necessary to allow commitment to a bonded fuselage in future military aircraft.

One of the critical areas which has been identified for additional development work is that of repair. It is recognized that processing anomalies and fabrication damage will occur when bonding primary structure. Repair methods must be available as an option to costly scrapping of the large components. Likewise, damage will occur in service. Operational requirements for the aircraft will necessitate that high quality repairs be made quickly to restore the damaged area to its pre-damaged level of strength and durability. It has been the purpose of this program to develop these kinds of repair procedures to support the PABST program.

The major goals of this program are defined as follows:

- Develop procedures, based on structural integrity, cost, and repair flow time considerations, that might best be used for the repair of adhesively bonded primary aircraft structures.
- Define facilities, equipment, and personnel skills that must be available at the depots to accomplish these procedures.

This five-phase program was performed over an 18 month period. The tasks and program schedule for each phase are shown in Figure 1.

The initial program tasks consisted of a coordination meeting with the Air Force/Douglas PABST team and subsequent preparation of a Master Program Plan. The information from the PABST review provided the following:

- A description of the overall PABST design configuration.
- Identification of critical structural areas for repair demonstration.

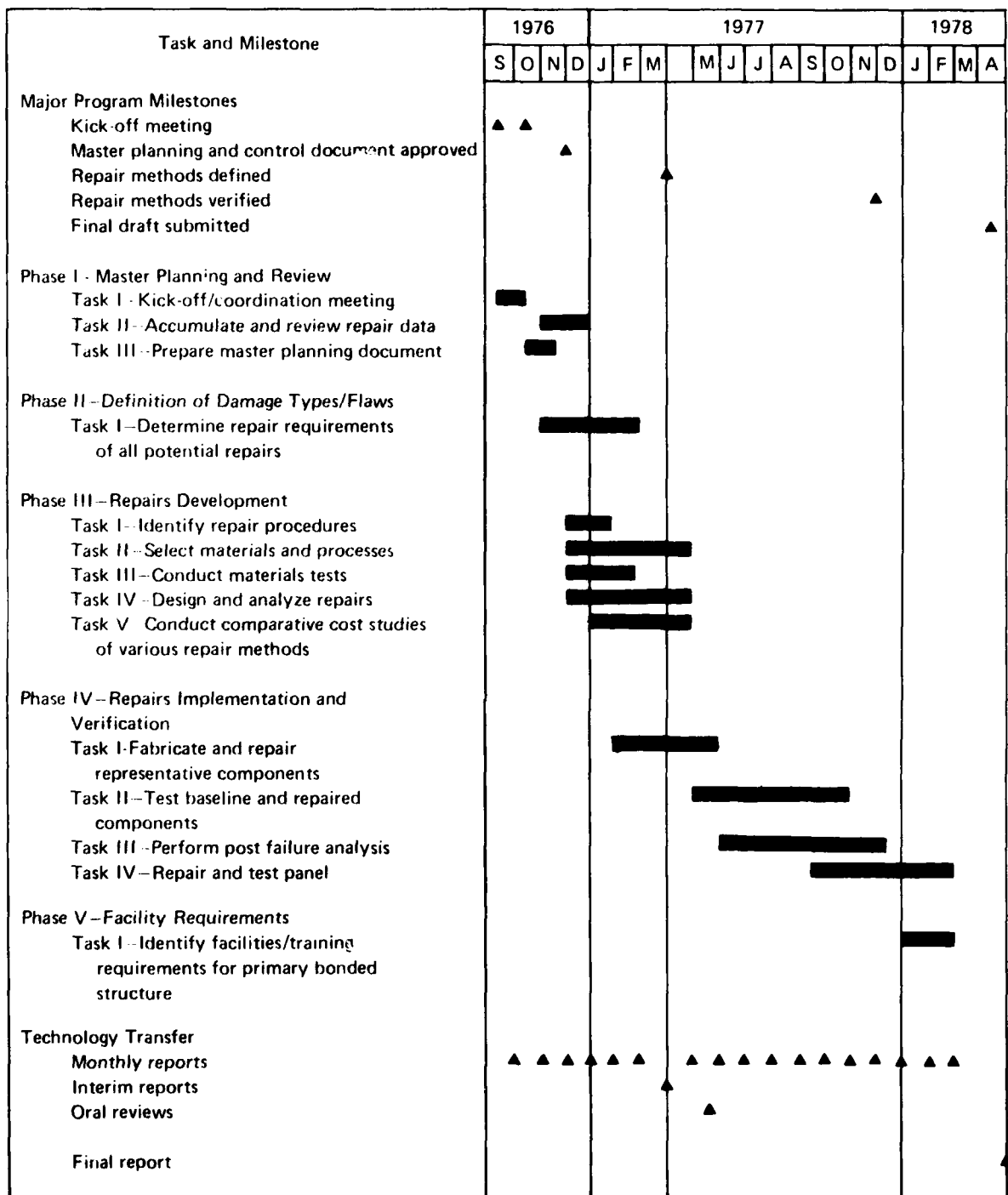


Figure 1.-Program Schedule

- Definition of PABST base structure and repair design criteria.
- Definition of baseline loads distribution and analysis data.

In addition to the information obtained, a large PABST test panel was identified as being available for repair method demonstration.

Since the Douglas YC-15 was selected as a baseline aircraft for PABST, a survey was conducted early in the program to determine types of fuselage damage that might be incurred by a typical medium STOL aircraft. Although the missions are not identical, past service experience with the C-130 aircraft was taken as indicative. Damage was principally divided into three categories. These were damage caused by ground handling equipment, operational incidents such as impact with runway debris or ground fire, and that caused by structural deterioration such as fatigue cracks and corrosion. In the final analysis, the most obvious repair solution was essentially independent of the cause of damage. Typically the damaged area would be removed and the material replaced.

Tests were conducted to select the adhesive system that would be used in subsequent repair demonstrations. Two 250°F curing epoxy adhesives, FM73 and EA9628, and a room temperature curing adhesive, EA9309, were evaluated. The phosphoric acid hand anodize method, previously developed during Air Force contract F33615-73-C-5171, was used for metal surface preparation. BR127 was selected for use as the corrosion inhibiting adhesive primer.

Tests on the adhesives were conducted using lap shear, peel and wedge specimens. Evaluation temperatures ranged from -67°F to 180°F. The tests included those conducted in critical environments with both steady state and cyclic loads. As a result of the tests, FM73 was selected for the follow-on repair work. This was primarily because of its superior durability as evidenced in the slow cycle fatigue testing.

Following selection of the adhesive system, test panels were fabricated. These represented areas of the bonded frame-to-skin attachment and the bonded longitudinal skin splice. Simulated repairs were incorporated. The repaired panels were tested both statically and with slow cyclic loading in an environment of 100% relative humidity and 140°F. The test results for the repaired panels compared favorably with those for unrepaired controls.

Two areas on the PABST fuselage were selected for repair demonstration. The PABST design utilizes both internal and external longerons. Consequently, the areas selected were at an intersection of a frame and internal longeron in the crown area and at a frame/external longeron intersection in the lower quadrant. Loads and baseline analysis data were furnished by Douglas to support a meaningful design study of repair procedures. The study included static, fatigue, and damage tolerance analyses.

Resulting repair designs were demonstrated on the large fuselage test panel obtained from Douglas. Three repairs were accomplished.

All work utilized procedures and equipment that would be adaptable to an on-the-aircraft repair situation. Phosphoric acid hand anodizing was used as the prebond surface preparation procedure. Mechanical fasteners were used in conjunction with springs to apply pressure for the first repair; vacuum pressure was used for the remaining two. Heating for all repairs was supplied by a Boeing-designed compressed air heater.

The repairs were nondestructively inspected and then cut up for coupon testing. The tests included lap shear and wedge specimens. The latter were exposed to 120°F and 100% relative humidity for 30 days.

Cost and flow time estimates were made to compare the vacuum and mechanical fastener methods of applying bonding pressure. It was concluded that for the repairs demonstrated, the vacuum bonding procedure was less expensive and could be accomplished more rapidly. However, the quality of the repair that was made using the mechanical fastener/bonding combination was quite acceptable and it remains a viable alternate procedure.

The facilities and training requirements that will be required to accomplish these repairs have been identified.

In general, it is concluded that these repairs, having primary structural quality, can be accomplished by repair depot personnel. With proper training, it is anticipated that a considerable amount of this type of repair work can also be accomplished at the base level.

2.0 DAMAGE CAUSES AND SEVERITY

A survey has been made to determine typical types of fuselage structural damage that might be encountered by the C-14/C-15 aircraft in service. This included a review of past C-130 incident damage experience (Ref. 1). In addition, discussions were held with Air Force maintenance personnel (Refs. 2, 3, 4).

Flight and ground handling damage for the C-130 and C-14/C-15 aircraft are, for the most part, expected to be similar. However, operational requirements differ. The C-130 is primarily employed on air drop missions and operates from improved runways. The C-14/C-15, by contrast, is designed for close, behind-the-lines battle support. As such, it will operate from semi-improved landing fields. It will be more susceptible to damage from runway debris. It will also be more exposed to enemy ground fire.

A second difference between the two aircraft lies in the construction methods. The C-130 is a conventional, mechanically fastened skin stringer design. The C-14/C-15 design proposed by PABST substitutes a significant amount of adhesive bonded attachment.

The expected types of damage are divided into three areas. These include ground handling, operational items, and structural deterioration. A further breakdown of these is as follows:

1. Ground Handling

a. Service Equipment

- Surface damage; dents, punctures, etc.

b. Loading Equipment

- Damage to the ramp hinge area
- Damage to the side of the door frame and the interior side of the body

2. Operational Items

a. Hard Landings

- Damage to the wheel well area and in proximity of the landing gear beams

b. Foreign Object Damage

- Bird strikes; primarily in the nose area
- Runway debris; including water
- Tire blowout debris
- Bullet damage; 30 cal to 23 mm high explosive (HE)

3. Structural Deterioration

- a. Fatigue cracks
- b. Corrosion
- c. Bondline delamination

TAC, at the Little Rock AFB, reports that their main problems with the C-130 are to the ramp hinge support bulkhead and landing gear wheel well area. Lockheed has repair kits for each of these. Damage due to service equipment occurs but is not a major consideration. This latter is concurred with by maintenance personnel at the McChord AFB (MAC).

The wheel well area is quite susceptible to damage from hard landings. Excess runway water causes damage to the wheel well doors. Other problems are caused by such items as fire extinguishers not being removed from in front of the aircraft prior to taxi for take-off, taxi collisions with other aircraft and deer, misfiring in flare launcher tubes, damage to tail skids due to nose-too-high landings, etc.

Battle damage (Refs. 5 and 6) can be categorized as follows:

- 1. Gunfire projectiles
 - a. Non-exploding
 - b. High explosive (HE)
- 2. Missile warheads

The non-exploding types are characterized by Soviet small arms projectiles (7.62 mm through 14.5 mm). These are comparable to the U.S. .30 and .50 calibers. Damage may be assumed as penetration roughly equivalent to the projectile size. Variation in damage is caused by such items as location of the strike, penetration angle, projectile velocity, skin thickness, and type of material.

Damage from high explosive shells is more extensive. Of these the Soviet 23 mm is considered the major threat. Its damage is simulated in test by the U.S. 20 mm. Typical damage to skin-stringer construction is shown in Figures 2a, b, and c. The projectile explodes on impact, creating a fragment cone. For large distances to the second penetration surface such as would be the case for a fuselage, the result would be a large scattering of small holes.

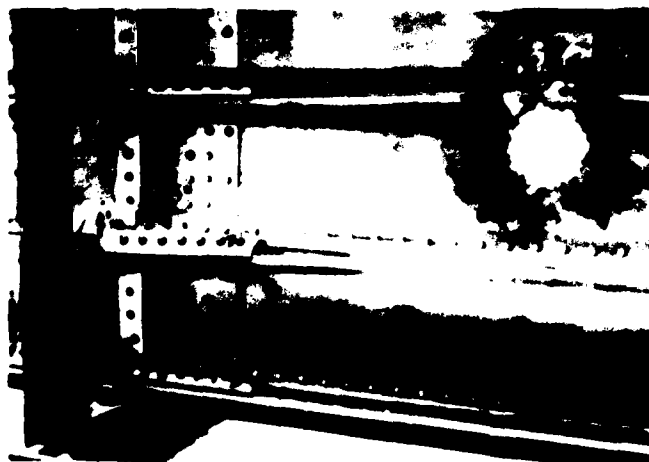
Structural damage from air-to-air missile warheads is due to the combined effects of the blast and the fragmentation. The fragment size and shape varies and includes cubes, pyramids, and rods. Typically, these are of a 180 grain size, i.e., approximately that of a .30 caliber projectile. The damage can be assumed as scattered multiple penetrations. The number and density are dependent on the explosion proximity.



(A) Impact into Stiffener, Entry Face, 7075-T6



(B) Impact into Stiffener, Exit Face, 7075-T6



(C) Impact Adjacent to Stiffener, 7075-T6

Figure 2.—Typical Entry Damage for 20-mm HE, Normal Impact

3.0 MATERIAL EVALUATION

3.1 SELECTION OF CANDIDATE ADHESIVE SYSTEMS

Three adhesives were evaluated in this program. The purposes were to select an adhesive for repair method demonstration and obtain preliminary data to support repair design and analysis.

Two elevated temperature curing adhesives, EA9628 and FM73, and one room temperature curing adhesive, EA9309, were candidate selections. EA9628 and FM73 were previously given preliminary evaluation in Air Force Contract F33615-73-C-5171. Results are reported in that program's phase II report (Ref. 7). Results for both adhesives were good.

FM73 was the adhesive selected for the PABST program. It was considered an advantage if that adhesive could also be used for repair.

EA9628 was selected as a companion to FM73 in the evaluation because it has shown superior tolerance to surface preparation quality. This characteristic is especially important for repair applications.

EA9309 was the room temperature adhesive selected by Douglas for PABST. Available data (Ref. 8) shows it to have better salt spray resistance than EA9320, which was another system initially considered as a candidate for evaluation.

3.2 TEST PLANS

Two groups of material tests were conducted. The types of tests conducted in Group 1 are shown in Table 1. These were static tests. They were used to evaluate strength versus temperature, resistance to environmental exposure, and toughness.

Additionally, some Group 1 tests were conducted using a differential scanning calorimeter (DSC) to determine glass transition temperatures. The purpose was to determine the minimum cure temperatures required to fully polymerize the elevated temperature cure and primer adhesives. The goal was to keep the repair cure temperature as low as practical. The reasons for this were:

1. To not heat the area adjacent to the repair any hotter than necessary and thus minimize the amount of restraining tool fixturing required.
2. Minimize residual stresses caused by cooling a localized area after heatup for repair.

It is recognized that some tolerance must be added to defined minimum cure temperatures since it will be difficult to closely measure or control temperatures in actual repair situations.

It has been indicated that slow cyclic loading, combined with humid elevated temperature, is a critical condition. This effect was investigated in the Group 2 series of tests.

Table 1. — TESTS OF CANDIDATE REPAIR ADHESIVE SYSTEMS USING HAND PHOSPHORIC ACID ANODIZE

Adhesive	Lap shear, psi				Variable lap length, lb			Metal-to-metal peel, lb-in./in.			Wedge test, in. *				
	R.T. control	14-day salt spray	180° F	60-day 600-psi	L = 0.5	L = 1.0	L = 2.0	R.T.	67° F	14-day 100% RH	Initial length	Crack growth			
												1 hr	4 hr	14 days	30 days
EA 9628 Cure A B	• •	•	• •	• •	•	•	•	•	•	•	• •	• •	• •	• •	• •
FM 73 Cure A B	• •	•	• •	• •	•	•	•	•	•	•	• •	• •	• •	• •	• •
EA 9309 RT cure	• • ***	• →	•	•	•	•	•	•	•	•	• •	• •	• •	• •	• •

Cure A- 90 min at 250° F, autoclave pressure
Cure B-2 hours at 200° F, vacuum pressure

* Test at -67° F, R.T., and 180° F

** 100% RH, 120° F, exposure

*** No primer

Five specimens for each condition except ten for the lap shear controls

All specimens primed with BR127

corrosion inhibiting primer except as noted.

The planned tests are indicated in Table 2. The stress levels were comparable to those used in the PABST program. The PABST exposure environment to 140°F and 100% relative humidity was also used. Since the tests were conducted over an extended time period, the specimens were not preconditioned. The test used a modification of the Douglas cycle as shown in Figure 3.

Table 2.—SMALL SPECIMEN SLOW CYCLE ENVIRONMENTAL FATIGUE TESTS

Adhesive	Cure	Static R.T. controls	Cyclic stress level		
			900 psi	1200 psi	1500 psi
FM 73	250° F, 90 min. autoclave	5	4	4	4
	200° F, 120 min. vacuum	5	4	4	4
EA 9628	250° F, 90 min. autoclave	5	4	4	4
	200° F, 120 min. vacuum	5	4	4	4
EA 9309	R.T., vacuum	5	4	4	4

Note: Exposure at 140° F., 100% R.H. See Figure 3 for cycle rate.

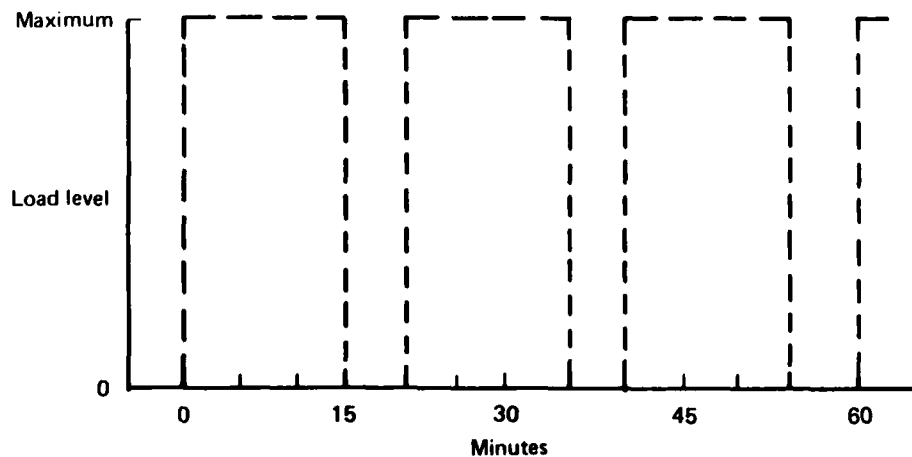


Figure 3.—Slow Rate Environmental Fatigue Cycle

Table 3. - LAP SHEAR AND PEEL TEST RESULTS

Adhesive	Cure	0.5 inch lap shear, psi				M M peel, lb in. in.		
		R.T.	180° F	14 day salt spray	Stressed ⁵ 60 day 600 psi	R.T.	-67° F	14 day 120° F 100% RH
EA 9628	Autoclave*	4598 S = 92	2896 S = 38	4604 S = 154	4610 S = 66	61.1 S = 5.6	11.6 S = 1.0	62.7 S = 3.9
	Vacuum**	4012 S = 93	2272 S = 72	4056 S = 38	4285 S = 64	None	None	None
FM 73	Autoclave*	3986 S = 87	2616 S = 88	4012 S = 92	3990 S = 125	56.4 S = 5.8	15.8 S = 5.5	56.7 S = 2.5
	Vacuum**	3778 S = 110	2388 S = 153	3920 S = 114	3820 S = 348	None	None	None
EA 9309	Vacuum***	3486 S = 442	576 S = 34	3462 S = 593	Failure in 5, 11, 14 & 18 days	55.8 S = 5.9	4.5 S = 1.2	43.9 S = 3.9

Notes:

1. Curing conditions

* 35 psi, 250° F, 90 min

** 25-28 in. hg, 200° F, 2 hr

*** 25-28 in. hg, R.T.

2. Specimens primed with BR 127

3. S = Standard deviation

4. 7075-T6 bare aluminum

5. Exposure at 120° F and 100% RH

It was planned that the specimens be tested for a minimum of 3000 cycles or to failure. Specimens surviving the maximum practical number of cycles were to be static tested to determine residual strength. The testing facility is shown in Figure 4.

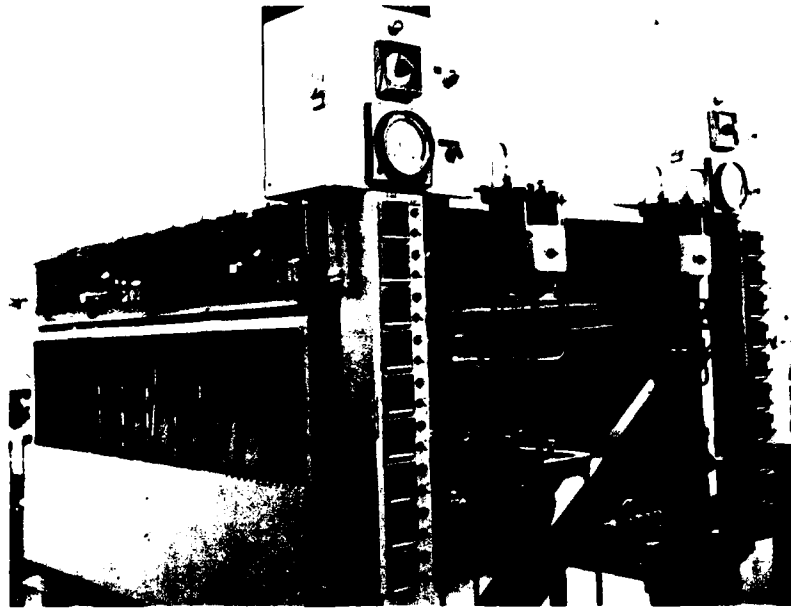


Figure 4.—Slow Cycle Environmental Fatigue Testing Facility

3.3 TYPES OF SPECIMENS

Three types of specimens were used for the Group 1 testing. These were lap shear, metal-to metal peel, and wedge specimens. The lap shear specimens were fabricated using 0.125 in. thick metal adherends. The material was 7075-T6 aluminum. Wide area bonded panels were laminated and cut into specimens 1.0 in. wide. Except for the specimens that were specifically made to evaluate the effect of lap length, the lap length of all specimens was 0.5 in. These were also used for the Group 2 cycle tests. The test lap area was accomplished by cutting two spaced slots on opposite sides of the specimen as shown in Figure 5.

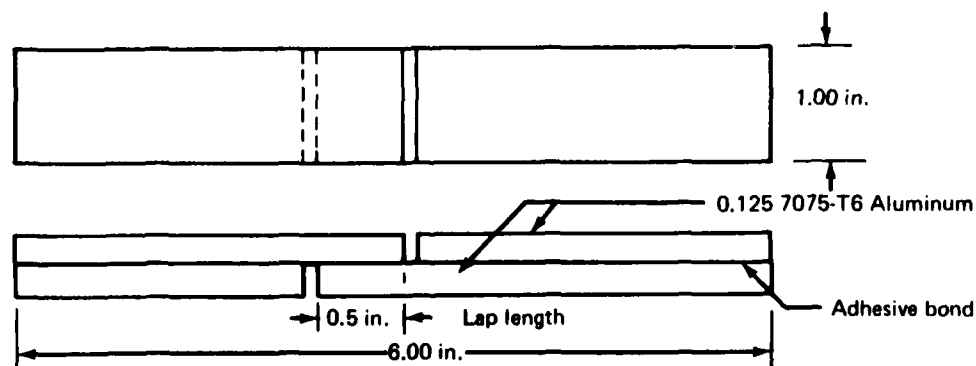


Figure 5.—Standard Adhesive Lap Shear Specimen

The metal-to-metal peel specimens were fabricated from laminated panels (14 by 17 in.) having 0.020 in. skins and 0.032 in. backing sheets. The panels were cut into 1.0 in. wide strips. The climbing drum peel specimen and test method are described in MIL-A-25463.

The configuration of the wedge test specimen assembly and the specimen details are shown in Figure 6. The laminated assembly was 6 by 6 in. The metal adherends were nominally 0.125 in. thick. A strip approximately 0.75 in. wide on one edge of the panel was left

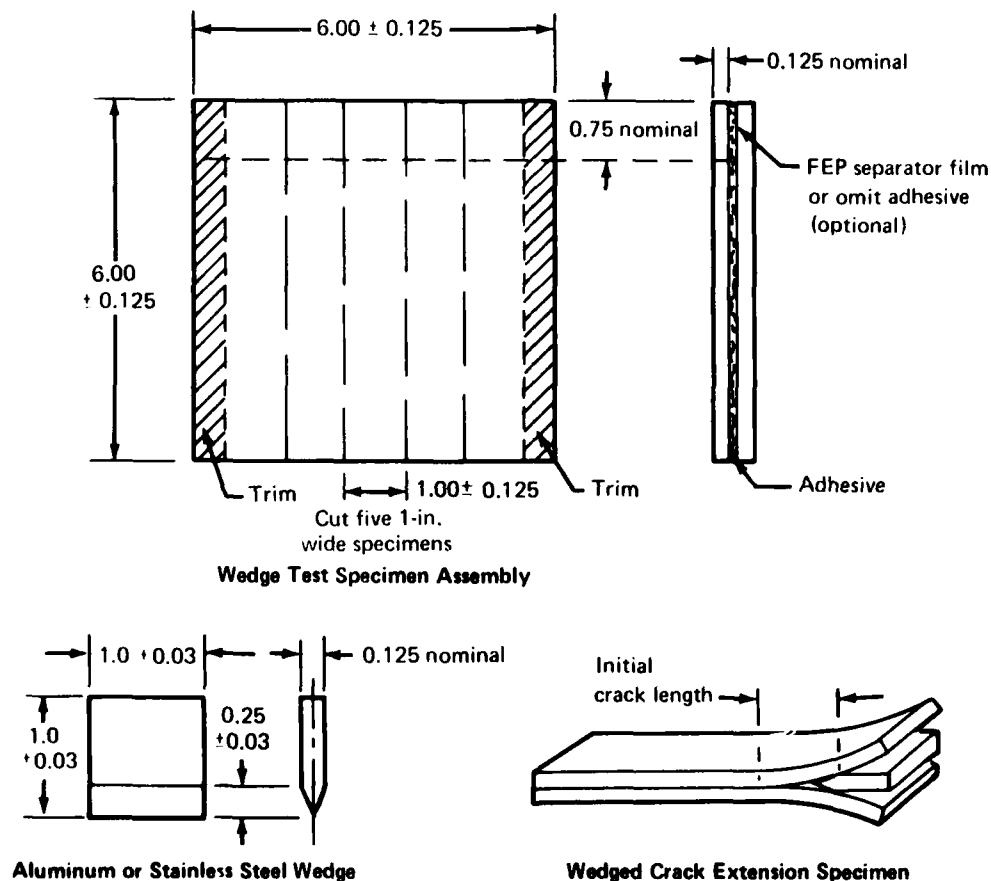


Figure 6.—Wedge Test Specimen Configuration

unbonded. After bonding, five 1-in. wide specimens were machined from the panel. The specimens were then marked with an identification prior to exposure. The testing procedure for the specimens consisted of the following:

1. The unbonded end of the specimen was precracked by inserting a wedge as shown in Figure 6. The wedge was inserted by using several light taps with a hammering device.
2. The wedge was positioned so that its end and sides were approximately flush with the specimen ends and sides.
3. Magnification of 10 to 30 power and adequate illumination was used to locate the tip of the initial crack. This was marked with a fine stylus or scribe. The reference point of crack initiation was located and marked. This was the point at which the shoulder of the wedge contacted the specimen surface: i.e., approximately 0.75 in. from the specimen end. The initial crack length was measured and recorded.
4. The wedge specimens were exposed to the selected environmental conditions: i.e., 120°F ±5°F and 95% to 100% relative humidity, for the specified time: e.g., 1 hour, 4 hours, 72 hours, 14 days, or 30 days.
5. The specimens were removed from the environment. The increase in crack length was measured and marked to 0.01 in.
6. Failure modes were determined by splitting the specimen open at the completion of the final crack growth measurement and examining the surface. The percentage of adhesive versus cohesive failure in the exposure crack growth region was recorded.

3.4 SPECIMEN PROCESSING

The processing methods that were evaluated were representative of those that can be used for on-the-aircraft repairs. These included the use of the phosphoric acid hand anodized surface preparation method developed in the F33615-73-C-5171 program (Ref. 7). Unless otherwise noted, bond surfaces were coated with BR127 corrosion inhibiting adhesive primer. The primer was bake cured prior to adhesive application. Since the primer requires a 250°F cure, only one set of EA9309 specimens was cured with primer. This was done to evaluate the value of using the primer with the room temperature curing system.

The elevated temperature curing systems were cured using two procedures. These were:

1. A vacuum bag and heating blanket; 200°F, 25 to 28 in. hg, 120 minutes.
2. An autoclave; 250°F, 35 psi, 90 minutes.

The former case is representative of the on-the-aircraft cure condition while the latter is a baseline for an as-manufactured comparison.

3.5 TEST RESULTS

Results corresponding to the Group 1 test plan shown in Table 1 are tabulated in Tables 3, 4 and 5. Shear strength versus overlap curves are plotted for EA9628 and FM73 in Figures 7 and 8. These curves are not plotted for the room temperature curing EA9309 adhesive because of its very low 180°F strength and the errantry of the -67°F data.

Table 4.—ULTIMATE LOAD VERSUS LAP LENGTH DATA

Adhesive	Test temperature	Ultimate load, lbs.		
		Lap length, inches		
		0.5	1.0	2.0
EA 9628 *	R.T.	2210 S = 34	4378 S = 88	7998 S = 240
	180° F	1730 S = 26	3008 S = 41	6018 S = 61
	-67° F	3572 S = 36	5028 S = 32	7848 S = 103
FM 73 •	R.T.	2035 S = 47	4348 S = 70	7865 S = 208
	180° F	1795 S = 177	2903 S = 297	5690 S = 98
	-67° F	3338 S = 88	4618 S = 156	7295 S = 264
EA 9309 **	R.T.	1877 S = 188	3563 S = 38	7178 S = 260
	180° F	304 S = 82	496 S = 33	835 S = 183
	-67° F	2780 S = 585	2003 S = 291	5838 S = 2499

Notes: 1. Curing conditions * 35 psi, 250° F, 90 min
 ** 25-28 in. hg, R.T.

2. 7075-T6 bare, 0.125 in. thick
3. Four specimens for each condition

In general, acceptable properties were obtained with both of the elevated temperature curing systems. The autoclave cured specimens gave slightly higher strengths than those cured under vacuum. Both systems showed some decreasing toughness at low temperatures. This was indicated by the drop-off in peel strength and the flattening of the shear strength versus overlap plots. The peel tests were rerun. The results are shown in Table 6. The -67° values were still quite low.

Table 5. - WEDGE SPECIMEN TEST RESULTS

Spec. design.	Adhesive	Cure	Initial crack length, in.	Crack growth, inches				
				1 hr	4 hr	24 hr	14 day	30 day
E-1	EA 9628	Autoclave*	1.48	.06	.09	.12	.19	.24
2			1.46	.06	.06	.12	.18	.21
3			1.41	.07	.11	.11	.17	.20
4			1.45	.06	.10	.12	.17	.20
5			1.55	.05	.08	.08	.13	.16
F-1	FM 73	Autoclave*	1.58	.05	.08	.11	.13	.17
2			1.56	.06	.06	.10	.13	.16
3			1.59	.05	.05	.05	.08	.14
4			1.53	.05	.05	.08	.11	.15
5			1.54	.06	.08	.11	.14	.16
VE-1	EA 9628	Vacuum**	1.59	.08	.11	.16	.20	.22
2			1.58	.07	.10	.12	.16	.19
3			1.54	.08	.12	.15	.18	.21
4			1.61	.06	.06	.11	.15	.15
5			1.59	.07	.11	.12	.19	.19
VG-1	FM 73	Vacuum**	1.55	.07	.07	.11	.14	.17
2			1.54	.09	.09	.12	.14	.17
3			1.54	.09	.09	.13	.16	.16
4			1.62	.06	.06	.10	.10	.10
5			1.72	.06	.06	.09	.09	.09
RE-1	EA 9309	Vacuum R.T.	1.53	.39	†	.78	1.09	1.47
2			1.43	.39		.62	.89	1.25
3			1.41	.41		.63	.87	1.28
4			1.46	.33		.58	.82	1.23
5			1.56	.34		.68	.98	1.32

- Notes:
1. Curing conditions * 35 psi, 250° F, 90 min
 ** 25-28 in. hg, 200° F, 2 hr
 2. All specimens primed with BR127 primer
 3. Specimens exposed to 120° F and 100% R.H.
- † No readings taken

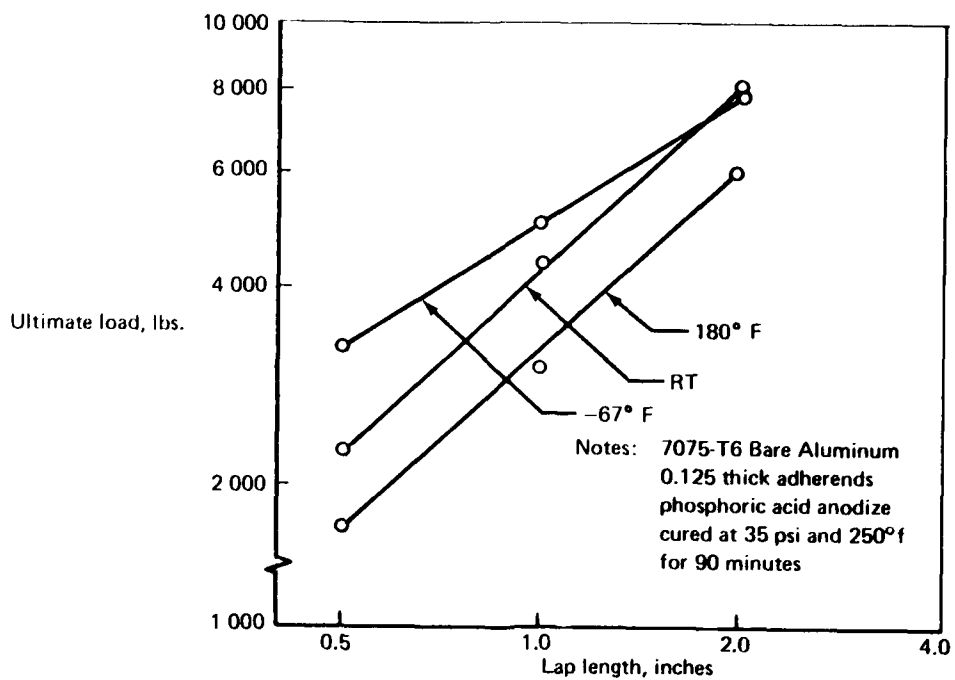


Figure 7.—Shear Load Versus Lap Length—EA9628 Adhesive

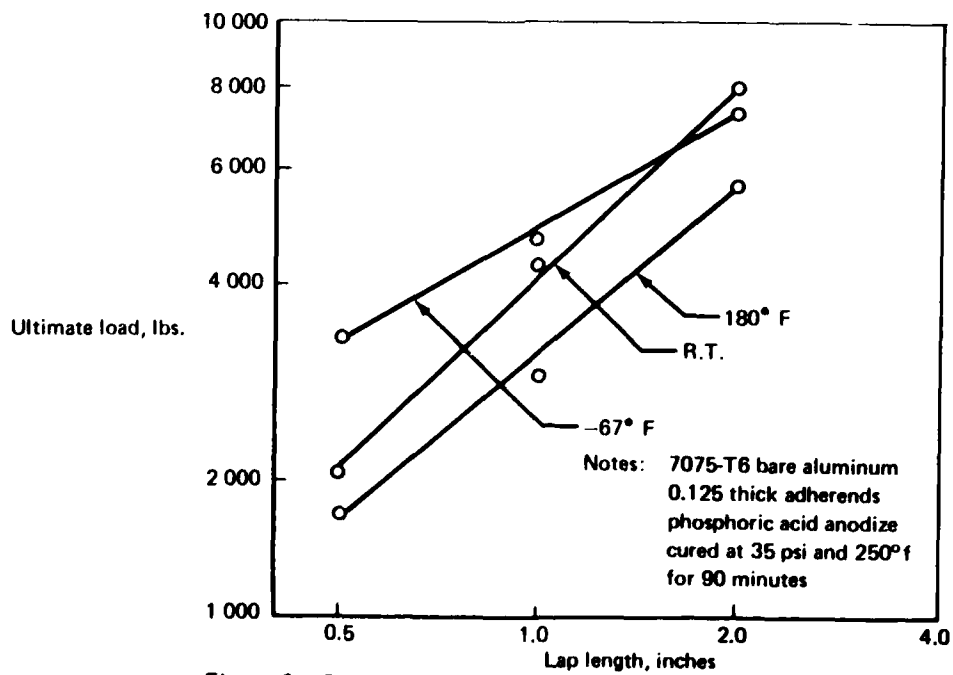


Figure 8.—Shear Load Versus Lap Length—FM73 Adhesive

Both EA9628 and FM73 showed good resistance to salt spray and to static stressed exposure at 120°F and high humidity. The wedge test crack growth data shown in Table 5 were also satisfactory.

Table 6. RETEST OF PEEL TESTS USING BOTH TANK AND NONTANK ANODIZE

Adhesive	Surface preparation	M/M peel, lb. in./in.	
		R.T.	67° F
EA 9628	Nontank anodize	40.5	25.5
		40.5	22.5
		40.5	22.5
			18.0
FM 73	Nontank anodize	108.0	24.0
		102.0	18.0
		81.0	18.0
			18.0
EA 9628	Tank anodize	40.5	21.0
		40.5	13.0
		40.5	9.0
			10.5
FM 73	Tank anodize	103.5	24.0
		105.0	13.5
		96.0	13.5
			16.5

Cure: 35 psi, 250° F, 90 min.

Less acceptable results were obtained with the room temperature curing EA9309 system. In addition to the unsatisfactory results obtained from the variable lap length tests, the specimens stressed to 600 psi at 120°F and 100% relative humidity failed after short time exposure. The -67°F peel test values were low. The crack growth rate for the wedge tests was also considerably higher than for the other systems.

Results of the glass transition tests are listed in Table 7. Various curing times and temperatures were evaluated for EA9628, FM73, and BR127 primer. In the test, the glass transition temperature of the test sample was compared to that of a control specimen that was known to be fully cured. In this case, the adhesive controls were cured at 250°F for 90 minutes. The primer control was cured at 250°F for 60 minutes. The results indicated that FM73 is not fully cured after 2 hours at 200°F. The 200°F cure was marginal for EA9628. Results for BR127 cured at 200°F were inconclusive.

**Table 7. -- RESULTS OF GLASS TRANSITION TESTS
ON ADHESIVES AND PRIMER TO DETERMINE CURE EFFECTIVITY**

Cure (temperature, time)	Adhesive		Primer
	EA 9628	FM 73	BR 127
250 ⁰ F, 90 min	212 ⁰ F *	242 ⁰ F *	202 ⁰ F *
250 ⁰ F, 60 min	215 ⁰ F	242 ⁰ F	
225 ⁰ F, 120 min	228 ⁰ F	244 ⁰ F	
225 ⁰ F, 60 min	223 ⁰ F	243 ⁰ F	
200 ⁰ F, 120 min	208 ⁰ F	202 ⁰ F	None ** Observed

* Controls

** No glass transition was observed. Samples were made three times, increasing the sample quantity each time (6, 12, 18 drops). Each group was cured in an oven separately. Regardless of the baseline slope, a straight line was obtained for all samples.

Results of the Group 2 cyclic load/environmental exposure tests are shown in Tables 8, 9, and 10. A bar chart comparison of the data is shown in Figure 9. The greater durability of the FM73 as compared to that of EA9628 can be noted. This is especially apparent for the 900 psi load.

3.6 TEST CONCLUSIONS

The results obtained with the EA9628 and FM73 adhesives were quite comparable except for the cyclic load/environmental exposure test. Here the FM73 system was significantly superior. As a result, the FM73 system was selected for use in repair method demonstration in subsequent tasks. The test values obtained on EA9309 adhesive indicate that it is unsatisfactory for repairing primary structures. No further work will be done with this system.

Table 8. - RESULTS OF CYCLIC LOAD/ENVIRONMENTAL EXPOSURE TESTING 900 PSI

Adhesive/primer	Cure cycle	Spec. no.	Hours to failure	Cycles to failure	Failure mode
EA9628/BR127	A (Auto-clave)	E-1	579.4	1738.2	95% Coh
		E-26	754.8	2279.4	95% Coh
		E-31	716.5	2149.5	85% Coh
		E-32	581.5	1744.5	95% Coh
EA9628/BR127	B (Vacuum bag)	VE-1	192.9	578.7	95% Coh
		-20	137.4	412.2	90% Coh
		-24	476.3	1428.9	95% Coh
		-31	353.5	1060.5	95% Coh
FM73/BR127	A (Auto-clave)	F-1	1		
		-6	1629.4	4888.2	90% Coh
		-31	2129.5	6388.5	90% Coh
		-37	1755.7	5267.1	85% Coh
FM73/BR127	B (Vacuum bag)	VF-4	1272.0	3816.0	85% Coh
		-22	1342.6	4027.8	95% Coh
		-26	1453.9	4316.7	90% Coh
		-31	1459.0	4377.0	90% Coh
EA9309/BR127	RT cure	1-25	4 minutes	less than	100% Coh
		-26	2 minutes	1 cycle	85% Coh
		-27	4 minutes	"	95% Coh
		-32	3 minutes	"	45% Coh

Note: 140° F/100% RH
900 psi = f_{max} for 15 minutes
0 psi = f_{min} for 5 minutes
3 cycles per hour

1 No failure after 7400 cycles; tested for residual at ambient (3350 psi)

Table 9. — RESULTS OF CYCLIC LOAD/ENVIRONMENTAL EXPOSURE TESTING—1200 PSI

Adhesive/primer	Cure cycle	Spec. no.	Hours to failure	Cycles to failure	Failure mode
EA9628/BR127	A (Auto-clave)	E-2	558.8	1676.4	95% Coh
		-5	498.2	1494.6	99% Coh
		-7	578.1	1734.3	70% Coh
		-8	753.8	2261.4	70% Coh
EA9628/BR127	B (Vacuum bag)	EV-1	90.4	271.2	95% Coh
		-3	207.1	621.3	95% Coh
		-5	202.1	606.3	98% Coh
		-7	245.2	735.6	99% Coh
FM73/BR127	A (Auto-clave)	F-5	872.2	2616.6	90% Coh
		-7	746.0	2238.0	80% Coh
		-13	703.2	2109.6	70% Coh
		-15	600.0	1800.0	90% Coh
FM73/BR127	B (Vacuum bag)	FV-2	642.7	1928.1	98% Coh
		-5	904.4	2713.2	95% Coh
		-9	795.8	2387.4	95% Coh
		-14	242.4	727.2	98% Coh

Note: 140° F/100% RH condition

1200 psi = f_{\max} for 15 minutes

0 psi = f_{\min} for 5 minutes

3 cycles per hour

**Table 10. — RESULTS OF CYCLIC
LOAD/ENVIRONMENTAL EXPOSURE TESTING — 1500 PSI**

Adhesive/primer	Cure cycle	Spec. no.	Hours to failure	Cycles	Failure mode
EA9628/BR127	A (Auto-clave)	E-3	191.3	573.9	100% Coh
		-6	142.7	428.1	98% Coh
		-9	185.1	555.3	95% Coh
		-10	163.5	490.5	98% Coh
EA9628/BR127	B (Vacuum bag)	VE-2	40.9	122.7	99% Coh
		-4	66.5	199.5	99% Coh
		-6	63.4	190.2	99% Coh
		-8	69.7	209.1	99% Coh
FM73/BR127	A (Auto-clave)	F-1	193.9	581.7	60% Coh
		-4	218.4	655.2	50% Coh
		-8	211.4	634.2	55% Coh
		-10	216.9	650.7	80% Coh
FM73/BR127	B (Vacuum bag)	YF-4	81.9	245.7	90% Coh
		-8	100.1	300.3	90% Coh
		-11	98.3	294.9	85% Coh
		-13	101.7	305.1	98% Coh

Note: 140° F/100% RH condition
 1500 psi = f_{max} for 15 minutes
 0 psi = f_{min} for 5 minutes
 3 cycles per hour

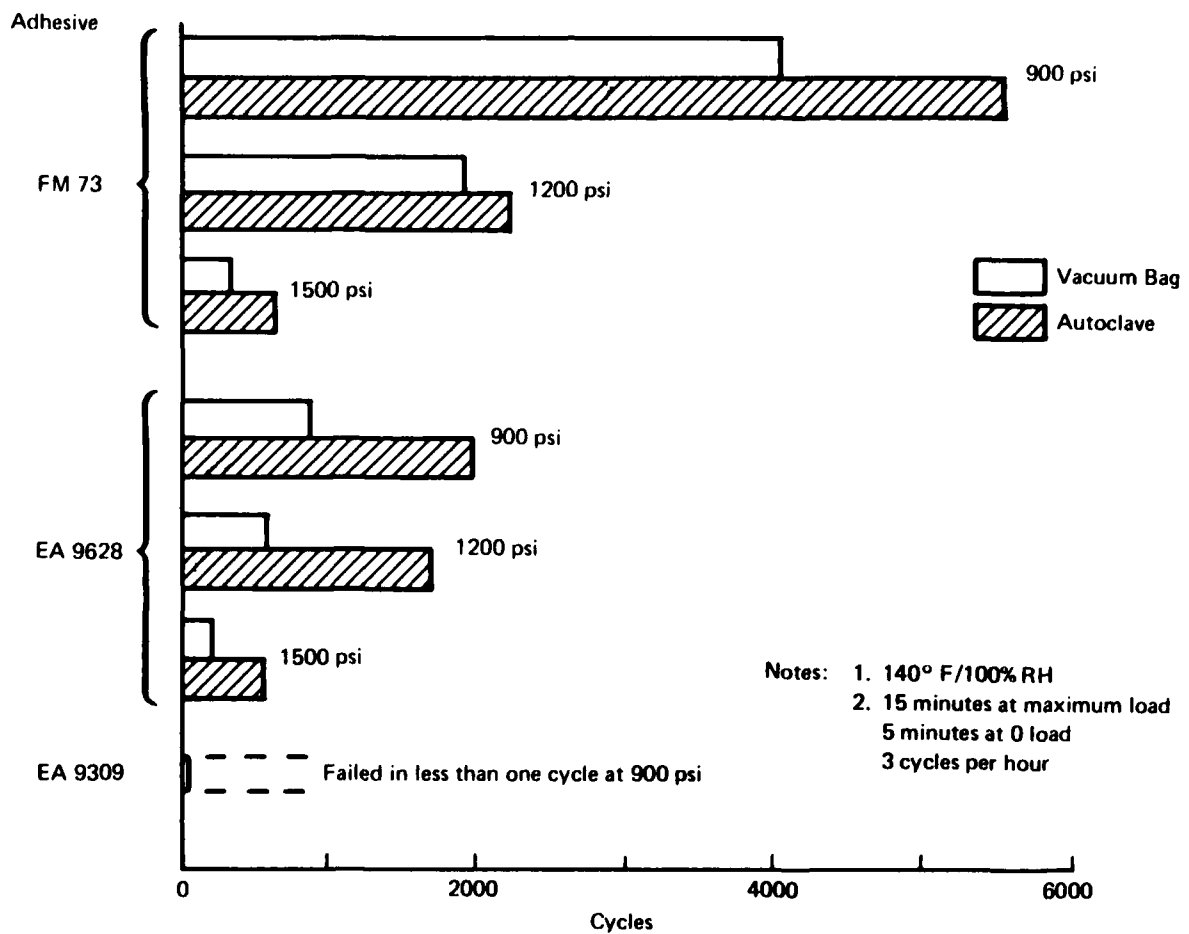


Figure 9.—Comparison of Cyclic Load/Environmental Exposure Data

4.0 EVALUATION OF REPAIRED PANELS

As part of this program, several panels were fabricated to provide a preliminary evaluation of the proposed repair procedures. The panels gave an opportunity to further demonstrate the utility of the phosphoric acid non-tank anodize method. There was special interest in demonstrating use of the method to prepare the surface of the bonded stiffeners where the metal splice details would be bonded.

Subsequent testing of the repaired panels and comparison with controls allowed verification that the repairs were adequate to meet the design requirements.

4.1 PANEL DESIGN

Repair demonstration panel configurations were selected based on critical structural conditions for the PABST fuselage. The types of panels and the modes of loading are shown in Figure 10. Two of the panel types represent repair of the skin/frame areas. The third represents repair to the bonded longitudinal skin splice.

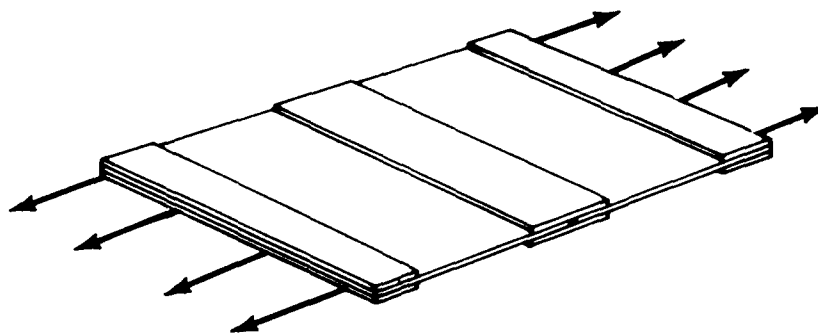
The panels with the frame tee allow two methods of testing. The first is a normal tension load on the tee. This occurs in-service due to fuselage internal pressure loads as the shell tries to expand and is restrained by the stiff frame ring. The tension load on the frame tee leg to skin bond is critical. The skin pillows between the stiff frames as pressure is applied. This tends to start a peeling action in the bond at the edge of the frame tee leg.

The other critical loading condition for the frame tee/skin is represented by shear along the frame. This is primarily caused by floor loads or may be caused by concentrated loads such as those introduced by the landing gear. The stresses in the longitudinal skin splice are caused by the fuselage pressure loads.

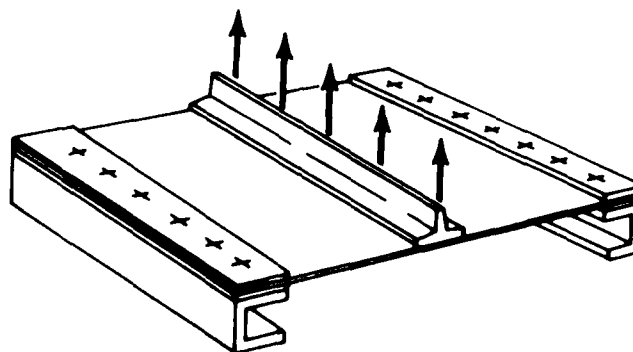
The designs of the repairs for the panels are shown by the sketches in Figures 11 and 12. The basic construction duplicates that of the PABST component. The skin for the panel is 0.050 in. thick 2024-T3 bare aluminum. The frame is detailed in Figure 13 and was fabricated from bare 7075-T6.

All of the panels were initially fabricated in the undamaged/unrepaired condition. Damage was then assumed for one-half of the panels and repairs were incorporated. The other half of the panels were used as controls. The repair design utilized bonded splice plates. In general, the splice overlaps were 2.0 in. The plates were 0.032 in. and 0.040 in. thick. They were stepped to provide edge tapering.

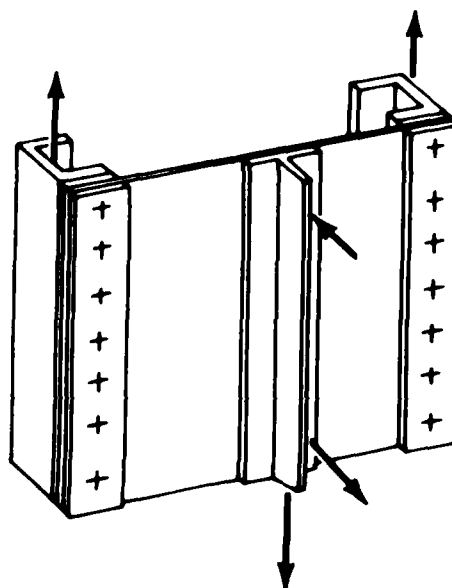
The stresses in the bondlines required to attain ultimate load in the metal were relatively moderate. The higher stresses were in the splice straps for the frame tee. These have a maximum 4.0 in. overlap length. Assuming an ultimate stress of 75 ksi for the 7075-T6 aluminum, the required average ultimate stress for the bond was 1380 psi. This is well within the adhesive's strength capability. If the low test point on the 180°F curve for FM73 adhesive in Figure 14 is reduced by 3 standard deviations and extrapolated to a 4.0 in. lap length, the allowable design value is 6200 lbs per in. of width or 1550 psi.



Tension—Longitudinal Skin Splice (18 by 24 in.)

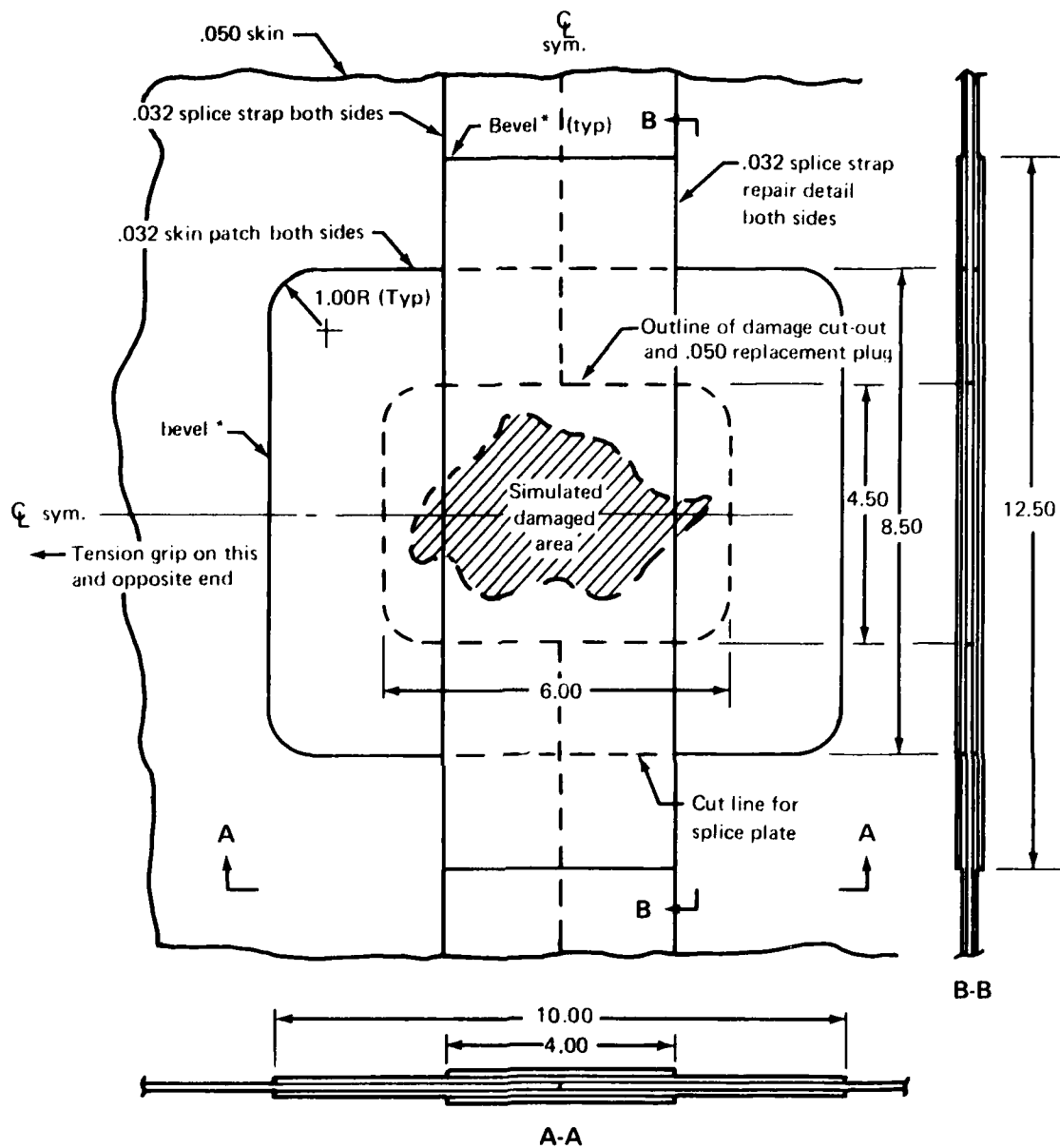


Tension—Frame Tee to Skin Joint (18 by 24 in.)



Shear—Frame Tee to Skin Joint (24 by 24 in.)

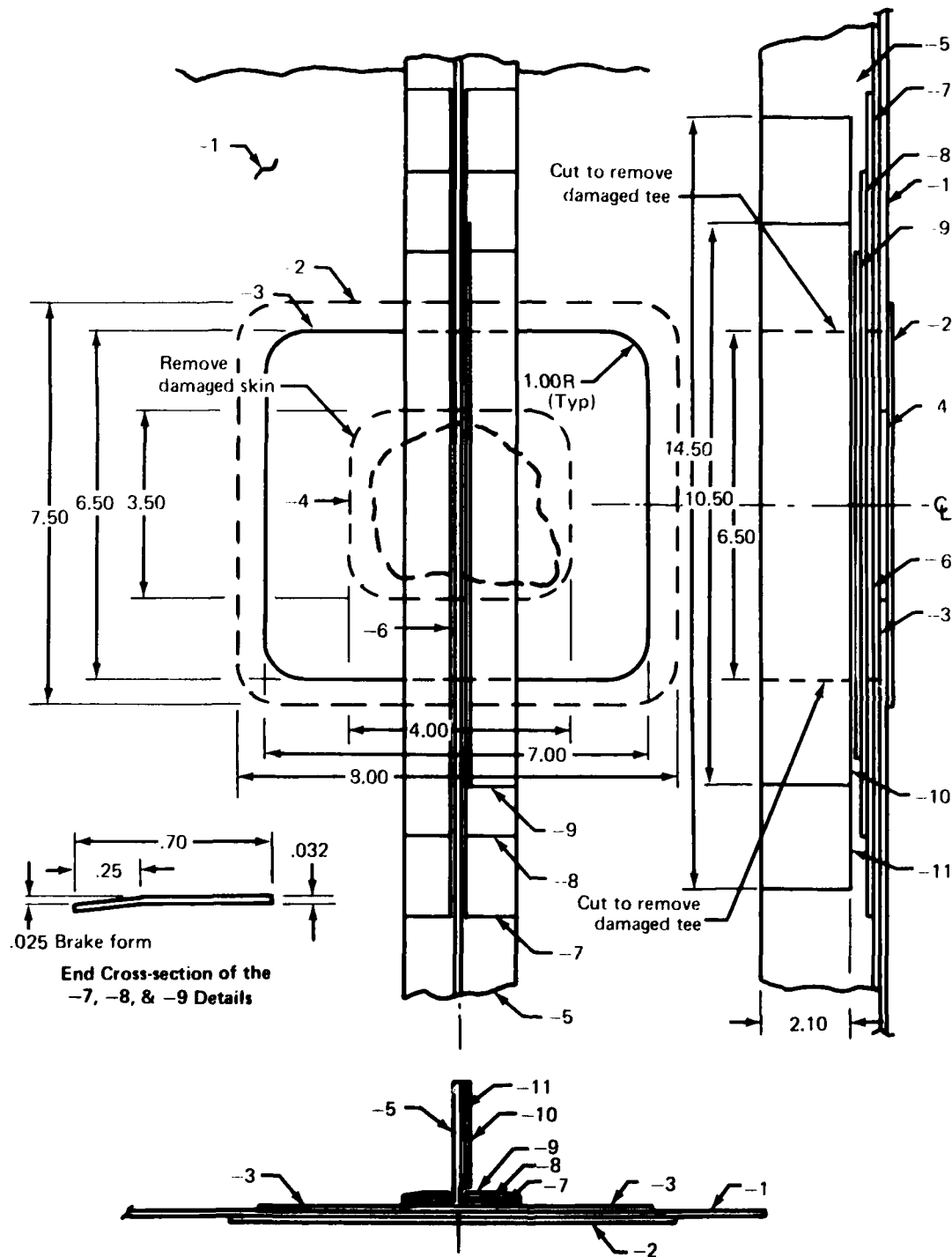
Figure 10.—Repair Test Panel Configurations and Loading Modes



*Bevel per repair handbook instructions

Notes: All metal 2024-T3 bare
use phosphoric acid anodize to prepare bond surfaces
prime with BR-127, bond with FM-73 adhesive
cure repair at 200 F, 2 hrs, full vacuum.

Figure 11.—Detail of Skin Splice Repair



Note: See next page for dash number description

☒ sym. except for splice plates on the side of the tee

Figure 12.—Detail of Frame Tee/Skin Repair

**Frame Tee Repair
List of Metal Details**

Dash No.	No. Req'd	Item	Description	Non-clad material	Notes
-1	1	Test panel skin	See test specification drawing for size	2024-T3	
-2	1	Outer skin splice plate	0.032 x 7.50 x 8.00	"	Radius corners and chamfer one side
-3	1	Inner skin splice plate	0.032 x 6.50 x 7.00	"	Radius corners
-4	1	Skin plug	0.050 x 3.50 x 4.00	"	"
-5	1	Frame tee	See Fig. 13 for cross-section	7075-T6	
-6	1	Frame tee plug	Same as -5 but 6.50 long	"	
-7	4	Splice strip filler	.032 x 0.70 x 4.50	"	
-8	2	Splice strip	.032 x 0.70 x 12.50	"	
-9	2	Splice strip	.032 x 0.70 x 9.50	"	
-10	1	Splice strap	.040 x 2.10 x 10.50	"	
-11	1	Splice strap	.040 x 2.10 x 14.50	"	

Figure 12.-(Concluded)

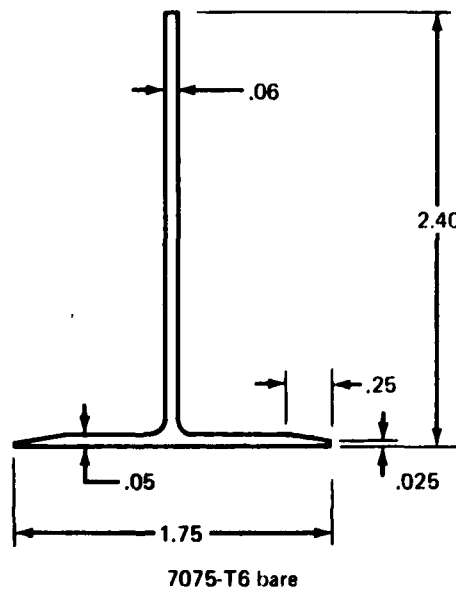


Figure 13.-Detail of Frame Tee

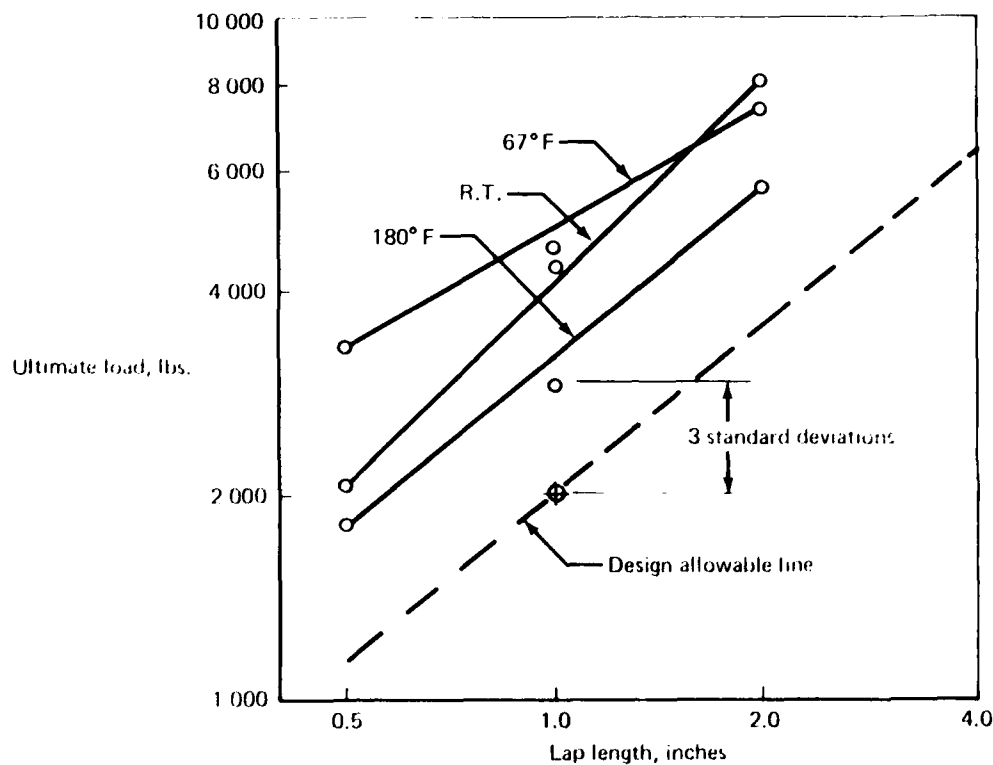


Figure 14. Design Curve Derivation - FM73 Adhesive

Bolted doublers were added to two sides of the panels where they were to be gripped for test loading. The frame tee for the shear panels was extended and tapered to a greater thickness for bolting to the test fixture as shown in Figure 15.

4.2 PANEL FABRICATION

Twelve panels were fabricated. The panel metal details were fabricated using conventional metal working techniques. The surfaces of the basic panel details were prepared prior to bond assembly by phosphoric acid anodizing in Boeing's production surface preparation tanks. The parts were then sprayed with BR127 corrosion inhibiting adhesive primer. The primer was cured by baking at 250°F for one hour. Subsequently, the panel was bonded with FM73 adhesive. The cure cycle was 250°F for 90 minutes at 50 psi. Wedge specimens were cured with the panels as controls. These gave satisfactory test results.

After bonding, the assumed "damaged area" was removed from one-half of the panels. Figure 16 shows the skin being cut with a high-speed router. The router is being used against a previously prepared metal template. A panel with the "damaged area" removed is shown in Figure 17. The organic finish has been removed from the area where the repair details are to be bonded.

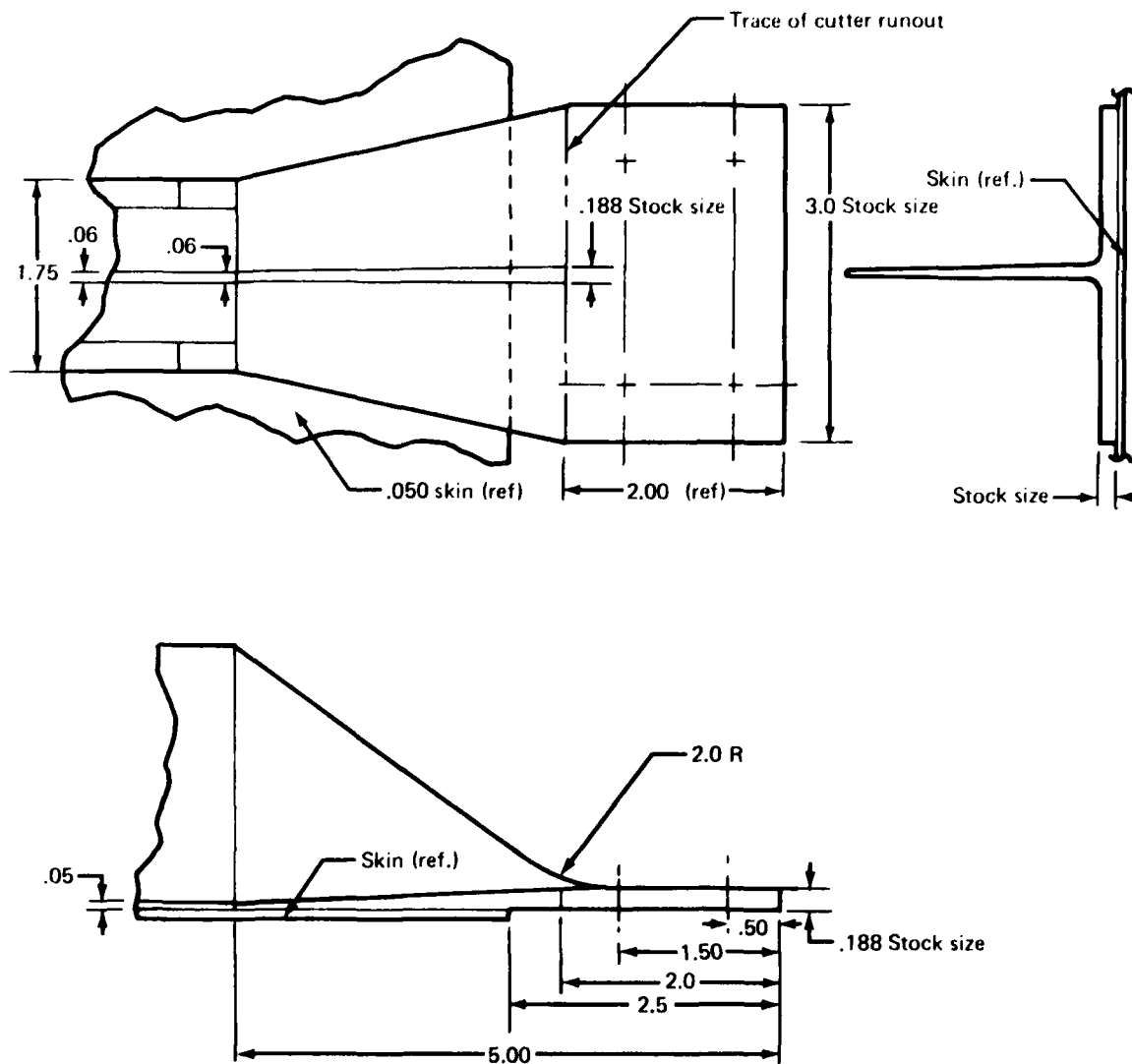


Figure 15.—Build-up Provided at End of Shear Panel Frame Tee for Test Loading.



Figure 16. Removal of the "Damaged Area" with High Speed Router

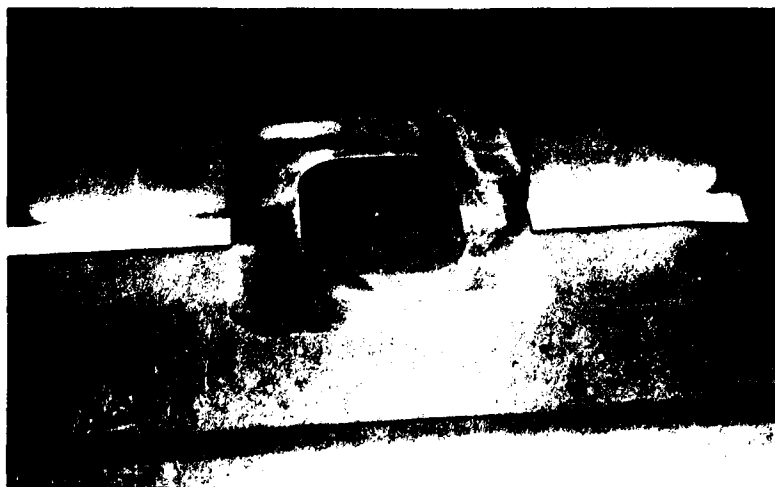


Figure 17. Panel with "Damaged Material" and Organic Coating Removed from Surfaces to be Bonded.

After damage removal, the repair details were fabricated. These are shown prior to bonding in Figure 18.

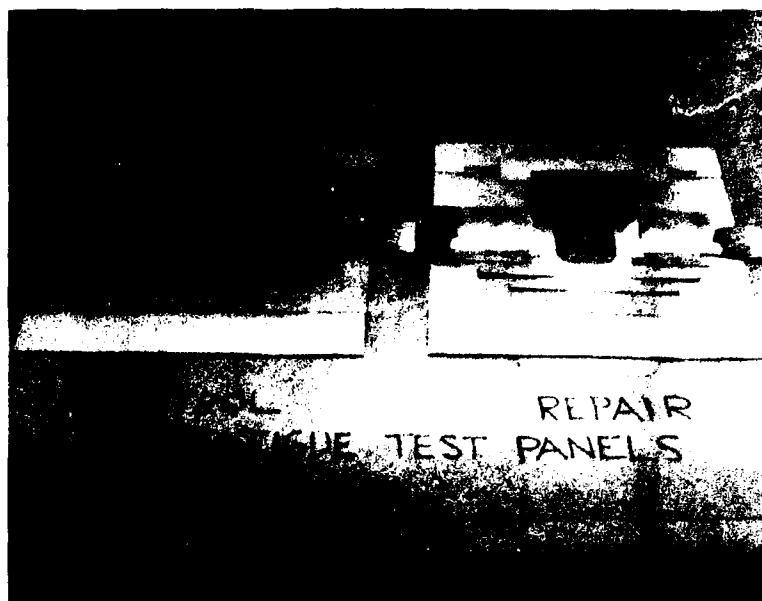


Figure 18. Fatigue Control and Repair Test Panel with Details Prior to Bonding

Surface preparation of the repair details was accomplished in production cleaning tanks. The phosphoric acid non-tank anodize method was used to prepare the surface of the panels. The area of the panels around the bond surfaces was masked and phosphoric acid gel applied as shown in Figure 19. The area was then covered with acid saturated gauze and a stainless steel screen. Anodizing is shown in process in Figure 20. The screen is connected as the cathode (-) and the panel as the anode (+). Anodizing was done at 6 volts for 10 minutes.

After anodizing, the acid was rinsed from the panel (Fig. 21) and the surface inspected for the iridescent, anodized color with a polarized filter (Fig. 22). The anodized area was subsequently primed with a Preval spray unit (Fig. 23) and the primer bake cured. The details were then assembled and the panels bonded at 200°F for 2 hours under full vacuum. A completed repaired panel and a comparable unrepaired control panel are shown in Figure 24. After repair, the panels were nondestructively inspected using the Fokker bond tester and ultrasonic water-coupled through transmission. The inspection indicated that all bonds were satisfactory.



Figure 19. -Applying Phosphoric Acid to Bond Surfaces Prior to Anodizing

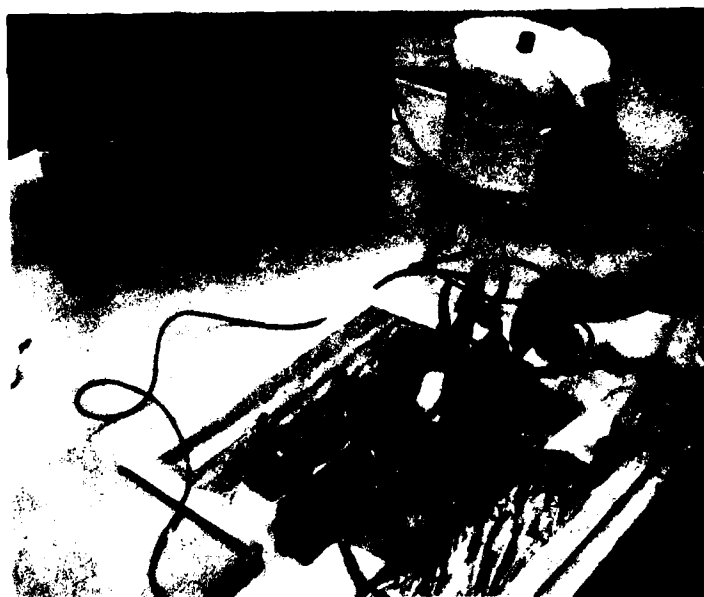


Figure 20. -Anodizing Repair Test Panel Prior to Bonding

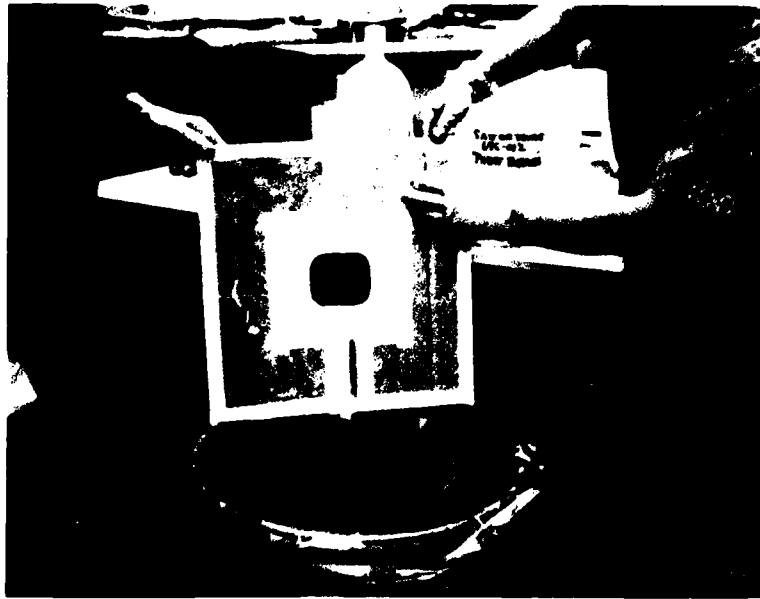


Figure 21. - Rinsing Panel after Anodizing

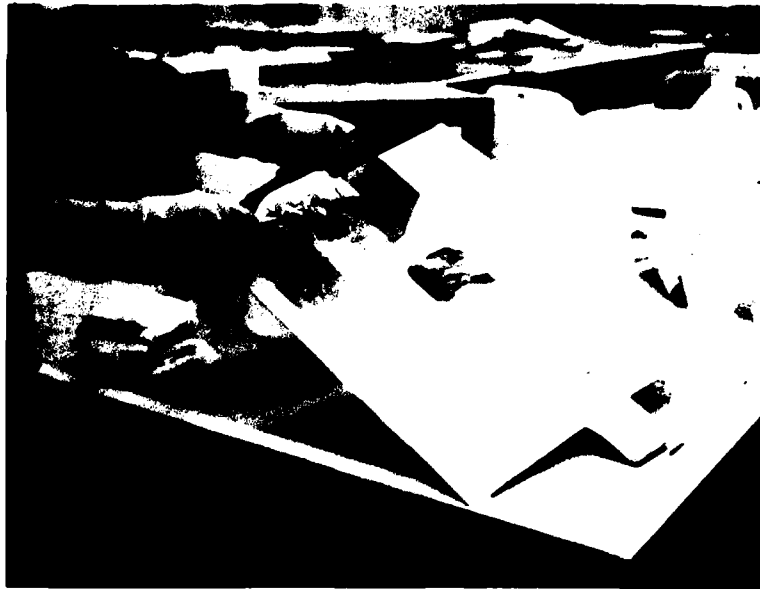


Figure 22. - Inspection of Anodized Surface with a Polarized Filter

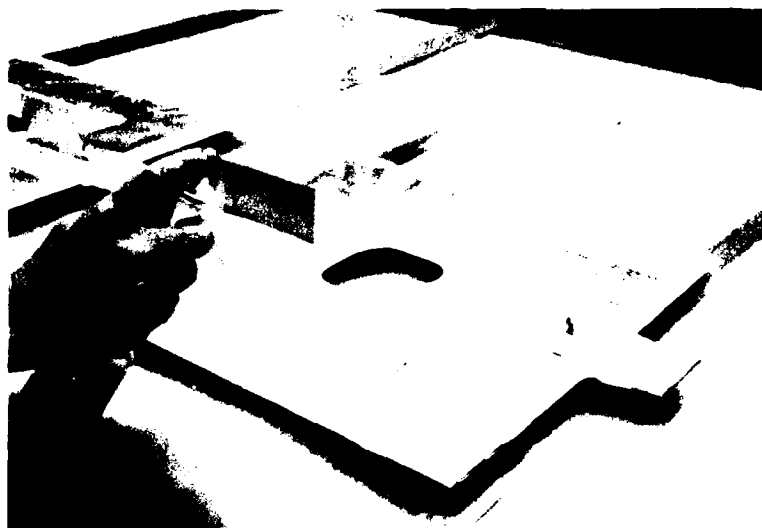


Figure 23. - Priming Surface with BR127 Primer

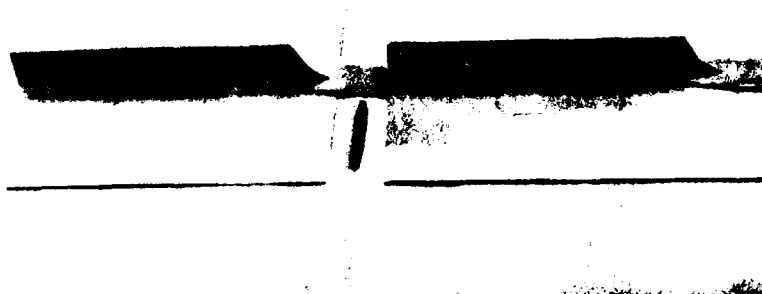


Figure 24. - Control and Repaired Shear Panel Prior to Test.

4.3 PANEL TEST AND RESULTS

One of each panel type was tested statically and in fatigue. The loads were applied to the panels using servo-controlled hydraulic actuators monitored by load cells. The six static specimens were strain gaged and a pretest strain survey taken to assure that the load distribution was acceptable. The static specimens were then tested at ambient conditions to failure.

The fatigue panels were tested in an environment consisting of 140°F and 100% relative humidity. The specimens were not preconditioned. Conditioning was accomplished during the test. The environment was created using a humidity generator and enshrouding the panel in plastic film. Temperature was controlled by thermocouples mounted on the panel surface. The humidity generator and two of the test panels are shown in Figure 25. This photo was taken during a pause in the testing for NDI evaluation. The plastic film and the thermocouples have been removed from the repaired longitudinal splice specimen in the foreground. Similarly, the repaired frame tee tension pull-off specimen is shown in Figure 26. A slow 20 minute fatigue cycle was used. Specimens were loaded to 50% of the ultimate strength of the comparable statically tested panel. The cycle consisted of the load being applied, held for 15 minutes, and then returned to no-load for 5 minutes. Specimens were loaded for 1000 cycles or until failure, whichever occurred first. The testing was halted after 350 and 700 cycles to allow nondestructive inspection with a Fokker bond tester to determine if degradation of the bond could be detected. The panels were also nondestructively

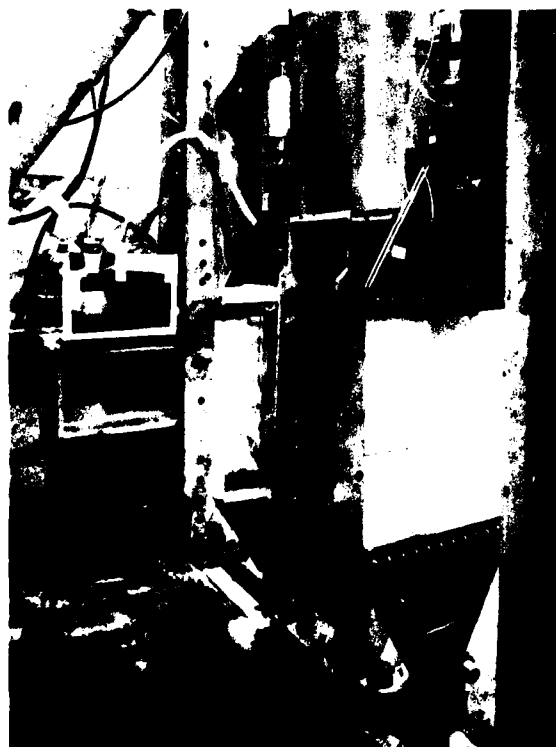


Figure 25.—Test Panels and Environmental Load Cycling Fixtures

inspected after completion of the 1000 cycles. Panels that sustained the 1000 cycles were then statically tested to determine their residual strength.



Figure 26. Frame Tee Tension Pull-off Test in Progress

Results of the static and fatigue tests are listed in Table 11. The repairs were considered successful. This was based on the design objective that the repaired specimens be as strong as the undamaged controls. For two of the panel types, the bondlines were in shear; failure, as expected, was in the base metal. These were the longitudinal skin splices and the frame/skin shear panels.

Typical failed skin splice panels can be seen in Figure 27. The base metal of all of these panels deformed considerably prior to failure. Failure was at the predicted ultimate metal strength and comparable for both the control and repaired units. Failure of the repaired fatigue panel at a lower stress than the control panel is attributed to normal data scatter.

Typical failures of the frame/skin shear panels are shown in Figure 28. All failures were in the tee at the transition of the frame to the padded end fitting. It would have been desirable to force the failure into the repair area. This was impractical, however, since the stresses were lower in the doubled-up repair area than in the surrounding base material. The load levels induced were satisfactory. Failure loads were very high as compared to the ultimate design requirements. Design ultimate shear in the skin was 260 lbs/in. Failure loads induced shear of approximately 830 lbs/in. It was felt that there was little possibility of failing the repair unless the skin buckled and induced high peel loads at the bond edge. This is an unrealistic condition and was not a test goal.

Table 11.—RESULTS OF CONTROL AND REPAIRED PANEL FATIGUE TESTS

Type of specimen	Static failure load, kips		Environmental stress cycles to failure	
	Control	Repaired	Control	Repaired
<u>Skin/frame tee panels</u>				
Tension	6.5	6.0	(5.47)	(5.32)
Shear	27.9	32.0	121	605
<u>Skin/splice panels</u>				
Tension	59.1	60.3	(61.27)	(60.00)

Note: Numbers in parenthesis denote residual failure load in kips after 1000 environmental stress cycles.

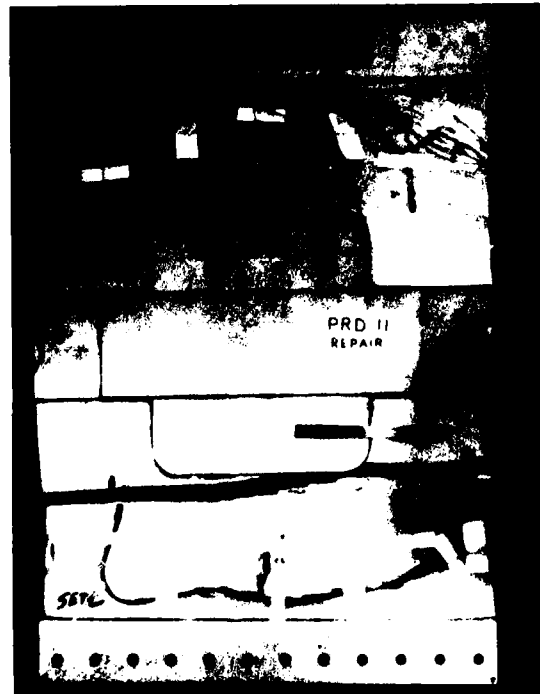
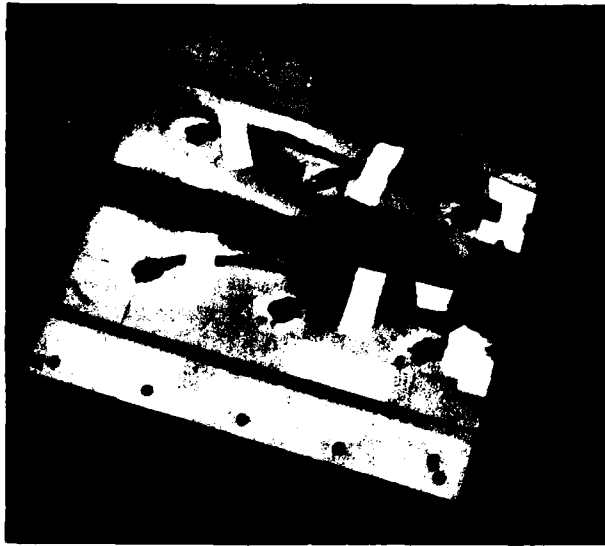


Figure 27.—Typical Failure of a Repaired Skin Splice Panel



a) Unrepaired Control Panel



b) Repaired Fatigue Test Panel

*Figure 28 – Typical Failure of the Frame/Skin
Shear Test Panels*

As noted in Table 11, the repaired frame/skin shear panels had higher static strength and a longer fatigue life. The reason for this can be seen by comparing Figures 28a and 28b. The bonded straps that were used in the repair to splice the frame tee base extended into the loading grip transition region and added a degree of reinforcement to that area.

A typical failure of the frame tee pull-off panels is shown in Figure 29. Failure was in the bond with the control specimens giving slightly higher results. The test, as seen previously in Figure 26, induced very high peel loads at the edge of the tee leg. Delamination started earlier in the repaired panel where splice doublers were bonded on the legs. This was because of the greater stiffness of the laminate build-up as compared to the initial tapered leg. A suggested solution is to extend the first splice strap to locally stiffen the skin and thus soften the load transition at that point. This can be seen in Figure 30.

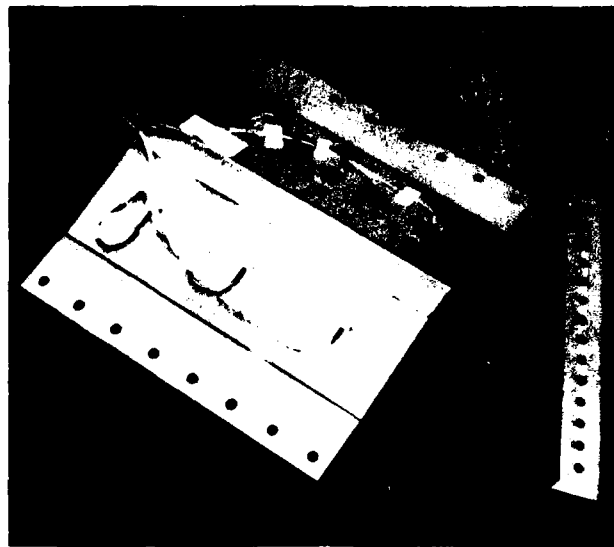


Figure 29.—Typical Failure of Frame Tee Tension Pull-off Panels

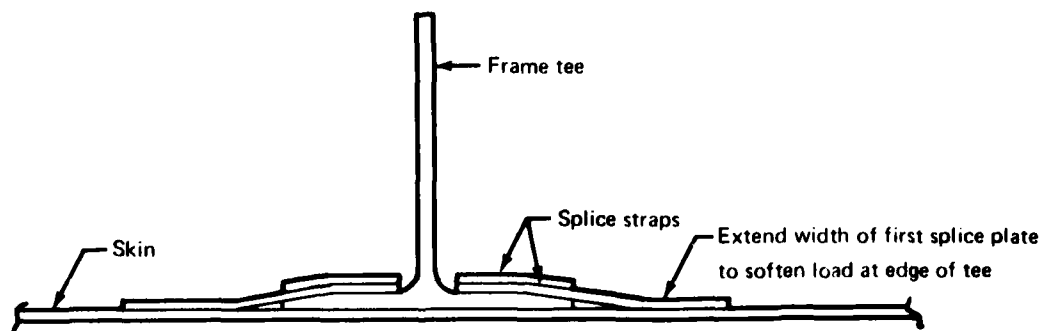


Figure 30.—Extension of Splice Strap Width to Reduce Peel Stresses at Edge of Frame Tee

The panels were progressively non-destructively inspected with a Fokker bond tester during the environmental fatigue cycles. This was done by using the same instrument for each inspection and calibrating it against a prepared standard before taking each set of readings. No indication of bond degradation could be noted with the exception of 2 delaminated areas that developed. One of these was in the repaired frame tee pull-off panel. Some initial delamination was detected under the edge of the spliced tee leg after 350 test cycles. This delamination did not progress during the remainder of the cycling. A second delaminated area, approximately 1.5 by 2.0 in., occurred in the frame tee/skin shear panel. This was noted under the tee in the tapered transition area. This panel failed prior to the next inspection period.

4.4 PANEL TEST CONCLUSIONS

No problems were encountered in using the non-tank phosphoric acid anodize method to accomplish these repairs. All repair bonds were of high quality.

The thickness of the metal for the panels, which were tested in this series, i.e., 0.050 in. to 0.060 in, was such that there was no problem of restoring the initial strength of the "damaged" panels as long as the bondlines of the spliced members were in shear. Conditions where bondline tension or peel stresses are critical, require more attention. It is suggested that where this condition is encountered, stresses be reduced by increasing the base of a tee. Care should also be taken to taper edges to minimize peel and other peak stresses.

The Fokker bond tester was effective for determining bond deterioration as manifested by delamination. It was not effective for detecting general degradation when the bondline remained intact.

5.0 DEMONSTRATION OF LARGE REPAIRS

The coupling of this program with the PABST contract has provided an excellent opportunity to develop and demonstrate large repair techniques for primary structure.

The PABST design and analysis results have been effectively utilized as baseline data. Relating this program to PABST has had additional advantages in providing a design representing structure that incorporates the most recent advancements in bonding technology. It has also been cost effective in providing the use of test hardware surplused from the PABST program, for repair demonstration.

In consideration of the trend to increase the use of structural bonding, the technology necessary to provide bonded repairs suitable for use on primary structure has been noticeably lacking. Repair methods are available for secondary components; however, the requirements of these repairs have not been sufficiently demanding to meaningfully apply this experience to primary applications. The differences are (1) the greater emphasis of primary structural design on reliability; (2) primary structures are typically much more highly loaded and must meet rigid requirements in regard to fatigue resistance and damage tolerance.

Current use of bonding in secondary applications is typified by wing trailing edge structure. These components are usually stiffness designed and the skin thicknesses are selected by minimum gage criteria. These are commonly 0.012 in. to 0.016 in. thick. Repair patch material is equally light and the bondline stresses are low. Quality of the repair is primarily a matter of economics. If the repair fails, safety of the aircraft is not threatened and the repair procedure must simply be repeated.

By contrast, primary structure typically utilizes much thicker gage material and the stress levels are much higher. Failure of the repaired component, if not the repair itself, will endanger the safety of the aircraft. These conditions, which will be encountered by the primary application of bonding, are adequately represented by the selected PABST fuselage component and its design criteria. In contrast to the minimum thickness skin gages for the described secondary structure, the skin gages for the PABST design range from 0.050 in. to 0.080 in. The bondline stresses are high. Additionally, the component provides many of the detail design, and hence repair situations, that may be encountered in an actual bonded fuselage.

5.1 DESCRIPTION OF THE BASELINE STRUCTURE

The structural configuration of the PABST fuselage is a combination external/internal longeron design concept. The longerons are external on the lower and side fuselage quadrants. They are internal on the upper quadrant. The longerons on the upper and lower quadrants are close-spaced, 10.25 in. to 12.38 in, while the side quadrant longerons are wide-spaced at 70 in. The basic frame spacing is 24 in. Intermediate frames having lesser height are additionally provided in the shear critical areas of the wide-spaced longerons.

A drawing showing structural details at a representative upper quadrant frame/longeron intersection is given in Figure 31. This particular location (Body Station 655) contains a longitudinal skin splice. The frame tee is bonded to the skin and longeron and splice plates are riveted. The inner rows of rivets are typically at 1.06 in. spacing. Spacing of the outer row of rivets for the wider internal splice plate is at 2.12 in.

The configuration of the intermediate frame used for the side quadrant is shown in Figure 32. A typical lower quadrant detail is shown in Figure 33. Dimensions are also given in the figure for the bulb tee external longeron. Except at the longitudinal splices, the longerons, as well as the frame tees, doublers and tear straps are bonded to the skin.

The lower fuselage section contains two bonded longitudinal skin splices. These are located approximately at the intersections of the lower and side quadrants. These splices are not at longerons but are double strapped butt joints as shown in Figure 34.

The materials for the PABSI program were selected based on potential future production application. The skins are 2024-T3. The material selected for the tear straps is 7475-T761. Because of procurement difficulties, however, the frames, longerons, and tear straps for the Douglas/PABSI demonstration component are fabricated of 7075-T6.

All metal surfaces are prepared prior to bonding by anodizing with phosphoric acid and then priming with BR127 corrosion inhibiting adhesive primer. Bonding is done with FM73 adhesive which cures at 250°F. The laying surfaces of the riveted joints are coated with PR1422 sealant prior to assembly.

5.2 SELECTION OF REPAIR DEMONSTRATION AREAS

Early in the program, meetings were held with the Air Force/Douglas PABSI team to discuss the objectives of the program and to select critical areas on the PABSI structure for repair demonstration. It was agreed that the repairs would be defined only for the basic structure and would not include special cases such as cut-outs for doors, etc.

Two demonstration areas were selected. These included the intersection of a frame/longeron in the crown area and a similar location in the lower quadrant. In the former case, the longeron was internal, passing through the frame. In the latter case, the longeron was external. The selection of these "critical case" conditions additionally gave solutions to less involved repair problems, e.g., where the skin and longeron or only the skin was damaged. Repairs at these locations were also felt to be adequate to demonstrate repair feasibility at a less critical candidate location in the side quadrant. Conveniently, specific points representing these areas were also selected by Douglas as critical analysis check points for the PABSI component. As such, loads and analysis data were available to permit meaningful fatigue and fracture analysis studies. The locations are shown in Figure 35. The "B" and "D" designations correspond to the designations used for these particular points by Douglas.

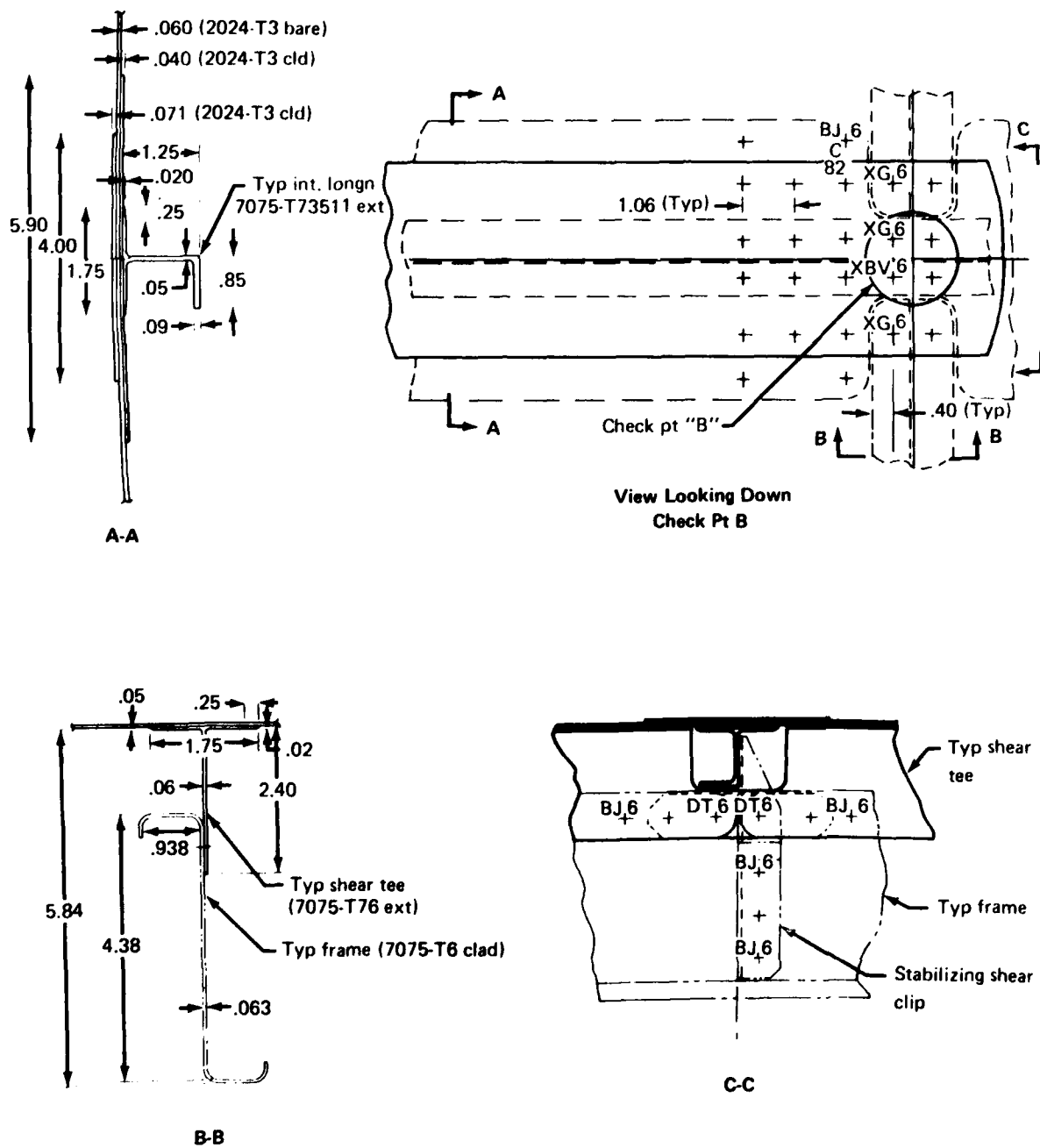
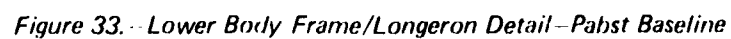
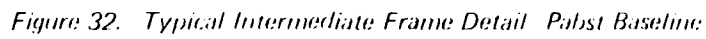


Figure 31.—Details of Upper Quadrant Frame/Longeron Intersection—Pabst Baseline



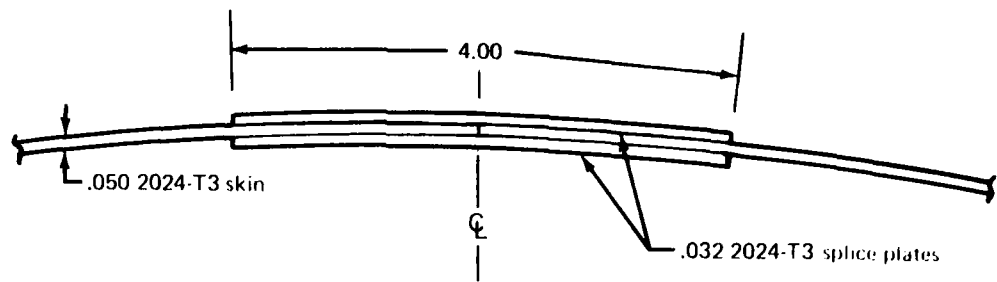


Figure 34. -- Bonded Longitudinal Splice Detail -- Pabst Baseline

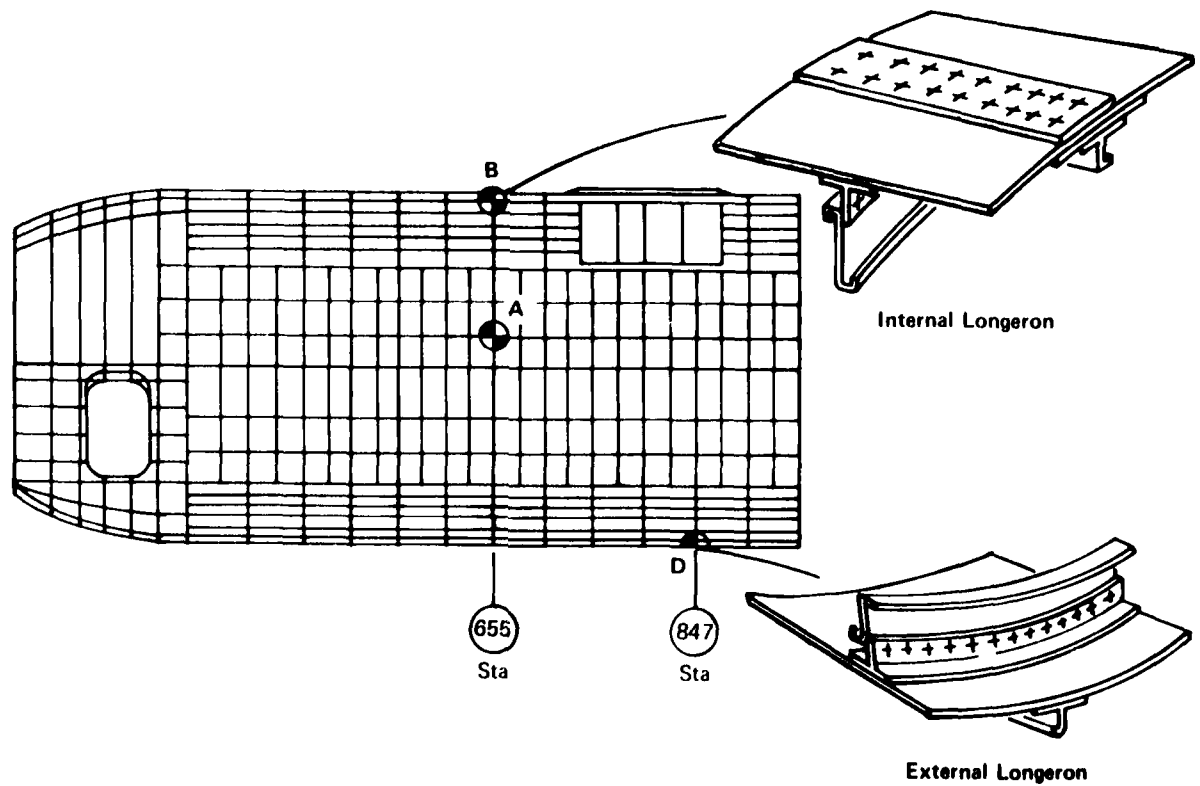


Figure 35. -- Areas on Pabst Structure for Repair Study

5.3 REPAIR REQUIREMENTS AND CRITERIA

The basic requirement for the repair is that the quality be such as to restore the structure to its original, undamaged level of strength and durability. The repair must meet the strength and rigidity requirements of the MIL-A-008860 series specifications. The fatigue life goal including the scatter factor is 30,000 hours with 19,000 pressure cycles. The basic structure is tested to two lives. It must meet the requirements for slow crack growth as specified in MIL-A-83444. In addition, the structure is required to equal DC-10 fail safe quality. This involves sustaining the following damage:

- A two-bay circumferential crack with the center stiffener failed at limit load.
- A two-bay longitudinal crack with the center frame intact but with the crack stopper failed if present at limit load.
- A 15 inch foreign object damage including a cut frame at the lesser of limit or one time maximum stress (20 lifetimes) - 1.5g inertia plus pressure were used for the DC-10.

The sophistication level of repair methods must be compatible with practical repair depot facilities and personnel capabilities. Because of the size of panels, repairs will largely be made on the aircraft. Sizeable repairs will be made at the ALCs. It must also be assumed that repairs of some limited size will be accomplished at the operational base.

Materials and processes will be defined considering practicality for repair depot use. This includes consideration of such items as tolerance ranges, heat-up rates and curing temperatures, working life of the resins, etc.

Minimum repair cost is an important goal. This is in agreement with the Air Force Merit Rating System appearing in the work statement for the PABST structure. This rates minimization of acquisition and maintenance costs as 90% in importance as compared to weight as 10%. The flow time required to accomplish the repair also must be considered. This may or may not be commensurated with cost.

Aerodynamic requirements for the PABST structure are not unduly strict. External repair doublers are allowable as is the use of button head rivets. The edges of external doublers should be tapered to a minimum thickness of 0.032 in. over a length of 0.25 in. The designated minimum skin gage is 0.050 in. This has been established to allow the use of countersunk fasteners and to minimize foreign object damage.

5.4 DESIGN

The general repair design approach has been to remove the damaged area and splice in new material as required to restore the previously undamaged structural strength. Three basic methods of attaching the repairs were considered. These are compatible with repair depot capability and the probability that repairs will be made on the airplane. These methods include the following:

1. Bonding using vacuum bag pressure and portable heating.
2. Bonding using mechanical fasteners for pressure and portable heating.
3. Riveting using an ambient temperature curing interface sealant.

All of these methods were shown to be satisfactory based on a static strength analysis. The subsequent fatigue analysis, however, indicated that the third method was not satisfactory and that structural bonding was required to meet fatigue quality requirements.

Repairs were designed for the two selected crown and lower fuselage locations. These designs were used as a basis for stress and cost analysis studies. They were subsequently demonstrated by performing the repairs on a large Douglas-furnished test panel.

Sketches of the repairs are shown in Figures 36 and 37. Splice plates were stepped to gradually transfer the load and minimize the effect of repair hard spots. Flat details were used where possible, so that they would conform easily to the contour of the curved skin or frame.

Matching stiff formed or extruded details to the frame contour may be a problem with these particular repairs. It is assumed that in actual practice consideration will be given to cutting these sections from stocked spare frame members. If these are not available, forming blocks or special roll forms may be required to fabricate the parts. This is not dissimilar to present requirements for obtaining these sections to repair current fuselage structure.

Rivets are used for the bonded repair in areas where they are used on the basic structure, e.g., for attachment of the formed frame zee to the tee leg. It is expected that the use of rivets will be allowable in some locations where bonded splice plates have increased the effective thickness and substantially reduced the gross area stress. The use of mechanical fasteners, where permissible, may be cost effective in alleviating the more exacting forming or machining tolerances that would be required if the details were to be bonded.

5.5 ANALYSIS

A conventional approach has been used for the static analysis. Load is transferred in or out of splice plates through rivets or adhesive bonds. The adhesive allowable stress has been conservatively determined from the ultimate load versus lap length values obtained from the material evaluation tests. This procedure was discussed previously in Section 4.1. A 2.0 in. splice lap length was used as a minimum length. Longer lap lengths were used as required.

Data was obtained from Douglas to perform fatigue analyses at the two locations selected for repair demonstration. The information package included the baseline structural drawings and the fatigue loading spectra. Douglas also furnished S-N curves for the baseline configuration. This allowed a comparability check of the Douglas and Boeing fatigue life predictions. This check indicated the two analysis procedures were closely comparable.

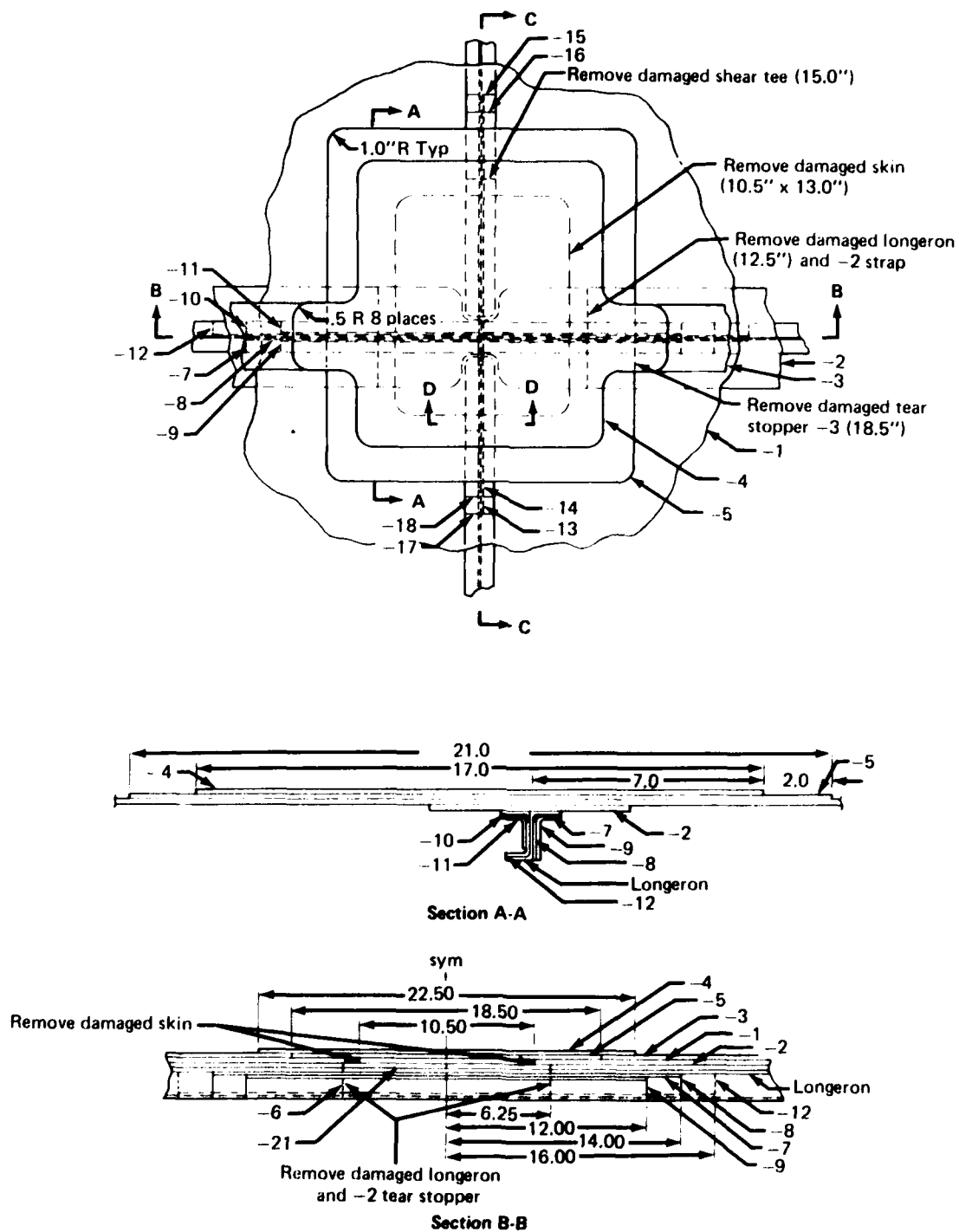
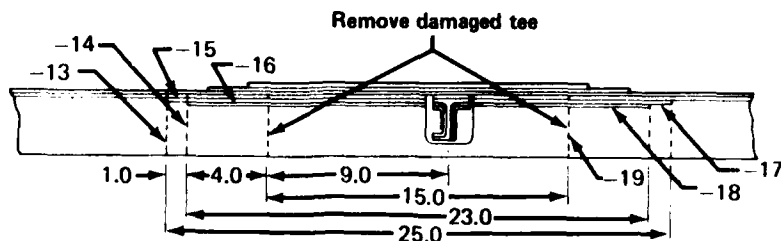
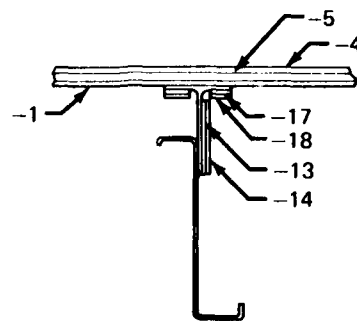


Figure 36.--Checkpoint "B" Repair Internal Longerons



Section C-C



Section D-D

Dash No.	No Req'd	Item	Description	Material
-1	1	Test panel skin	.050	2024-T3
-2	1	Splice strap	.025 x 4.00	"
-3	1	Splice strap	.025 x 3.00	"
-4	1	Splice plate	.025 x 17.0 x 22.0	"
-5	1	Splice plate	.025 x 18.5 x 21.0	"
-6	1	Long. plug	12.5	7075-T6
-7	1	Long. strap	.050 x 0.80 x 28.0	"
-8	1	Long. strap	.050 x 1.15 x 28.0	"
-9	1	Long. angle	.050 x 1.05 x 24.0	"
-10	1	Long. strap	.050 x 0.80 x 28.0	"
-11	1	Long. angle	.050 x 1.05 x 24.0	"
-12	1	Long. angle	.050 x 1.05 x 32.0	"
-13	1	Shear tee strap	.040 x 2.10 x 25.0	"
-14	1	Shear tee strap	.040 x 2.10 x 23.0	"
-15	2	Shear tee strap	.032 x 0.70 x 13.0	"
-16	2	Shear tee strap	.032 x 0.70 x 12.0	"
-17	2	Shear tee strap	.032 x 0.70 x 9.5	"
-18	2	Shear tee strap	.032 x 0.70 x 8.5	"
-19	1	Shear tee plug	15.0	"
-20	1	Skin plug	0.50 x 10.5 x 13.0	2024-T3
-21	1	Tear strap plug	.025 x 4.0 x 12.5	"

Figure 36.-(Concluded)

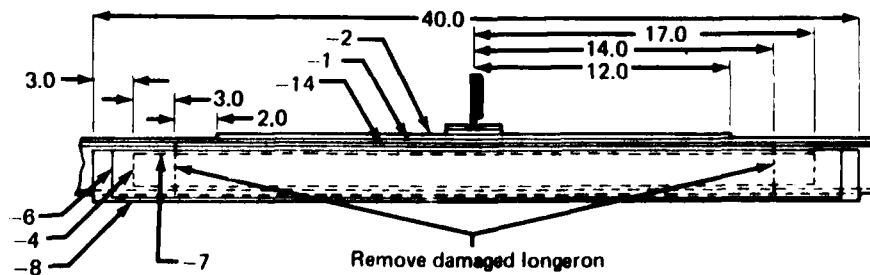
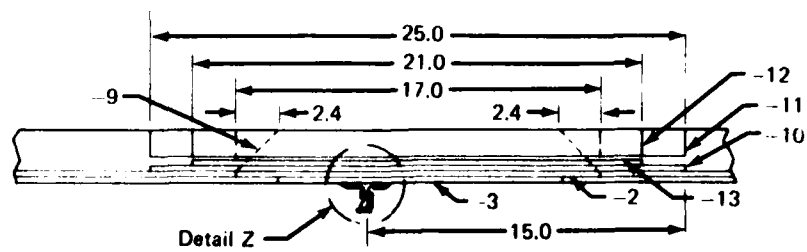
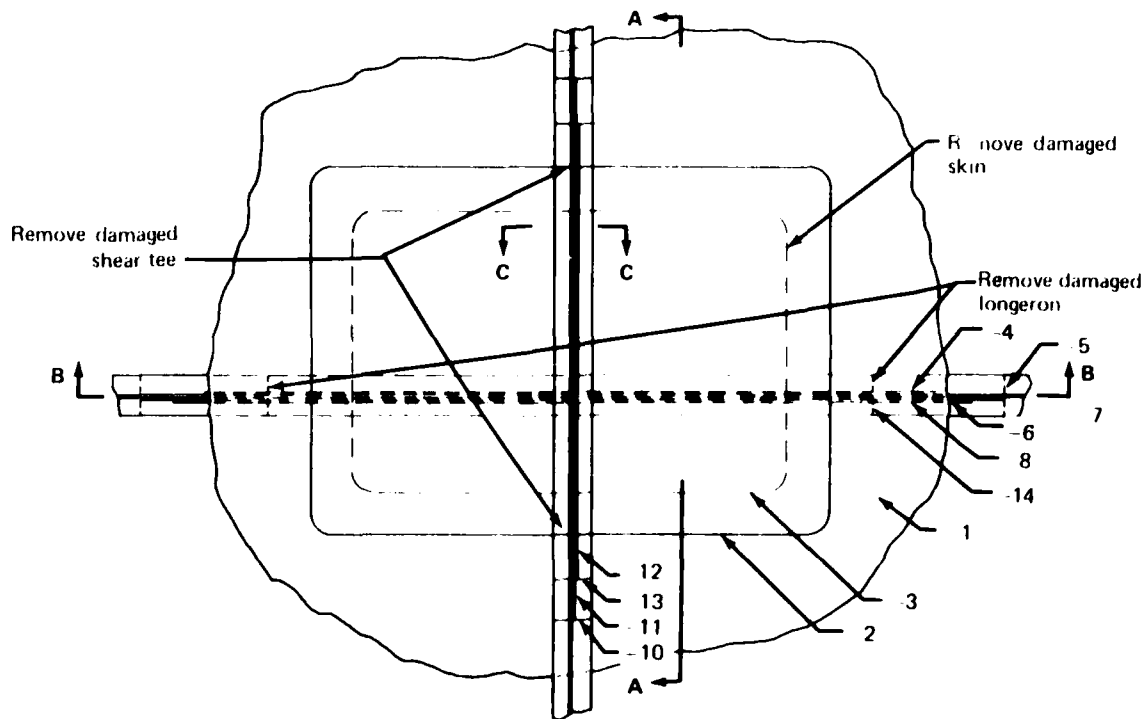
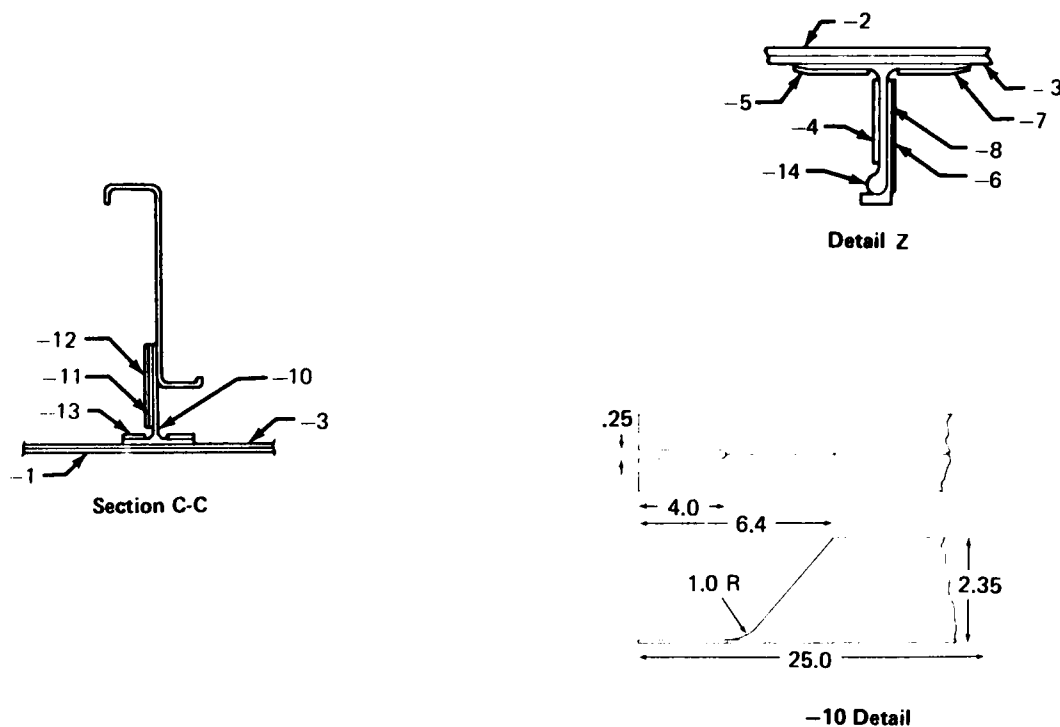


Figure 37.—Checkpoint "D" Repair External Longeron



Dash No.	No. Req'd	Item	Description	Material
-1	1	Existing skin	.050	2024-T3
-2	1	Splice plate	17.0 x 24.0 x .050	2024-T3
-3	1	Skin plug	13.0 x 20.0 x .050	2024-T3
-4	1	Long. strap	34.0 x .45 x .050	7075-T6
-5	1	Long. strap	40.0 x .70 x .050	7075-T6
-6	1	Long. strap	37.0 x .95 x .032	7075-T6
-7	1	Long. strap	4.0.0 x .70 x .050	7075-T6
-8	1	Long. angle	40.0 x .95 x .050	7075-T6
-9	2	Filler	.060	2024-T3
-10	1	Shear tee	25.0	7075-T6
-11	1	Shear tee strap	25.0 x 2.1 x .040	7075-T6
-12	1	Shear tee strap	21.0 x 2.1 x .040	7075-T6
-13	2	Shear tee strap	21.0 x 0.7 x .040	7075-T6
-14		Long. plug	28.0	7075-T6

Figure 37.—(Concluded)

The fatigue analyses of the repairs entailed utilizing the Douglas/PABST fatigue load spectra, Boeing's computerized fatigue program and Boeing's detail fatigue performance charts, and modification factors. The latter were used to determine the fatigue quality level of the repair design details. The procedure was as follows:

1. Representative levels of fatigue quality were assumed for each of the selected repair locations. The Douglas/PABST load spectra for the particular locations were then used with the Boeing fatigue program to produce curves of fatigue quality versus fatigue life. The two curves for the crown and lower fuselage area are shown in Figure 38.
2. The fatigue performance qualities or ratings of the baseline designs and candidate repair methods were determined and plotted on the appropriate curve. These ratings were based on the detail configurations and were obtained from Boeing's detail fatigue rating design charts. The charts provide fatigue ratings for the particular detail design configurations. These ratings are appropriately modified depending on the type of fasteners and hole preparation, material surface treatment, countersink configuration, and such additional considerations as material stack-up and bolt clamp-up effects, etc.

The analysis for the purely mechanical fastened repair was treated conventionally with allowance for the faying surface sealant. In the cases where a structural adhesive was used for attachment and mechanical fasteners were used to apply the bonding pressure, the adhesive bond was designed to take all the transfer load. Load transfer through the mechanical fasteners was considered to be negligible.

The acceptability of the repair methods was measured by requirement that their fatigue life be equivalent or greater than that of the baseline. A comparison of the methods is shown in Figure 38. It was indicated that the purely bonded repairs were acceptable. The bonded repairs with mechanical fasteners were also satisfactory, assuming that the fasteners were in the padded-up areas and nonloading transferring. The mechanical fastened repairs using only an interface sealant were not acceptable.

Crack growth analyses were conducted for structural repairs to the fuselage crown and belly areas (check points B and D). Results of the study showed that both the candidate mechanical fastener/bonded repairs and the purely bonded repairs satisfied the design life requirements. The Douglas structure was designed to satisfy the slow crack growth certification requirements of MIL-A-83444. The Boeing repairs were evaluated using the same slow crack growth certification requirements.

All inputs for the analyses were identical to those used by Douglas in their PABST evaluation studies. The loading spectrum was representative of several different mission types. For example, the spectrum for the crown location contained 111 blocks and 510,376 cycles per 1000 flight hours. The stresses include those induced by typical flight and pressure loadings.

The analysis procedure required a unique approach in order that the Boeing results would be equitable to the Douglas baseline data. The Douglas analysis used the Willenborg crack growth retardation model that was modified to provide a good match between predicted and test results. The Douglas modified retardation model was not accessible to Boeing, but

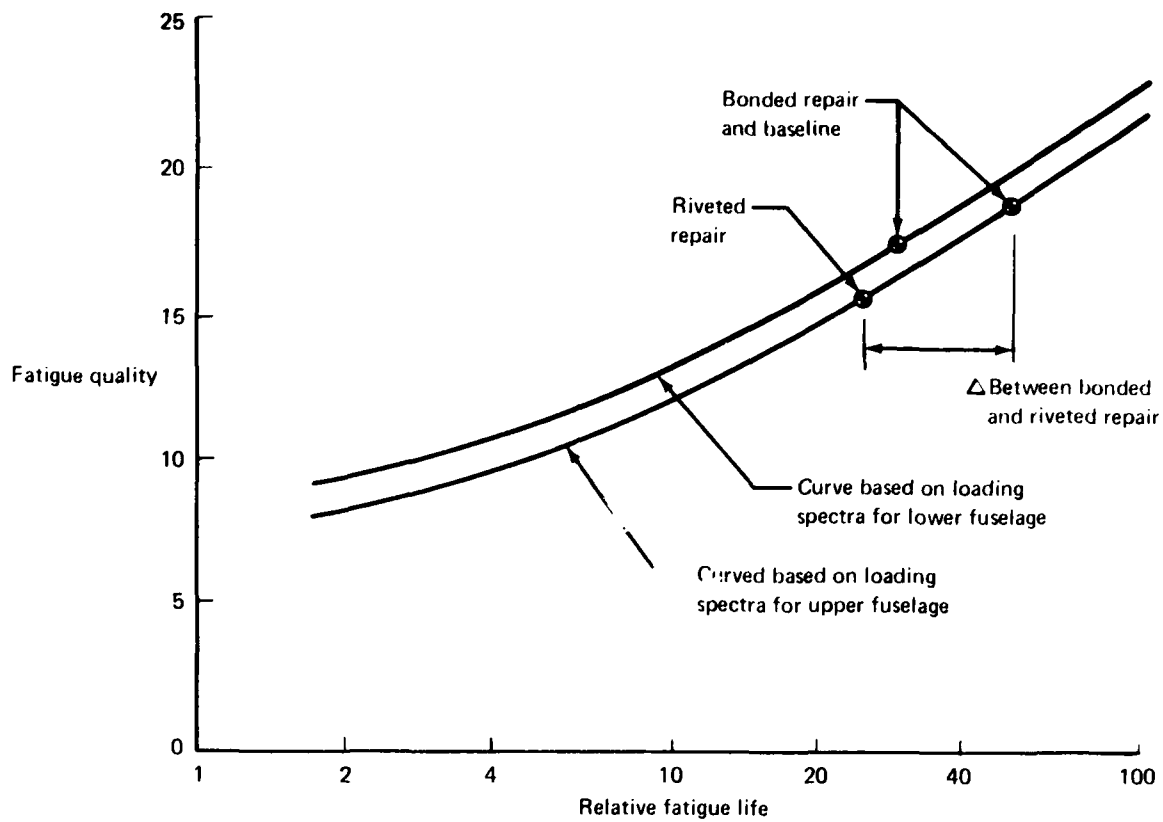


Figure 38.—Comparison Between Fatigue Quality of Repair and Baseline

the baseline crack growth curves (crack length versus time) were provided. These Douglas crack growth curves were differentiated and normalized to a geometry represented by a standard thru-thickness crack in an infinitely wide sheet (i.e., the geometry correction factors were unity for all crack lengths.) Then the crack growth behavior of the repair detail was obtained by integrating this established relationship and correcting for the particular detail geometry. Figure 39 is a comparison of the crack growth performance for an 0.250 in. thru-thickness crack as defined by Douglas and as computed by Boeing. (Douglas has identified the 0.250 in. thru-thickness crack condition as being critical in contrast to an 0.050 in. crack at a hole).

The stress intensity geometry factors for the Boeing repair were generated using the stress intensity factor relationship defined for flaws in holes which was developed by Shaw and presented in ASTM STP 590. These included the finite width and back surface factors. Small flaw effects were not included.

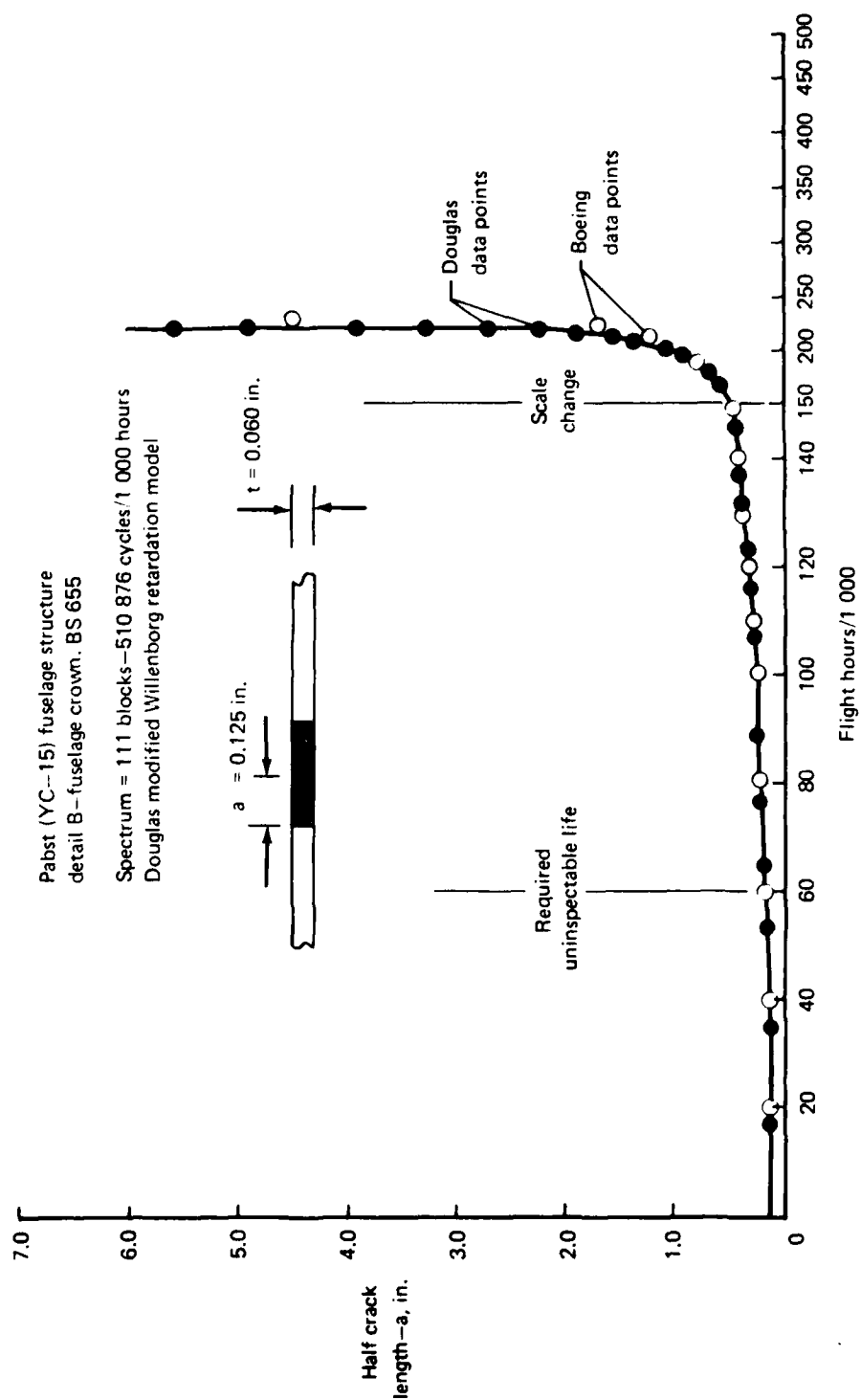


Figure 39.—Comparison of Douglas and Boeing Crack Growth Analysis Results

Geometry magnification factors for flaws located at the edge of fastener holes in representative sheet thickness have been computed (Figs. 40, 41, 42, and 43). These geometry magnification factors were established using the following assumptions:

1. The adhesive was fully effective in distributing the load through the repair splice elements; there was negligible load transfer through the fasteners.
2. The adhesive did not restrict the crack opening displacement in the individual sheets.
3. The load in the crack tip was not transferred to adjacent elements through the adhesive.

These assumptions are considered to be representative or conservative (i.e., lower performance than demonstrated by test).

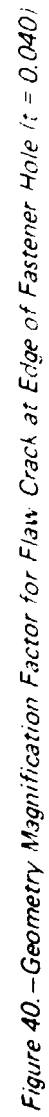
The above factors were used to make a comparison of the crack growth behavior of the Douglas 0.25 in. thru-thickness surface flaw located away from a fastener and an 0.050 in. corner hole flaw at a "no load transfer" fastener in the repair area. This is shown in Figure 44. MIL-A-83444 permits consideration of a smaller flaw ($a=0.125$). The higher stress intensity resulting from the fastener causes the hole flaw to initially grow at a faster rate. This trend is followed until the crack grows out of the direct influence of the hole. At that point the growth rate of the surface flaw becomes greater because it is growing at both crack tips while the hole flaw is growing at only one tip. This comparison shows that the Douglas analysis was correct in selecting the surface flaw as being more severe than a hole flaw.

Figure 45 is the crack growth performance for an initial 0.050 in. hole flaw in 0.060 in. skin material at four fastener areas in the repair design for checkpoint B. Station 1 is in the joint area just outside the repair splices. Stations 2, 3, and 4 are in the repair splice area and differ only by the addition of the repair doublers. The analysis indicated that the repair splice is less critical than the baseline.

The addition of the repair doublers may add sufficient stiffness to pull additional load into the area and thus not provide the projected stress reduction. The limiting case is considered to be that of the doubler elements picking up sufficient load (due to the increased stiffness) to provide no decrease in stress level. In that case, the crack growth performance would be the same as the original basic splice structure (i.e., strain compatibility restraints result in the same gross stress distribution throughout the detail).

Since the critical flaw condition was found to be away from the fastener holes, this analysis is equally applicable to the all-bonded type repair.

The analysis approach for the lower fuselage (checkpoint D) was the same as that used for analysis of the crown; however, only a bonded repair was analyzed.



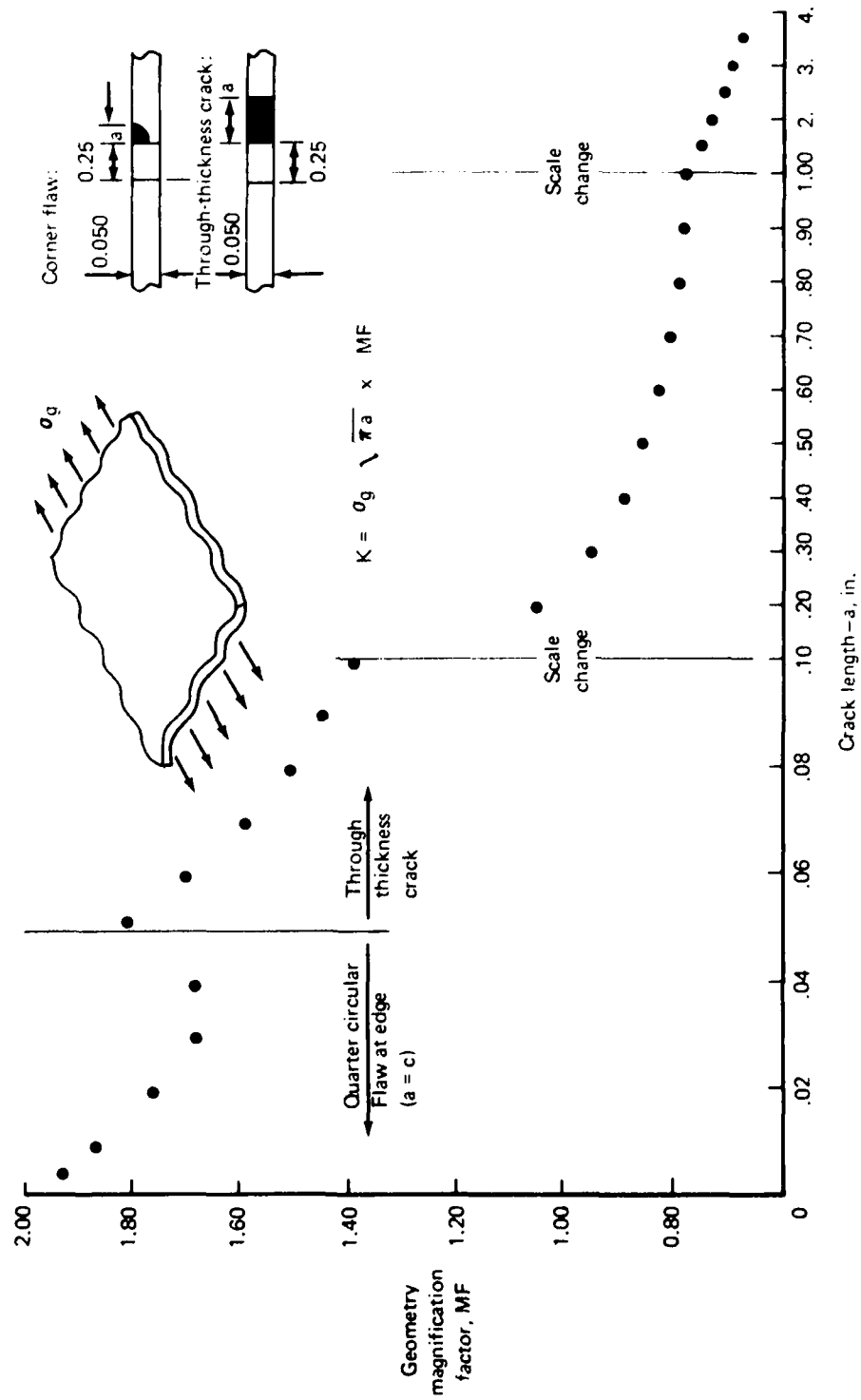


Figure 41.—Geometry Magnification Factor for Flaw Crack at Edge of Fastener Hole ($t = 0.050$)

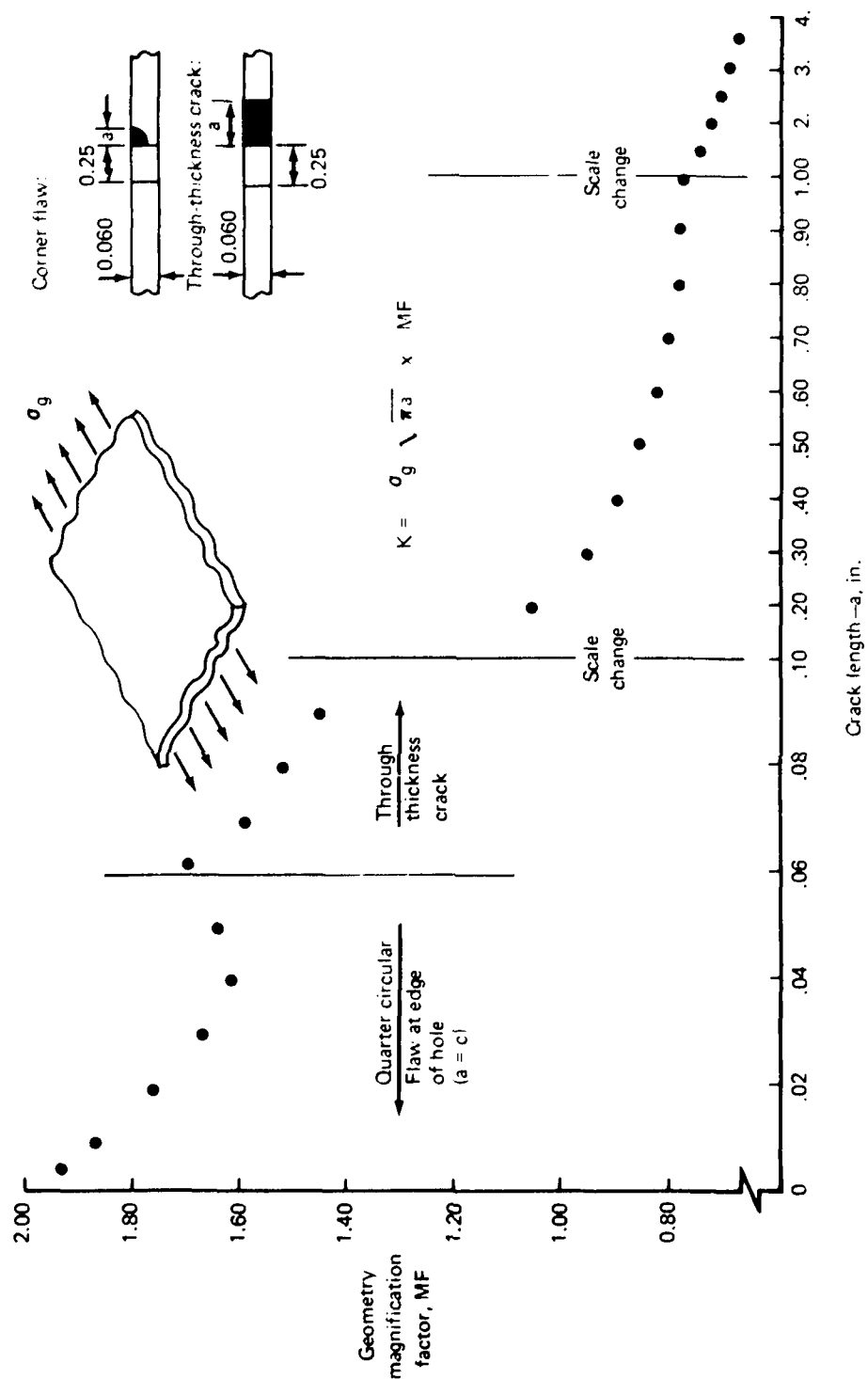


Figure 42.—Geometry Magnification Factor for Flaw Crack at Edge of Fastener Hole ($t = 0.060$)

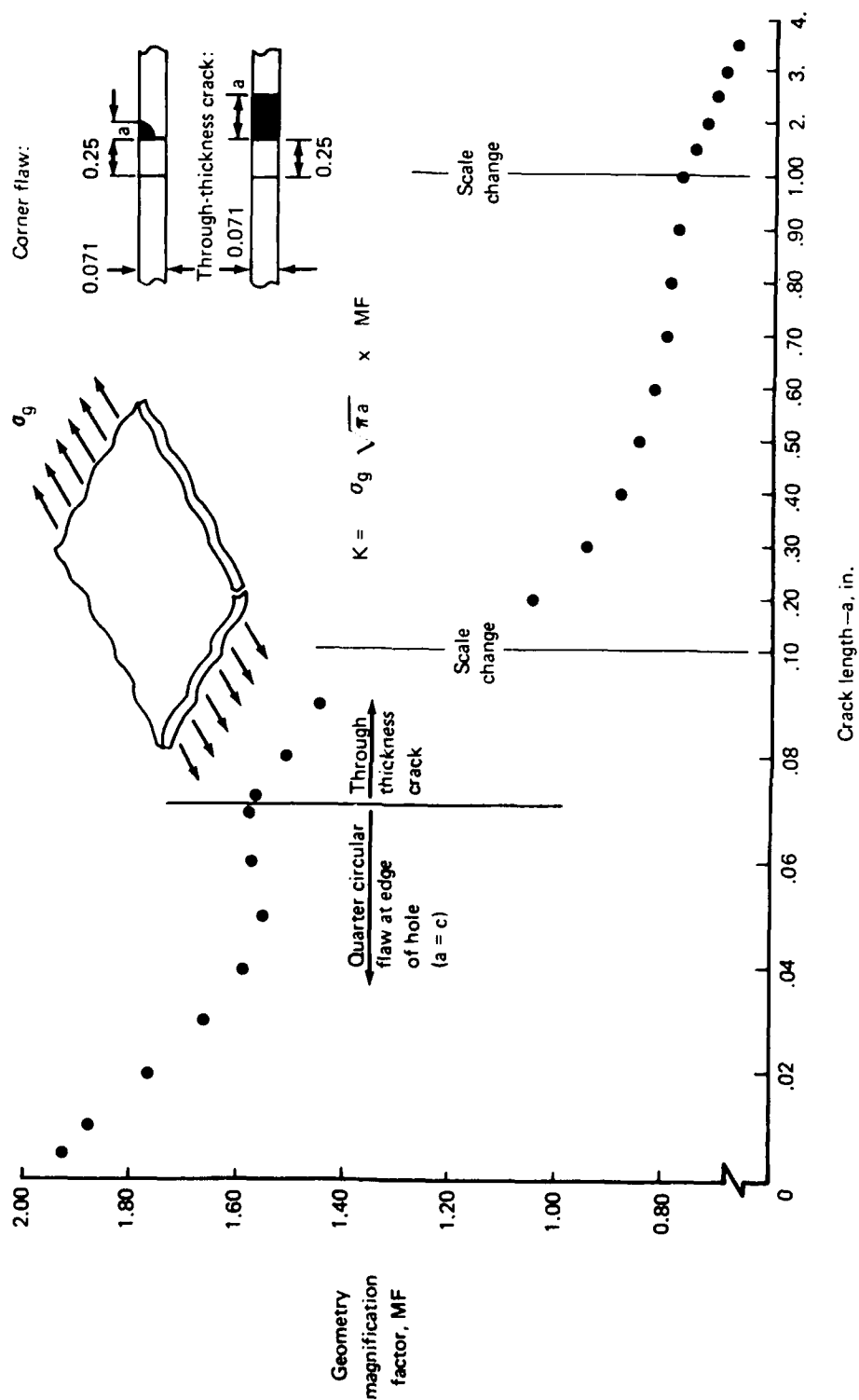


Figure 43.—Geometry Magnification Factor for Flaw Crack at Edge of Fastener Hole ($t = 0.071$)

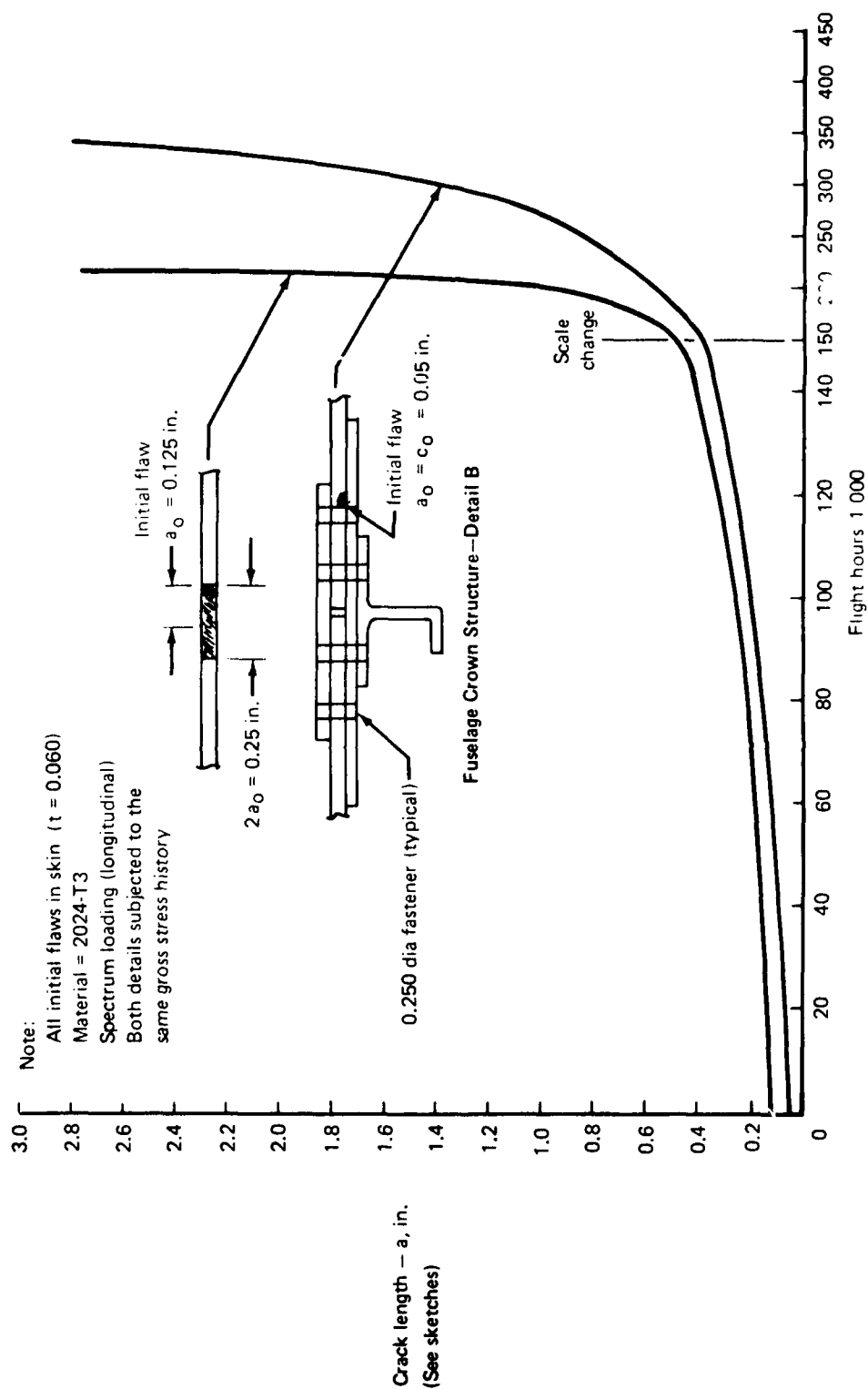


Figure 44.—Comparison of Crack Growth Behavior of Surface Flaw and Flaw at a Hole

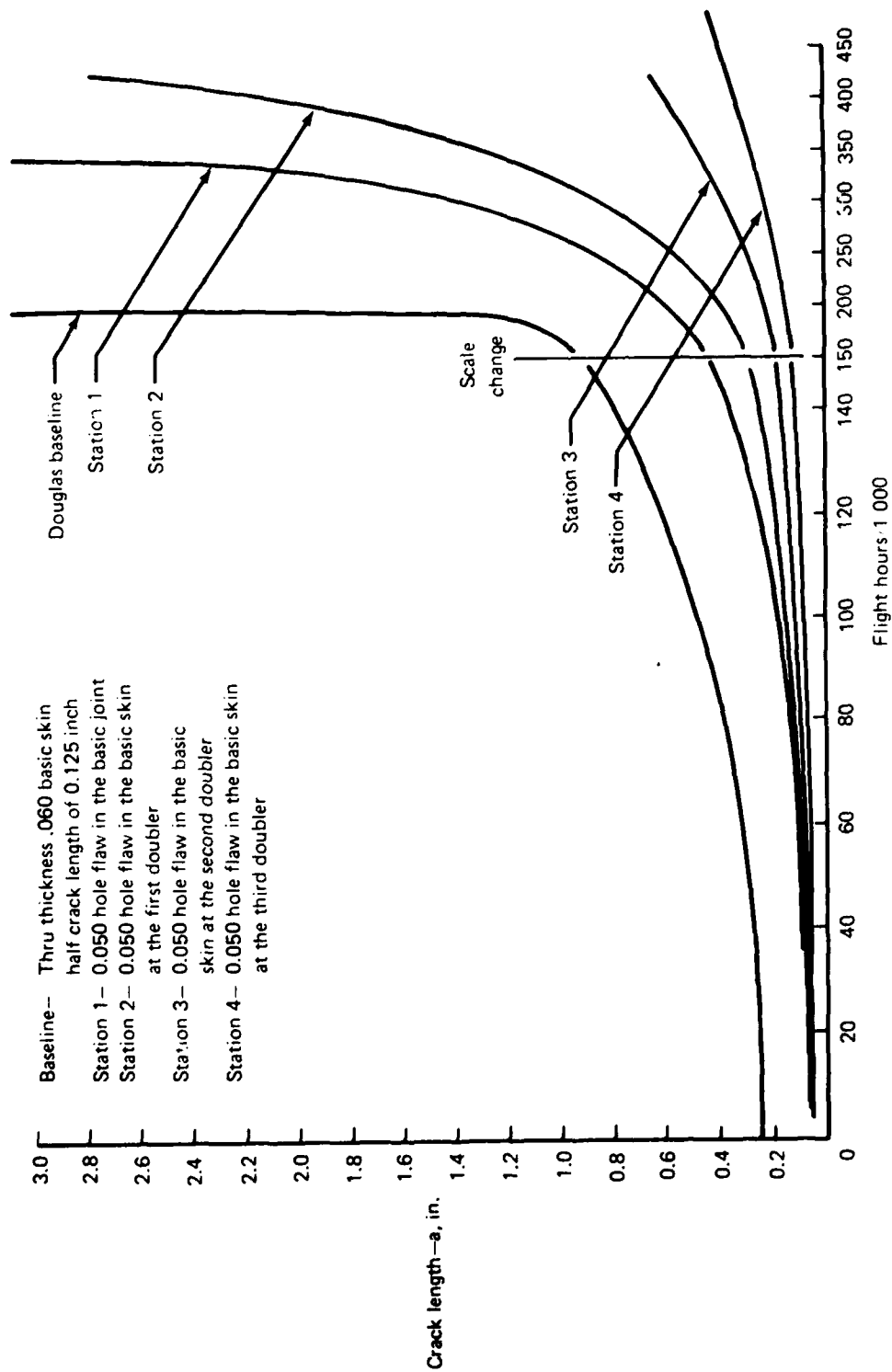


Figure 45.—Corner Hole Flaws Comparison

Crack growth analyses were performed for a flaw located adjacent to and under the bonded repair doubler. These results, and the performance of a flaw in the basic structure, are presented in Figure 46. The flaw located adjacent to the bonded doubler (Location b) had exactly the same load environment as the flaw in the basic structure. The flaw under the bonded doubler (Location c) had exactly the same load environment as the flaw in the basic structure. The flaw under the bonded doubler (Location c) had a 50% reduction in stress level. The crack growth rates of both the b and c locations are less than that of the baseline as shown. In this analysis, no credit was taken for the bonded doubler restricting the crack-opening displacement. This phenomena should reduce the stress intensity factor and result in a lower crack growth rate than that indicated.

The performance of a flaw under the bonded frame repair was also investigated. The Douglas analysis showed that a flaw in the skin between the frames was more critical than a flaw under the frame. In this analysis, it was assumed that the performance of a skin crack under the frame was as bad as that defined by Douglas for the worst possible location. The performance of the repair structure was then computed. A comparison of these two performance levels is shown in Figure 47. The results show that the growth of a flaw in the skin under a bonded repair will not propagate sufficiently to be significant in the design life-time of the aircraft.

5.6 FABRICATION OF THE REPAIRS

During coordination with Douglas, a large PABST pressure test panel (110 in. x 168 in.) was identified on which testing had been completed and which could be surplused to this program. The panel, shown in Figure 48, had been used for damage tolerance testing and had several temporary repairs that had been made to permit test continuity. Adequate areas remained, however, where permanent repairs of a structural type could be demonstrated.

Three areas where repairs could be accomplished were selected. These are shown in Figure 48. The first area was at the intersection of an internal longeron and frame. Pressure for bonding, in this case, was obtained by using mechanical fasteners.

The second repair was accomplished at the intersection of a frame and external longeron. The panel, as received from Douglas, did not have an external longeron. Consequently, a longeron section was fabricated and bonded to the panel.

Both the first and second repairs were made with the panel in the vertical position. Subsequently, a third repair was accomplished with the panel overhead. This involved repair of a frame/skin "damage" location. The repair was less complex than the former two repairs in that it did not additionally involve a longeron. It did, however, adequately meet its objectives in demonstrating use of the hand anodizing process in the more difficult overhead mode.

A more detailed discussion of the repair demonstrations is included in the following sections:

Pabst (VC-15) Fuselage Structure
Detail D—Fuselage Lower Lobe B.S. 823

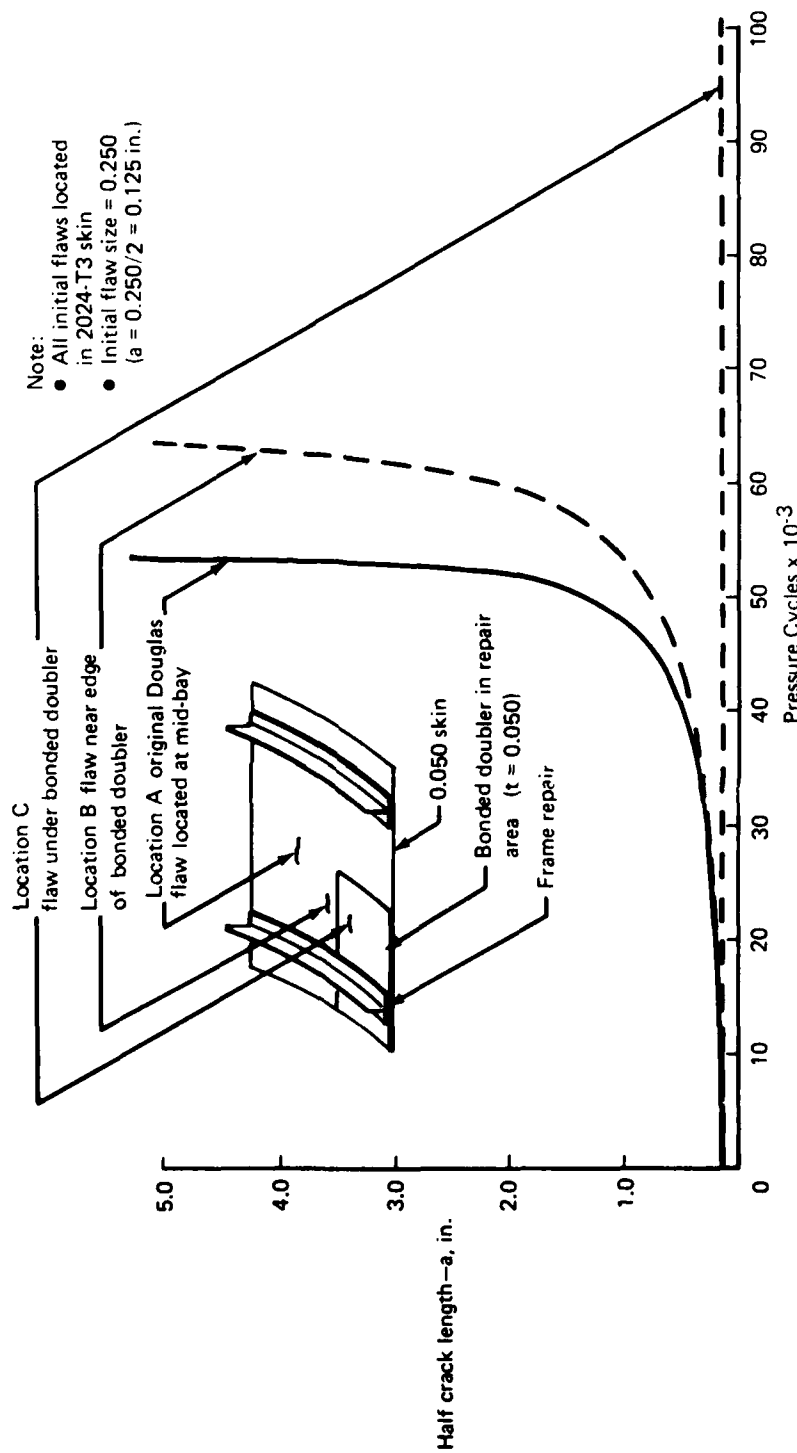


Figure 45.—Skin Crack Growth Behavior Adjacent to and Under Bonded Repair Doubler

Pabst (YC-15) Fuselage Structure
Detail D—Fuselage Lower Lobe, B.S. 823

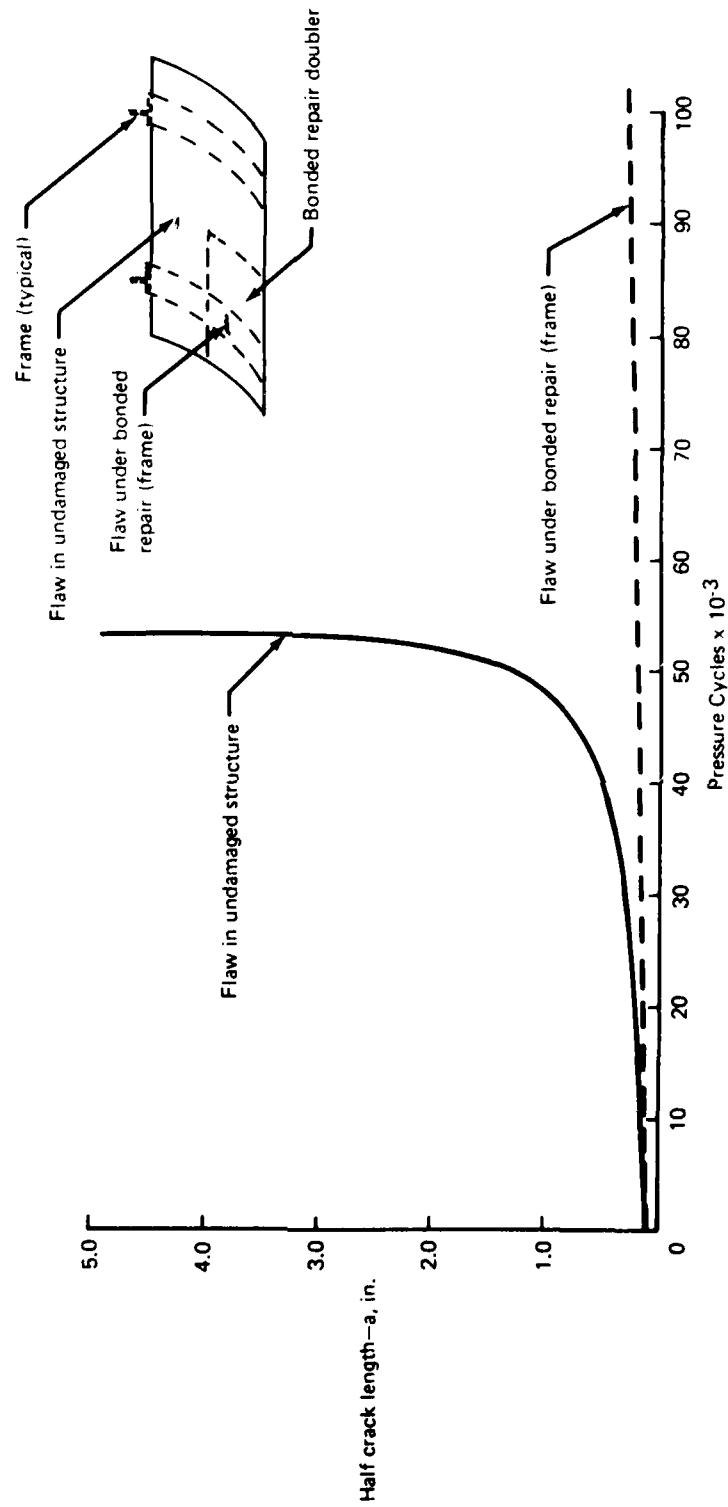


Figure 47.—Skin Crack Growth Behavior in Basic Structure and Under Bonded Frame Repair

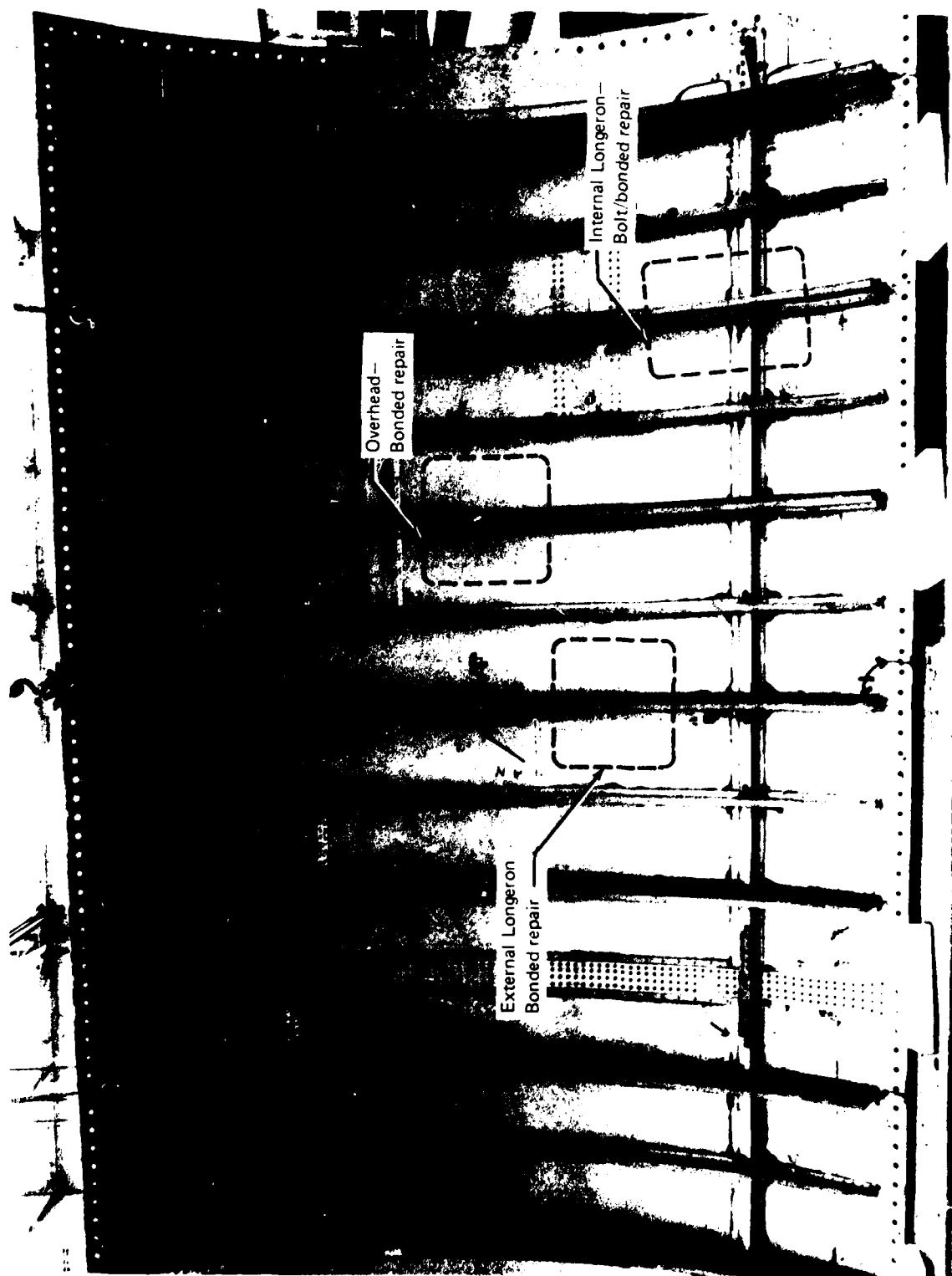


Figure 48. —Location of Repair Demonstration Areas—Pabst Panel

5.6.1 MECHANICAL FASTENED/BONDED REPAIR

During the design and analysis studies, emphasis was placed on defining repairs that had strength and durability equal to those of the original construction. Consideration was also given to procedures that could practically be used at base or depot locations and that would involve minimum cost and time to accomplish.

One method that has advantages is the use of mechanical fasteners to apply the bonding pressure to the adhesive. A factor in favor of this procedure is that, after the parts are assembled, only one curing cycle is required. This is in contrast to more time consuming multiple cycles that might be required if vacuum pressure was used. It also may be difficult to seal a vacuum bag around a complex area such as that having frames and longeron members. Another advantage is the higher pressure that can be obtained with fasteners. This can be utilized to more effectively force parts into intimate bonding contact.

An investigation was conducted before starting the repair to determine if rivets could be used or if a bolt/spring procedure would be required for pressure application. The problem anticipated was that the adhesive would flow out of the riveted joint and relieve the bonding pressure during cure. This was evaluated by curing a laminate using both procedures. Laminates were assembled incorporating six bondlines. This was representative of the repair in the longeron/frame area. The panels are shown in Figure 49. The edges of the two panels are shown after the cure in Figure 50 and the voids between the rivet-bonded plate can be quite clearly seen. The adhesive interface in the riveted panel was porous, indicating that the rivet method was not satisfactory. As a result, the bolt/spring procedure was used for the demonstration repair.

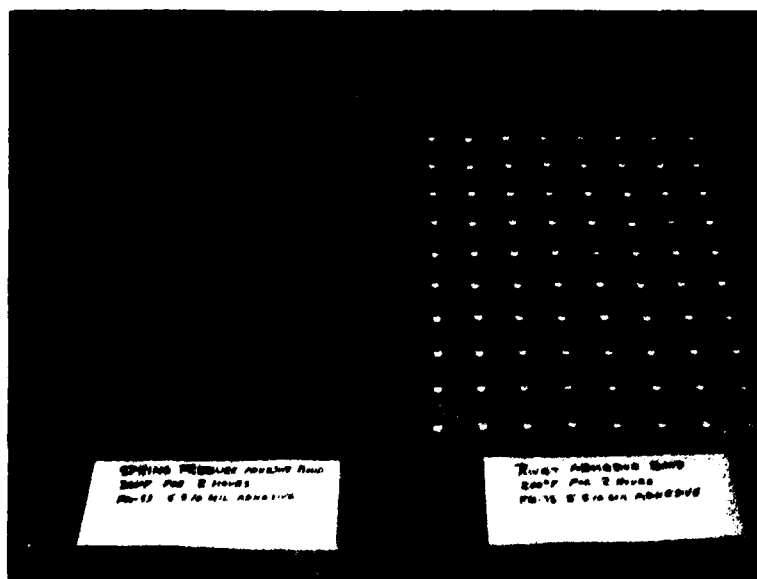


Figure 49. Laminated Panels to Evaluate Rivets Versus Bolt/Springs for Cure Pressure

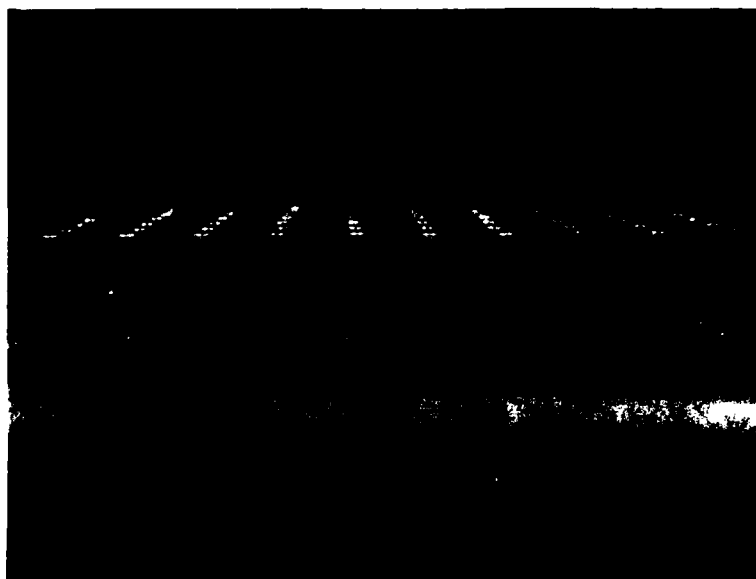


Figure 50.—Edge View Showing Porous Edge of Panel Pressurized with Rivets (Top) as Compared with More Dense Bolt/Spring Bonded Panel (Bottom)

The start of the first repair on the large panel is shown in Figure 51. The riveted rib web was removed. Guide holes were drilled and then a hole saw was used to radius the corners of the cut-out area. Templates were attached to the panel as shown in Figure 52, to act as a guide for the router cuts. The frame tee and longeron were cut back beyond the skin edge to provide a splice overlap for the repair details. Removal of the "damaged" material is shown completed in Figure 53.



Figure 51.—Start of Damage Removal



Figure 52.—Attaching Bar Templates to Guide High-speed Router

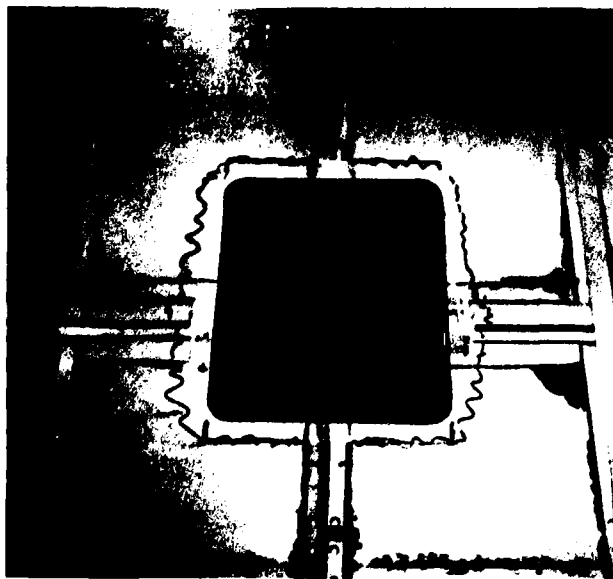


Figure 53.—All "Damaged" Material Removed from Panel

After the "damaged" material was removed, the metal repair details were fabricated. These are shown in Figure 54. They were assembled prior to bonding, i.e., prefit, to ensure proper mating of bond surfaces (see Fig. 55). The details were cleaned and primed in regular production facilities.



Figure 54. --Metal Detail Pieces Used for Repair



Figure 55. Detail Parts Prefit Prior to Surface Preparation and Bonding

The organic coating was removed from the panel areas where the splicing material was to be bonded. This is shown for the back side of the panel in Figure 56. The material around these areas was protective masked with aluminum tape prior to preparation of the bond surfaces. The anodizing process is shown being accomplished in Figure 57. The procedure involved



Figure 56. Organic Removed from Bond Area and Masking Applied Around Periphery

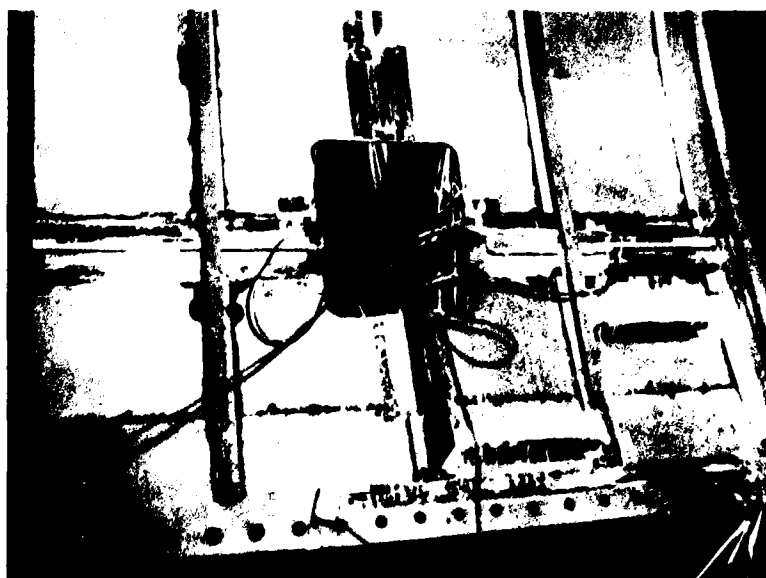


Figure 57. Anodizing the Surfaces to be Bonded

laying several thicknesses of gauze saturated with 12% phosphoric acid paste over the bare metal bond surfaces. A stainless steel screen was embedded in the acid over the gauze; care was taken to prevent the screen from touching, i.e., shorting, to the metal. Electrical connections were made to the screen and to the panel; the screen was connected as the cathode and the panel as the anode. Anodizing was accomplished using a potential of 6 volts dc for 10 min. The current flow was approximately one and one-half amperes.

Immediately following anodizing, the screen and gauze were removed and the area rinsed thoroughly with water. The area was allowed to dry and then inspected. Inspection was accomplished by viewing the surface with a polarized filter. The surface gave an iridescent color, indicating that the anodizing process was successful.

After inspection, the surface was ready for priming. This was done using BR127 corrosion inhibiting adhesive primer. The primer was applied by spraying with a portable Preval unit. Curing of the primer was accomplished using a portable compressed air heating unit and shrouding the area with a plastic tent (shown in Figure 58). The air flow was baffled as it entered the tent to provide even heat distribution. Temperature level was regulated at 200°F for two hours, using thermocouples and a controller/recorder. An overall view of the curing process is shown in Figure 59.

After curing of the primer, the repair details were assembled and location holes drilled. The parts were pinned in position with Cleco fasteners and the remainder of the holes drilled as shown in Figure 60. Following drilling, the parts were disassembled and the holes deburred. The bond surfaces were then wiped with methylethylketone (MEK) and the parts reassembled with the interleaving adhesive film. The bolt/spring system that was used to apply the bonding pressure is shown installed in Figure 61.



Figure 58. Curing BR127 Adhesive Primer with a Portable Compressed Air Heater

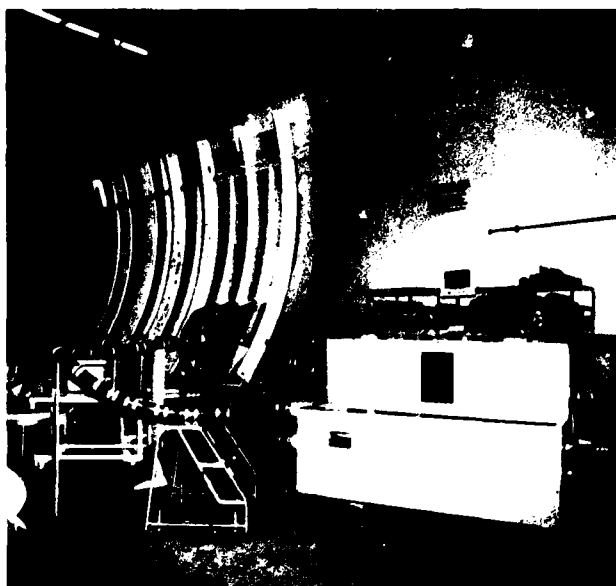


Figure 59. --Overall View Showing Compressed Air Heater and Heating Set-up

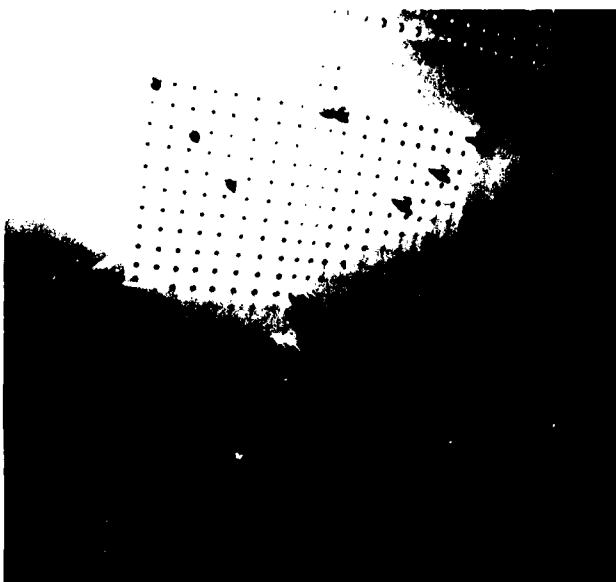


Figure 60. --Holes Drilled in Repair Details Prior to Installing Pressurizing Bolts and Springs

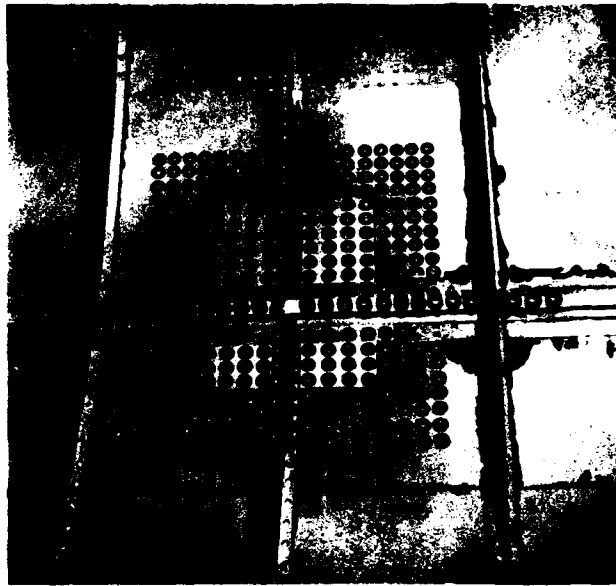


Figure 61.—Pressurizing Bolts and Springs Installed for Cure of the Bond

Curing of the adhesive was accomplished by heating the area at 200°F for 2 hours. This was done with a compressed air heater similar to the procedure that was used for curing of the primer. Heat was applied to both sides of the panel.

After curing, the bolts were removed, the holes reamed, and rivets installed. Completed repair is shown in Figure 62.

5.6.2 VACUUM BONDED REPAIR—EXTERNAL LONGERON

Two tasks were accomplished prior to start of the second repair. (1) One stiffener was bonded to the exterior of the panel. This was a bulb tee duplicating the external longeron design used for the PABST fuselage (Fig. 63); (2) a fiberglass bond tool was fabricated to match the external panel surface. This was subsequently used to maintain the curved surface contour during bonding of the repair details. The tool was reinforced with integral stringers to provide necessary rigidity. Layup of the tool is shown in Figure 64, the tool is shown bagged for cure in Figure 65, and the completed tool is shown in Figure 66. Removal of the "damaged" material with a high-speed router is shown in Figure 67. This procedure was similar for each of the three repairs.

Organic coatings were removed from the surface to be bonded. Aluminum masking tape was applied around these areas as shown in Figure 68. The phosphoric acid anodizing procedure is shown being accomplished in Figure 69. Priming of the surface and curing of the primer are shown respectively in Figures 70 and 71.

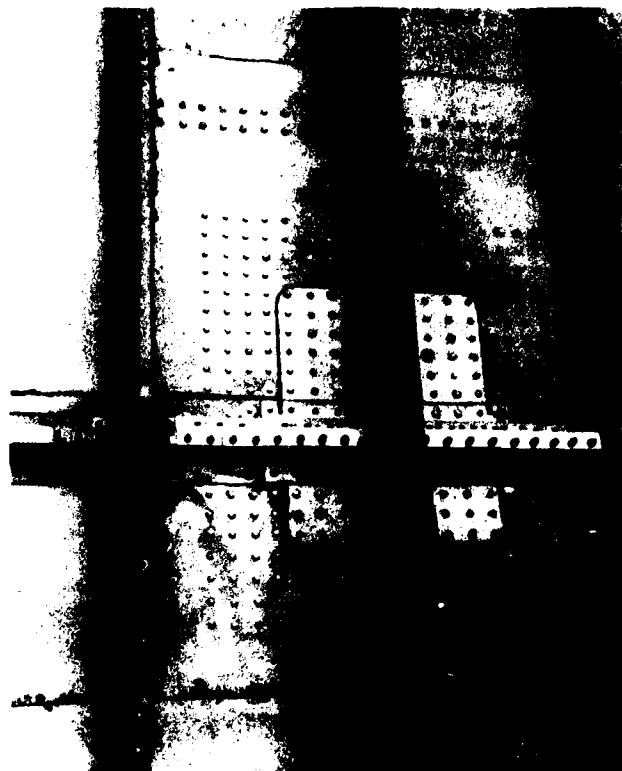


Figure 62.—Repair Complete—Rivets Installed after Removal of Bolts

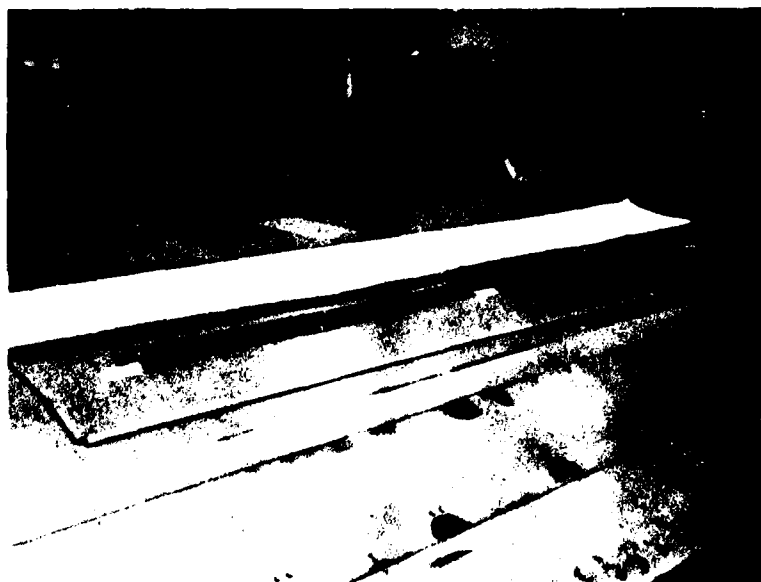


Figure 63.—Bonding an External Longeron on Repair Demonstration Panel

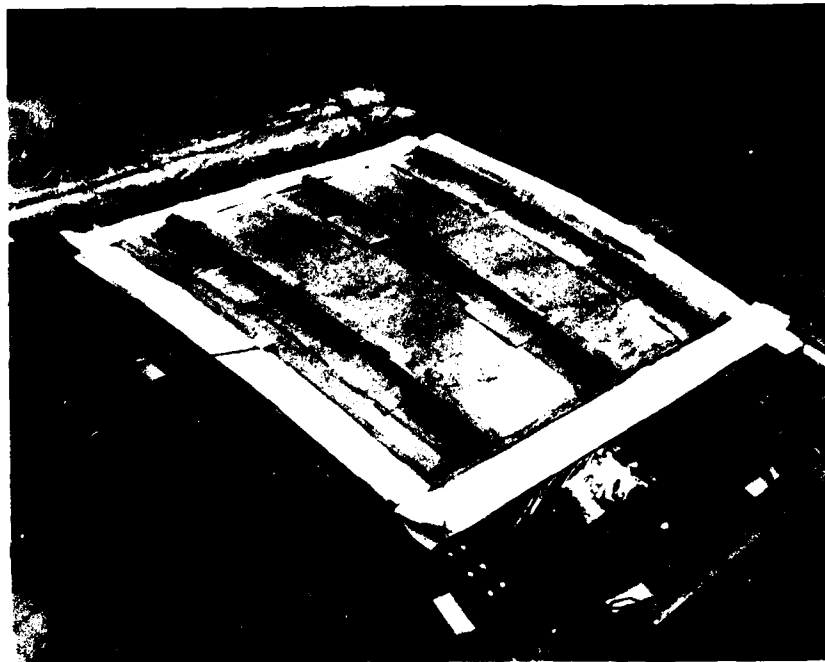


Figure 64.—Lay-up of Fiberglass Tool to be Used to Maintain Surface Contour During Subsequent Repair Bonding

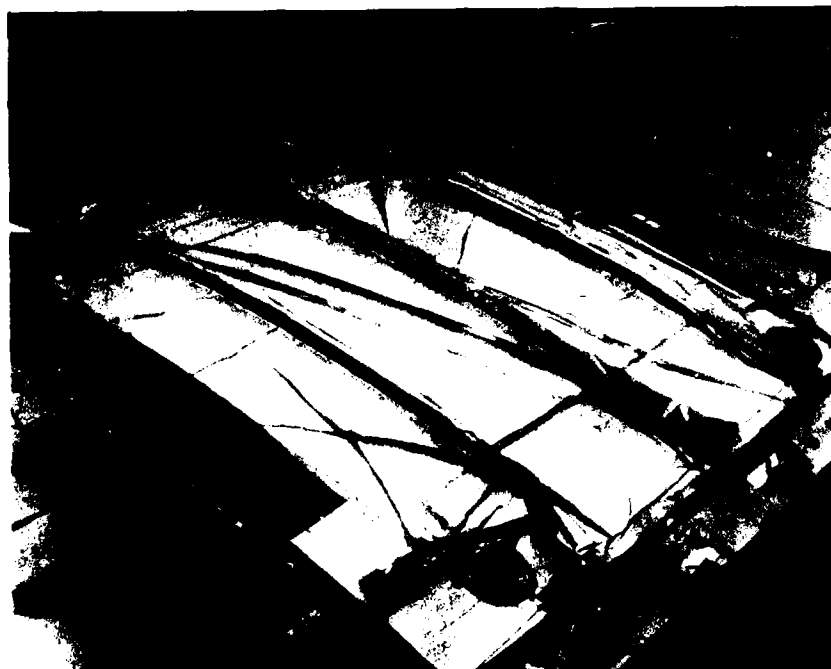


Figure 65.—Curing Fiberglass Bond Tool

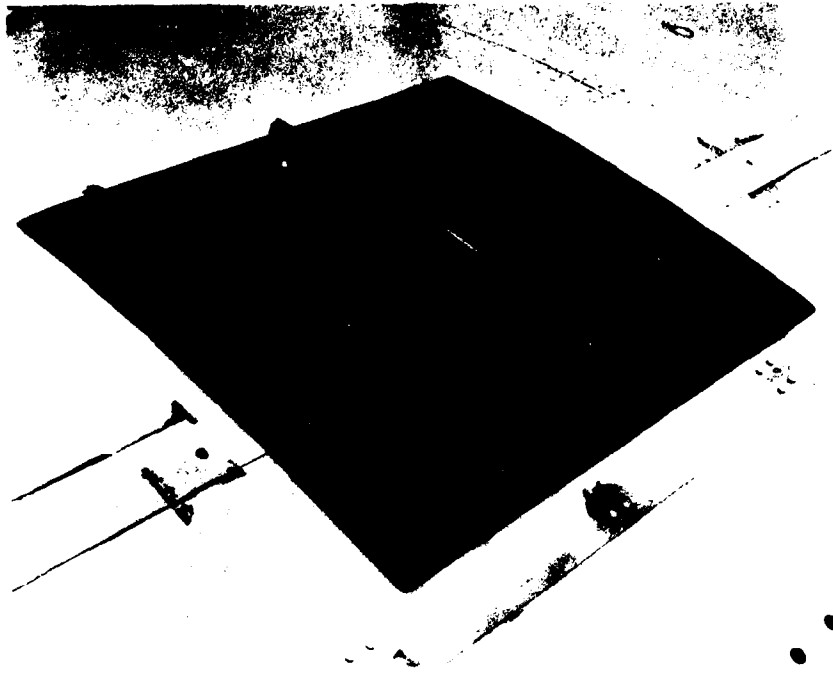


Figure 66.—Fiberglass Bonding Tool—Fabrication Complete



Figure 67.—Removal of Material for Bonded Repair

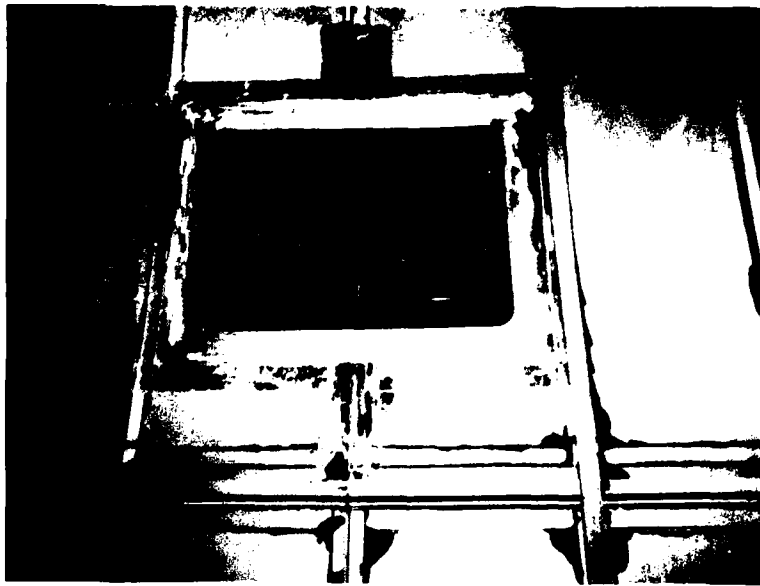


Figure 68.—Bond Area Ready for Surface Preparation



Figure 69.—Phosphoric Acid Anodizing Aluminum Surface to be Bonded



Figure 70.—Spray Application of BR127 Adhesive Primer



Figure 71.—Curing Adhesive Primer

Bonding of the repair details was accomplished in two stages. The skin plug and patch plate were bonded in the first stage. This was accomplished using the fiberglass tool to maintain the contour and a vacuum bag to apply the pressure (Fig. 72). The compressed air heater was again used for the cure. The bond was inspected after the cure using a Fokker bond tester (Fig. 73). The frame tee and longeron splice details were then bonded in place using vacuum pressure and the compressed air heater. The completed repair is shown in Figure 74.

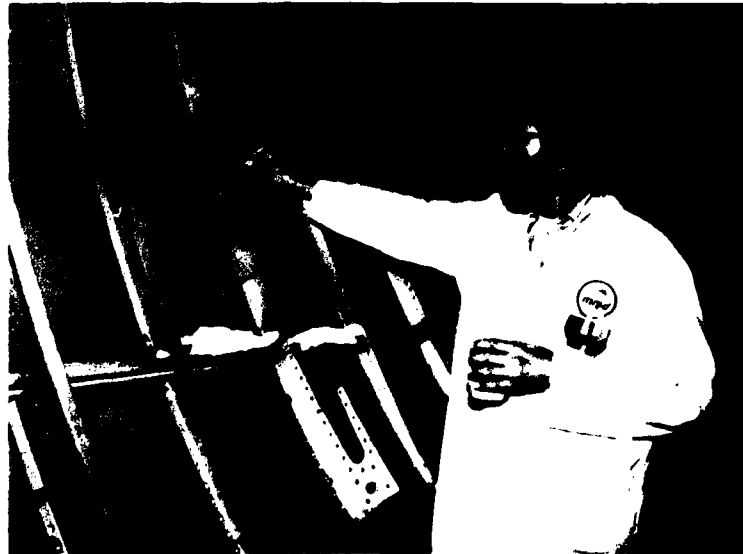


Figure 72.—First Stage Bond of Skin Patch and Plug



Figure 73.—Inspection of Skin Patch with a Fokker Bond Tester

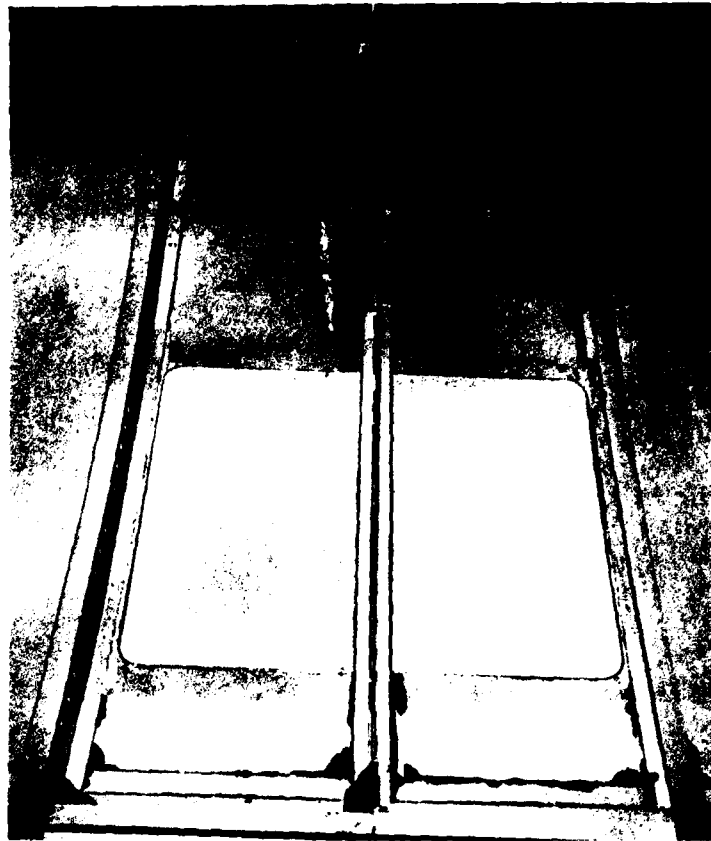


Figure 74.—Completed Repair—External Longeron

5.6.3 VACUUM BONDED REPAIR—OVERHEAD

The primary purpose of the third repair was to demonstrate the feasibility of using the phosphoric acid hand anodizing procedure in the overhead mode. The panel is shown mounted in the overhead position in Figure 75. The repair included a section of the skin and frame tee. The removed material is shown in Figure 76. After removal of the metal, the organic coating was removed from the bond areas and peripheral masking applied.

Since the skin patch was to be bonded to the undersurface, it was necessary to devise a means of keeping the phosphoric acid saturated gauze pressed up against the under surface during anodizing. This was accomplished by placing insulation gauze, the stainless steel screen, and additional gauze saturated with phosphoric acid on an aluminum supporting plate. (The plate was previously roll formed to the panel curvature.) The acid paste is shown being applied to the gauze in Figure 77. The plate was clamped against the panel surface as shown in Figure 78. Leads were attached to the screen and to the panel. Care was taken that an electrical short did not exist between the screen and plate or the screen and panel (evidence of a short would be indicated by a high amperage reading). The anodizing was



Figure 75.—Panel Mounted for Making Overhead Repair



Figure 76.—Material Removed for Overhead Repair

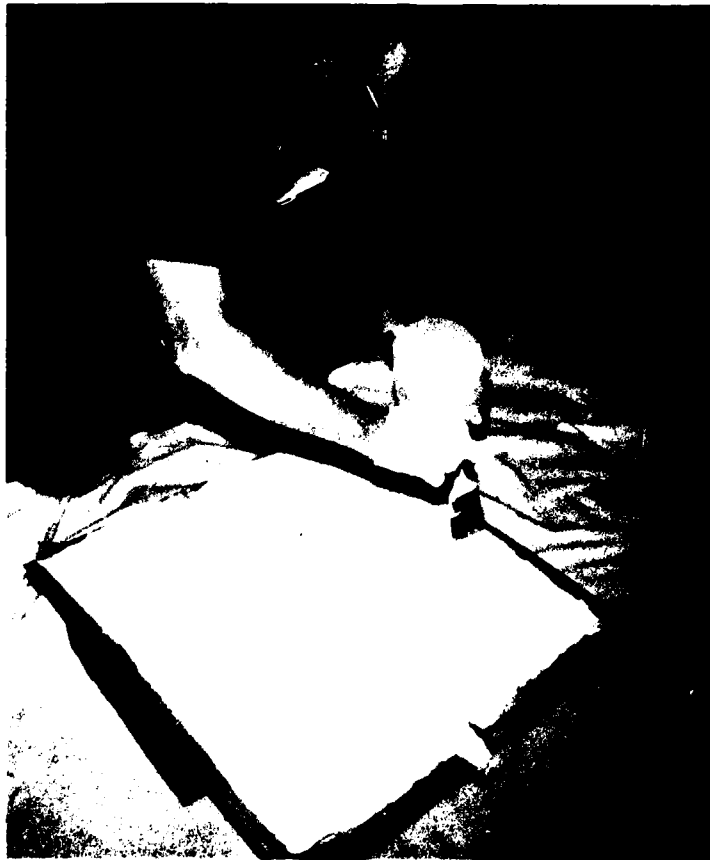


Figure 77.—Applying Phosphoric Acid to Gauze on Plate to be Used to Press Against Lower Surface

accomplished using a rectifier. Six volts were applied for 10 min. After anodizing, the surface was immediately rinsed and dried. Success of the anodize was checked by viewing the surface with a polarized filter. The surface showed an iridescent color indicating that the anodizing had been successful.

Following anodizing, the bond surface was spray primed with BR127 primer. Curing of the primer is shown in Figure 79. The details were then assembled with the FM73 adhesive film. Vacuum pressure was applied and the cure accomplished at 200°F for 2 hours.

This completed the three repairs (Figs. 80 and 81).

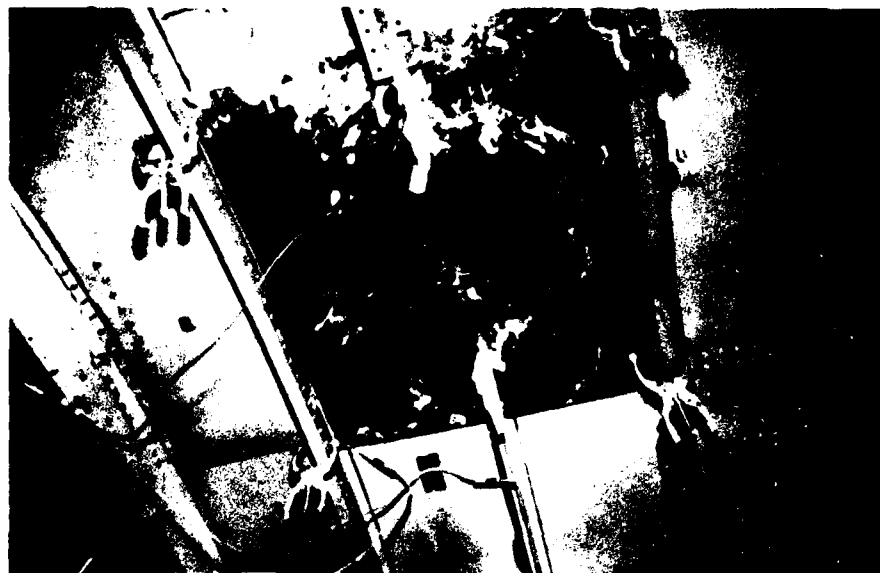


Figure 78.—Plate Clamped Against Lower Surface and Anodizing Clips Attached

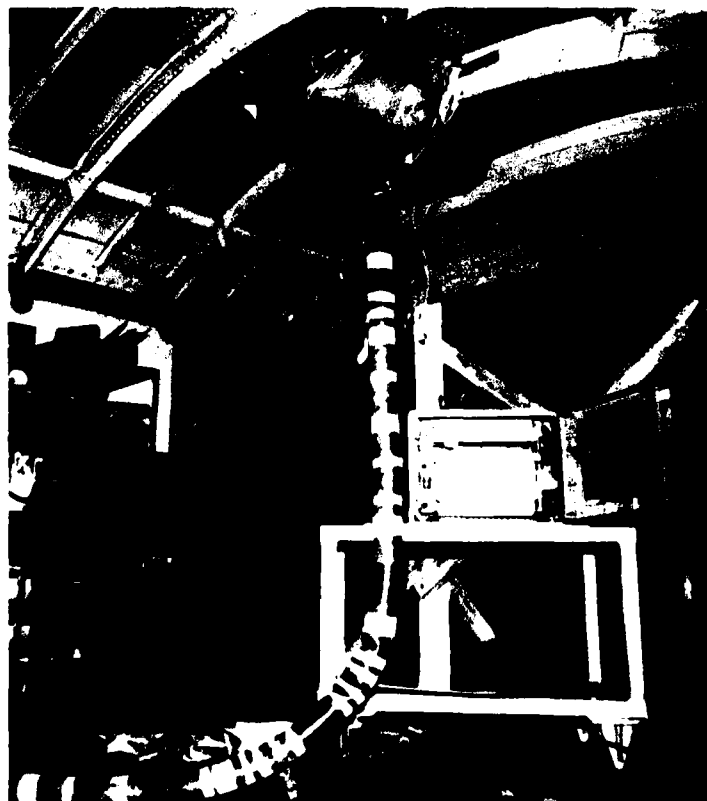


Figure 79.—Curing Adhesive Primer with Portable Compressed Air Heater

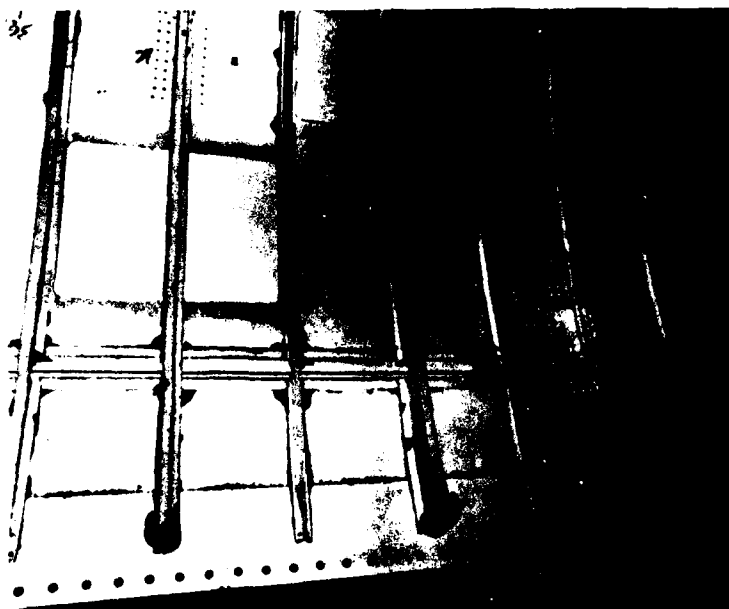


Figure 80.—Interior View of Completed Repairs



Figure 81.—Exterior View of Completed Repairs

5.6.4 POST-REPAIR EVALUATION

Following each of the repairs, the repair was inspected with a portable Fokker bond tester. This represented the type of inspection that is recommended for an on-the-aircraft evaluation. This method primarily determines the presence of voids or delaminations in the bondline. In the case of these repairs, no voids or delaminations were detected.

After all of the repairs were completed, the panel was again inspected. This second inspection was accomplished using Boeing's water-coupled ultrasonic through-transmission unit (TTU). The panel is shown being inspected in Figure 82. The unit can detect much smaller defects than can be found using the portable Fokker instrument. The TTU scans the panel utilizing multiple water jet coupling and a computerized planform printout. Again, as previously, no voids were detected.

Following nondestructive inspection of the repair areas, coupons were cut from the repairs for fabrication of lap shear and wedge specimens. Emphasis was placed on selecting coupons from areas where the bond surfaces had been hand anodized. Locations are shown in Figures 83 and 84. The "L" in the specimen number designation indicates location of a lap shear specimen. The "W" indicates a wedge specimen.

Location of specimens taken from the overhead repair were the same as for the first vacuum bonded repair except that it did not involve the external longeron. The specimens with those number designations, therefore, are omitted, i.e., specimens number 4, 5, 6, and 7.



Figure 82.--Inspection of Repairs with Ultrasonic Water Coupled Through Transmission Unit

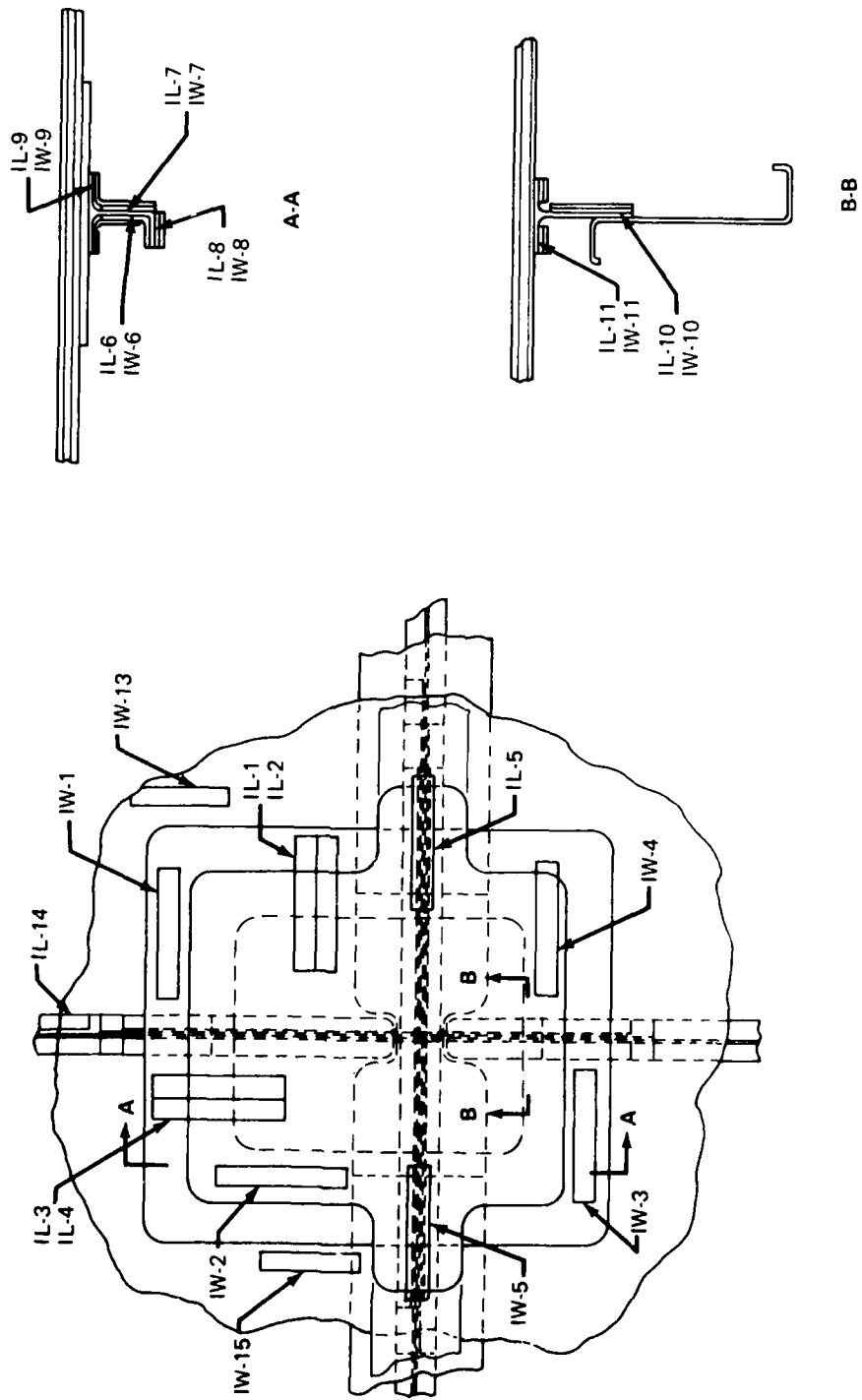


Figure 83. -- Location of Specimens Cut from Internal Longeron Repair

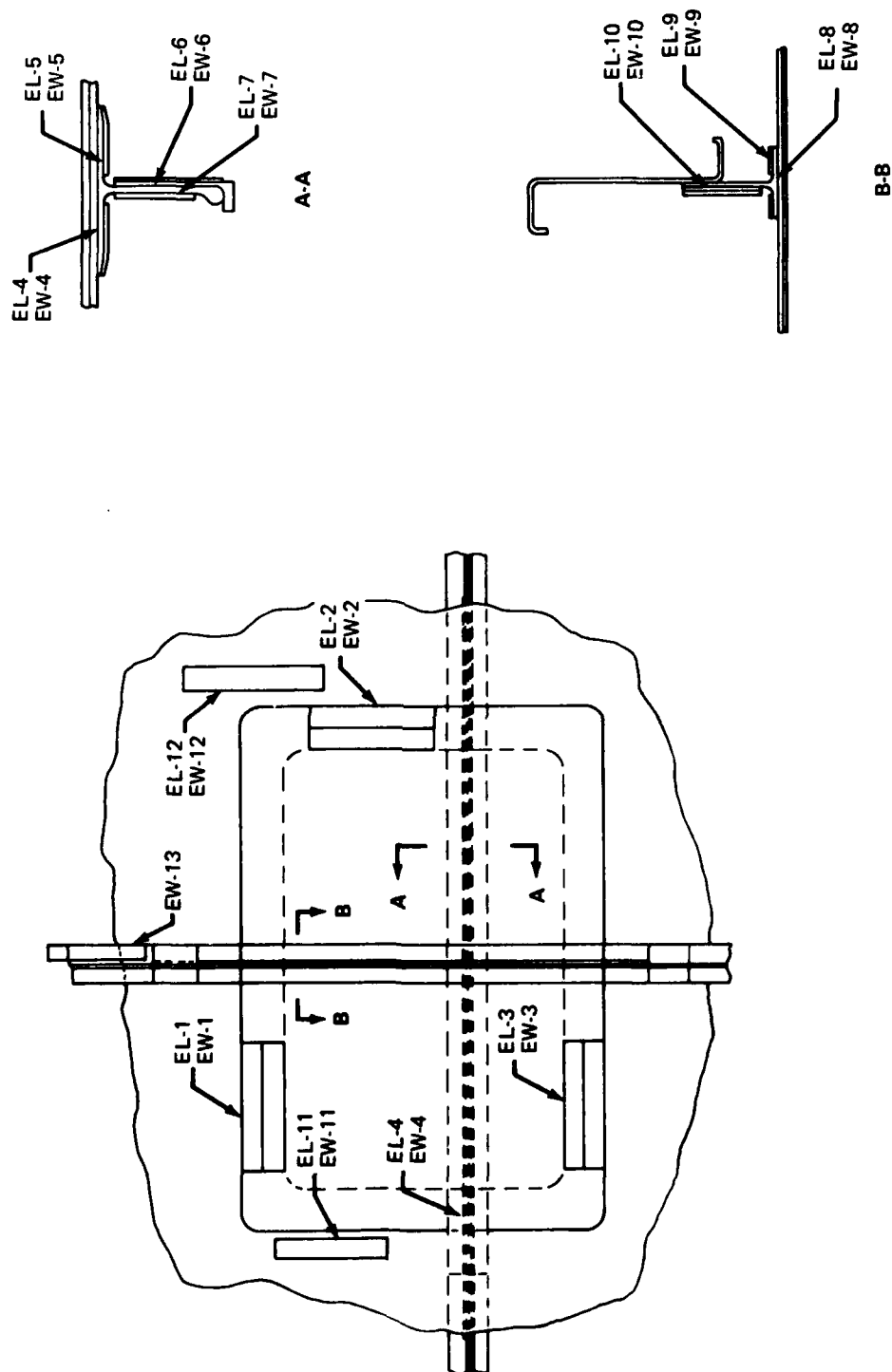


Figure 84.—Location of Specimens Cut from External Longeron Repair

It can be noted that coupons were taken both from the repair and from adjacent areas. The latter were samples of the original bond under the frame tee. The purpose was to see if the adjacent bond had been degraded by the repair and to compare the repair properties with those of the original bond.

Where multiple bondlines existed in the coupons, the proper bondline to be evaluated was identified. The laminate metal thicknesses were measured. Thicknesses of metal were then added or removed to approximate the normal specimen metal thickness of 0.125 in. Sufficient thickness was important for the lap shear specimens to ensure that the metal did not yield during testing. Proper thickness was also important for the wedge specimens since the metal thickness can significantly influence both the initial crack opening and also the residual stress on the bond. This in turn influences the rate of crack growth.

Results of the tests are listed in Tables 12, 13, and 14. The lap shear results were satisfactory. The lap shear values were quite comparable to values that were obtained earlier on laboratory prepared specimens (Ref. section 3). The range of values was also acceptable. Some amount of scatter was expected due to damage that might have occurred during removal of the coupons or in subsequently preparing the specimens. This was especially of concern where rivets had to be removed. This did not develop as a significant problem.

The concerns with the wedge specimen test results are primarily in obtaining an initially high crack opening, a high crack growth rate, or a bondline separation that is adhesive rather than cohesive. Any of these three conditions are undesirable and are indicative of possible unsatisfactory surface preparation.

Photos of the failure surfaces of the wedge specimens are shown in Figures 85, 86, and 87. Although the majority of the failure surfaces are cohesive, six of the specimens have partial

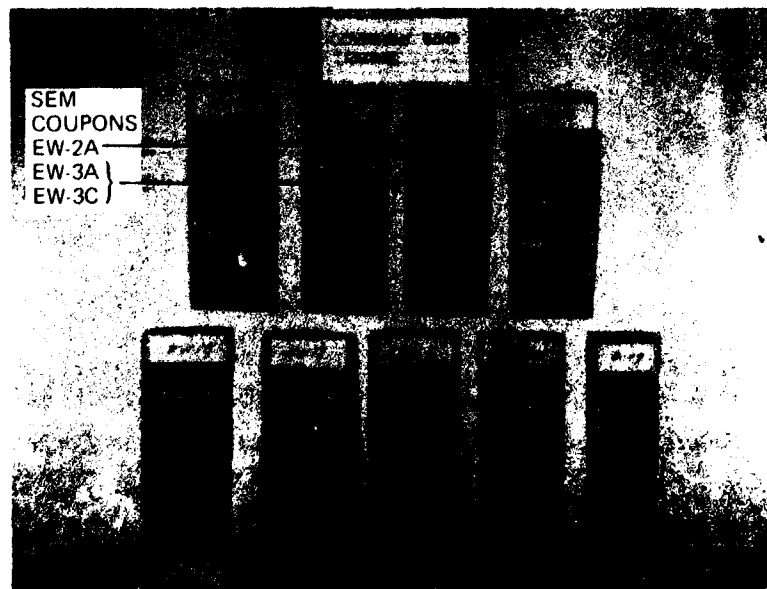


Figure 85.—Failure Surfaces of Wedge Specimens From the Overhead Bonded Repair

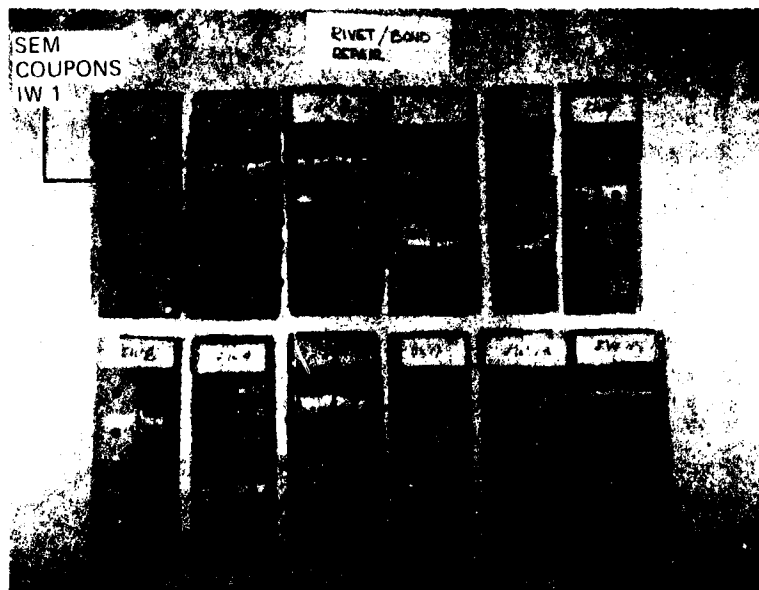


Figure 86.—Failure Surfaces of Wedge Specimens From the Mechanical Fastener Bonded Repair

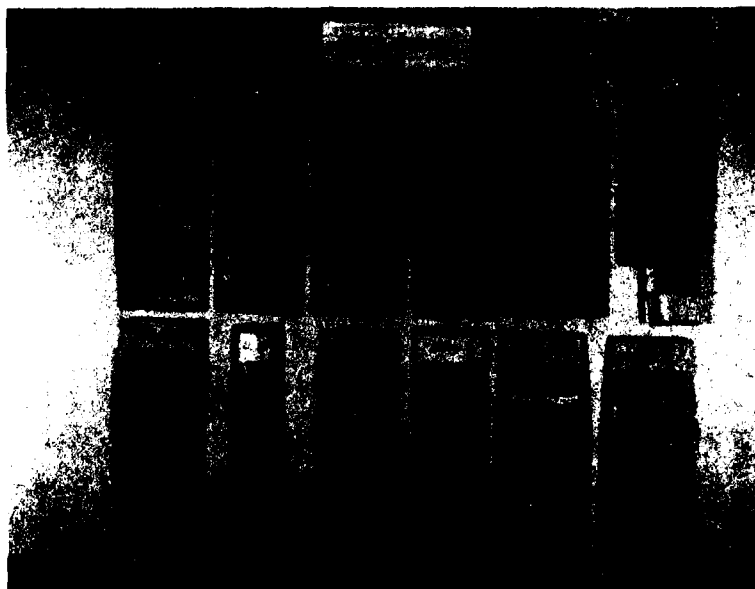


Figure 87.—Failure Surfaces of Wedge Specimens From the External Longeron Repair

Table 12. - RESULTS OF TESTS ON SPECIMENS CUT FROM BOLT/SPRING BONDED REPAIR-INTERNAL LONGERON

Specimen no.	Lap shear at R.T. psi	Specimen no.	Wedge test 120° F/100%RH						Failure mode
			Initial, inches	1 hr	4 hrs	24 hrs	14 days	30 days	
IL 1	5011	IW 1	1.35	0	0	.04	.33	.38	Adhesive
2	3956	2	1.37	0	0	0	.08*	.08	Cohesive
3	5150	3	1.14	0	0	0	.06	.06	Cohesive
4	4356	4	1.34	0	0	0	.11	.11	Cohesive
6	4680	6	1.01	0	0	0	.11	.16	Cohesive
7	4570	7	1.96	0	0	.08	.18	.23	Cohesive
8	4395	8	1.44	0	0	0	.19	.19	Cohesive
9	4632	9	1.44	0	0	0	.11	.11	Cohesive
10	4925	10	1.11	0	0	.04	.09	.09	Cohesive
11	4770	11	1.75	0	0	0	0*	0	Cohesive
14	5346	* 13	1.05	0	0	0	0	0	Cohesive
		15	1.10	0	0	0	.05	.05	Cohesive

Note: Specimens 13, 14, and 15 were taken from the frame tee to skin bond in an area adjacent to the repair.

* Crack jumped to next bondline

Table 13.—RESULTS OF TESTS ON SPECIMENS CUT FROM VACUUM BAG BONDED REPAIR—EXTERNAL LONGERON

Specimen no.	Lap shear at R.T. psi	Specimen no.	Wedge Test 120° F/100% RH							Failure mode
			Initial, inches	1 hr	4 hrs	24 hrs	14 days	30 days		
IEL 1	5216	IEW 1	1.32	.49	.49	.63	.63	.68	Adhesive	
	5333	2	1.35	.99	.99	.99	.99	.99	Adhesive	
	4743	3	2.43	0	0	0	.05	.12	Adhesive	
	4946	4	1.33	0	0	0	.05	.09	Cohesive	
	4767	5	1.34	0	0	.06	.06	.06	Cohesive	
	4700	6	1.24	.09	.09	.09	.18	.18	Cohesive	
	3726	7	2.32	.08	.08	.08	.16	.16	Cohesive	
	3809	8	1.51	0	0	0	0	0	Cohesive	
	4729	9	1.74	0	0	0	.12	.12	Cohesive	
	5081	10	1.15	0	0	.04	.08	.08	Cohesive	
	4947	11	1.09	0	0	.06	.06*	.11	Cohesive	
	4947	12	1.00	0	0	0	0	.05	Cohesive	

Note: Specimens 11 and 12 were taken from the frame tee to skin bond in an area adjacent to the repair.

*Crack jumped to next bondline

Table 14.—RESULTS OF TESTS ON SPECIMENS CUT FROM OVERHEAD VACUUM BONDED REPAIR

Specimen no.	Lap shear at R.T. psi	Specimen no.	Wedge test 120° F /100% RH						Failure mode
			Initial inches	1 hr	4 hrs	24 hrs	14 days	30 days	
EL 1	5025	EW 1	1.52	0	0	.03	.24	.24	Adhesive
2	5151	2	1.51	0	0	.08	.08	.12	Cohesive
3	5236	3	2.60	0	0	0	0	0	Adhesive
8	4160	8	1.42	0	0	.06	.06	.06	Cohesive
9	4341	9	2.17	0	0	0	.23	.41	Cohesive
10	5093	10	1.31	0	0	0	.08	.08	Cohesive
11	4916	11	1.29	0	0	0	.16	.16	Cohesive
12	4932	12	1.20	0	0	0	.04	.04	Cohesive
		13	1.25	.06	.06	.06	.06	.06	Cohesive

Note: Specimens 11, 12, and 13 were taken from the frame tee to skin bond in an area adjacent to the repair.

adhesive failure. These specifically are specimens EW1, EW3, IW1, IEW1, IEW2, and IEW3 and represent all three repairs. The adhesive surface appearances correlate with the "higher than normal" initial crack opening lengths and growth rates listed in Tables 12, 13, and 14.

Post failure analysis of selected surface areas were subsequently conducted with the scanning electron microscope (SEM). Areas where the SEM coupons were taken are shown in the figures. The resulting surface appearances were compared with those of coupon surfaces previously studied under Air Force contract F33615-C-73-5171 Mod 7 and reported in Reference 11. The results of this analysis are as follows:

- Specimen EW-2
This is a baseline wedge specimen taken from the overhead repair. The specimen gave a cohesive failure with only 0.12 in. crack growth during 30 days of high humidity exposure. SEM photos of the surface are shown in Figure 88. The anodize oxide formation is uniform and of adequate thickness and is comparable to satisfactory surfaces reported in Reference 11.
- Specimen EW-3
This specimen, again from the overhead repair, had an adhesive type failure and a high initial crack length. The SEM coupon, EW-3A, taken from the hand anodized surface, is shown in Figure 89. The surface has almost no oxide formation. A direct comparison can be made with Figure 88.

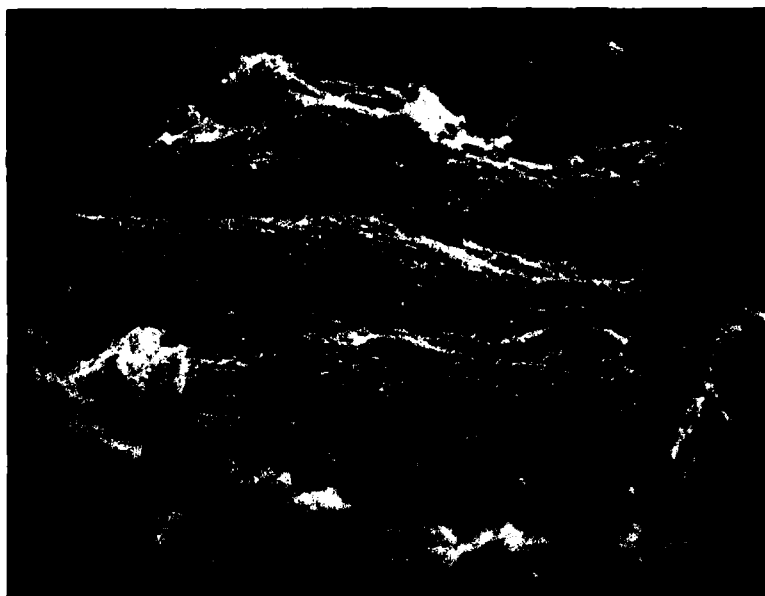
This is similar to surfaces anodized in the Reference 1 study where the voltage was too low, i.e., 1 volt and consequently, the current flow was inadequate. In this case, the six volts used is considered adequate. Low current flow presumably resulted from high local resistance. This was undoubtedly caused locally by lack of a dense current path through the acid saturated gauze/screen combination, probably due to a slight buckle in the screen.

The results indicate that a greater level of care must be taken to ensure uniform contact between the aluminum surface and the anodizing materials. The use of a foam pad and a pressure plate over the screen is suggested, especially for the more difficult situations such as for anodizing large areas or anodizing vertical or overhead surfaces.

A second SEM coupon, EW-3C, was taken from the mating surface of the EW-3 specimen which was tank anodized. The anodized surface is shown in Figure 90. The oxide thickness and density appear satisfactory.

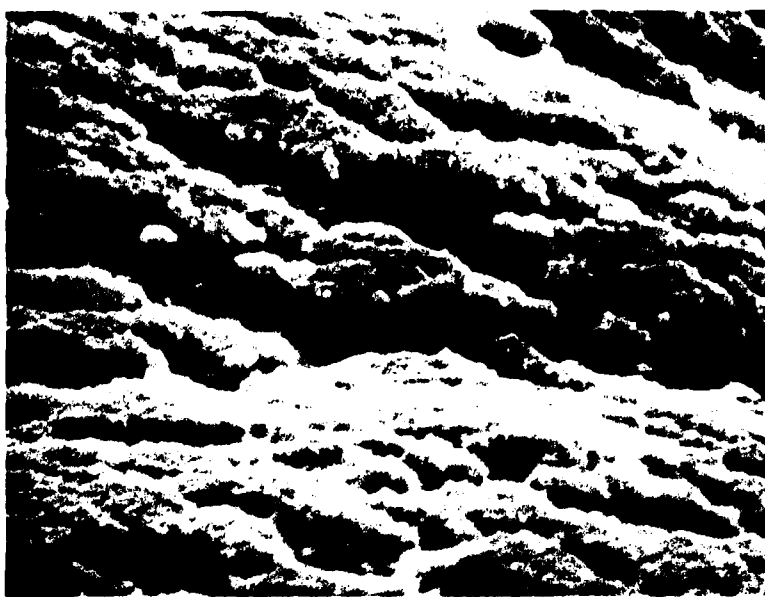
- Specimen IW-1
This wedge specimen was from the bolt/spring bonded repair. The failure mode was adhesive. The crack extension was moderate (0.38 in.) after 30 days exposure. The surface is shown in Figure 91. The oxide layer is comparable, in general, to those of satisfactory bonds. No explanation for the adhesive failure is offered. Since the crack growth was moderate, perhaps there should be no concern.

No SEM examination was made for the third repair.



3600x

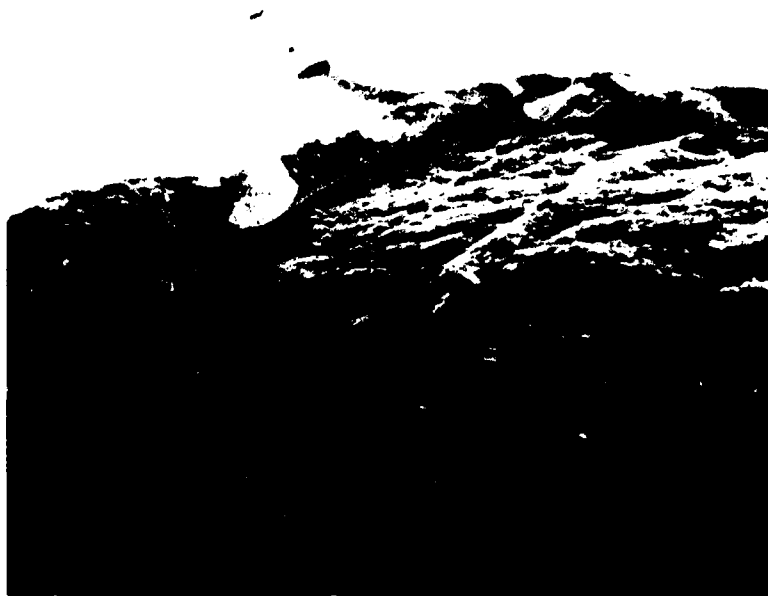
(a)



12,000x

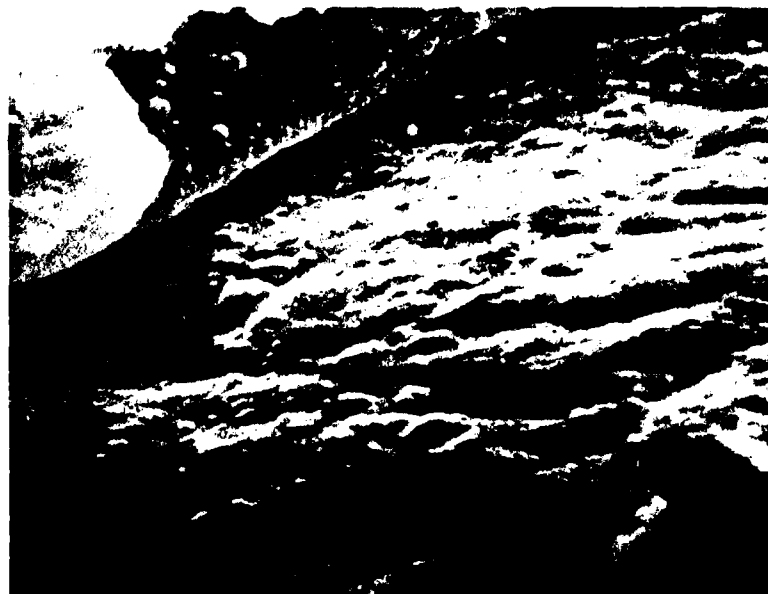
(b)

*Figure 88.—SEM Photos Showing Satisfactory Oxide Layer
on the EW-2 Specimen Hand Anodized Surface*



3600x

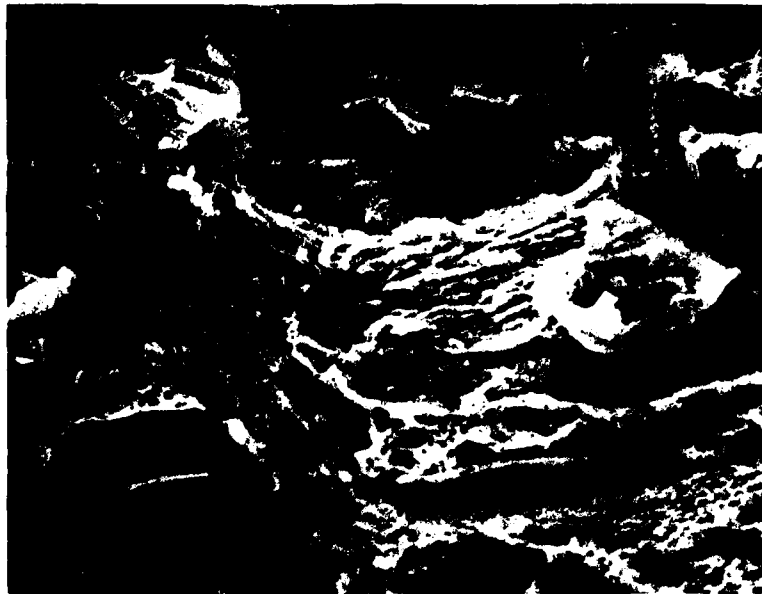
(a)



12,000x

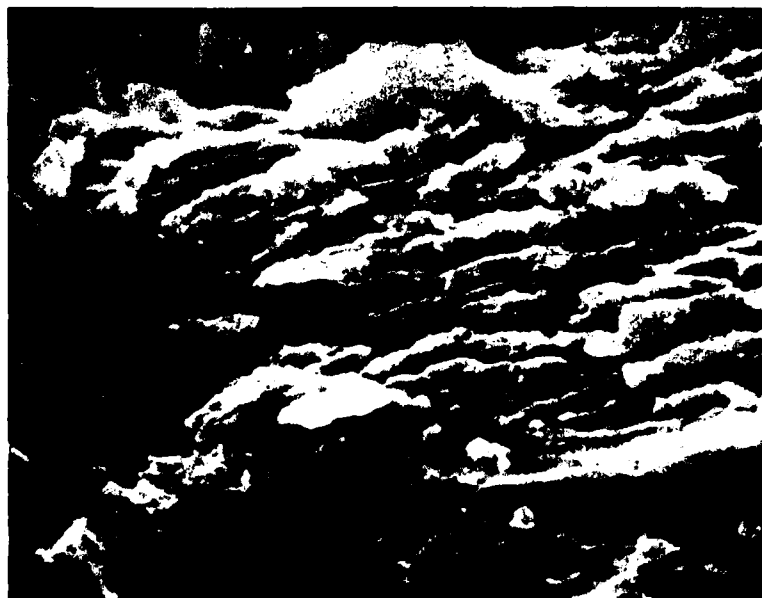
(b)

*Figure 89.—SEM Photos Showing Lack of Oxide Build-Up
On the EW-3 Specimen Hand Anodized Surface*



3600x

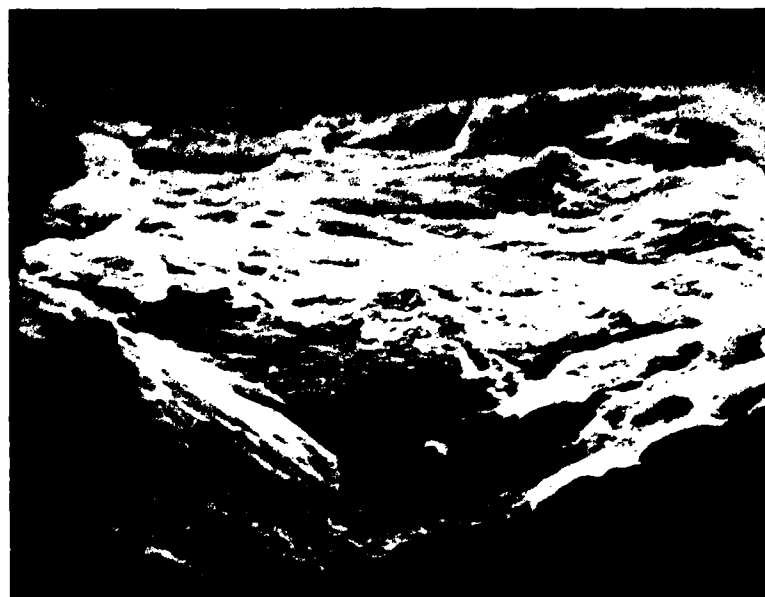
(a)



12,000x

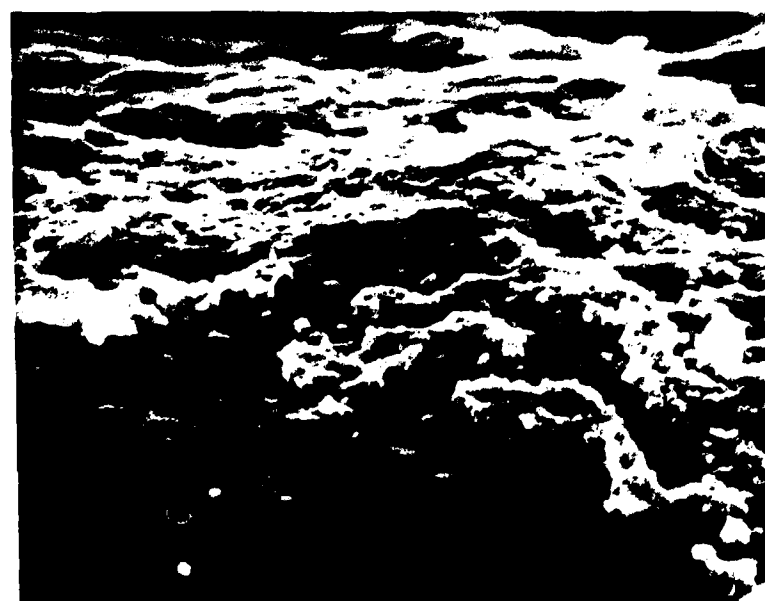
(b)

*Figure 90.—SEM Photo Showing Satisfactory Oxide Build-Up
On the EW-3 Specimen Tank Anodized Surface*



3600x

(a)



12,000x

(b)

*Figure 91.—SEM Photo Showing Satisfactory Oxide Build-Up
On the IW-1 Specimen Hand Anodized Surface*

5.7 COST AND FLOW TIME STUDIES

As a result of the design and analysis tasks, it was determined that two alternate procedures could be used to accomplish repairs on the PABST fuselage. These were the all-bonded repair method with the cure pressure applied by means such as a vacuum bag and a second procedure utilizing pressure provided by mechanical fasteners. Following satisfactory demonstration of these two procedures, a study was made to determine the cost and flow time that would be required to accomplish each of the three repairs by these two methods. The experience obtained from the demonstration repairs was used to supplement standard shop estimating procedures.

Ground rules for the cost and fabrication flow time estimates included the following items:

1. Repairs were assumed to be made on the aircraft fuselage. Metal details requiring surface preparation for bonding would be processed in tanks. Surface preparation on the structure was to be done by hand anodizing. After anodizing, the surfaces were sprayed with BR127 primer and the primer bake cured.
2. Preparation of bond surfaces using bolt/spring pressure was identical to that used for the conventional vacuum pressure bonded repairs. Adhesive tape was placed at the interfaces. The details were fixed in place and the assembly drilled and bolted. After cure, the bolts were removed and replaced by rivets.
3. Flow times estimates are based on the repair being accomplished by one person. Two people were assumed only when required to accomplish a particular operation; e.g., installing the bolts and springs and riveting.
4. The cleaning and priming of the metal details was considered to be accomplished concurrent with similar work on the basic panel.
5. The time required for fabrication of the sheet metal details was included. The time required to fabricate circumferential tees, machined parts, etc. was not included. It was assumed that these latter items would be purchased.
6. The repairs were considered to be one time operations. Both recurring and non-recurring cost items were included in estimates.
7. The cost of material was not included.

The comparative man-hours cost and the flow times required to complete repairs by the two methods are shown in Figures 92 through 95. For the particular repair situations studied, the all bonded procedure was estimated to be both less expensive and quicker to accomplish. The reason for this can be seen by reviewing the time required for the individual processing steps listed in the flow charts. Essentially, the time required to lay out and drill the fastener holes, disassemble, deburr, reassemble, etc. was considerably longer than that required for the vacuum bagging procedure.

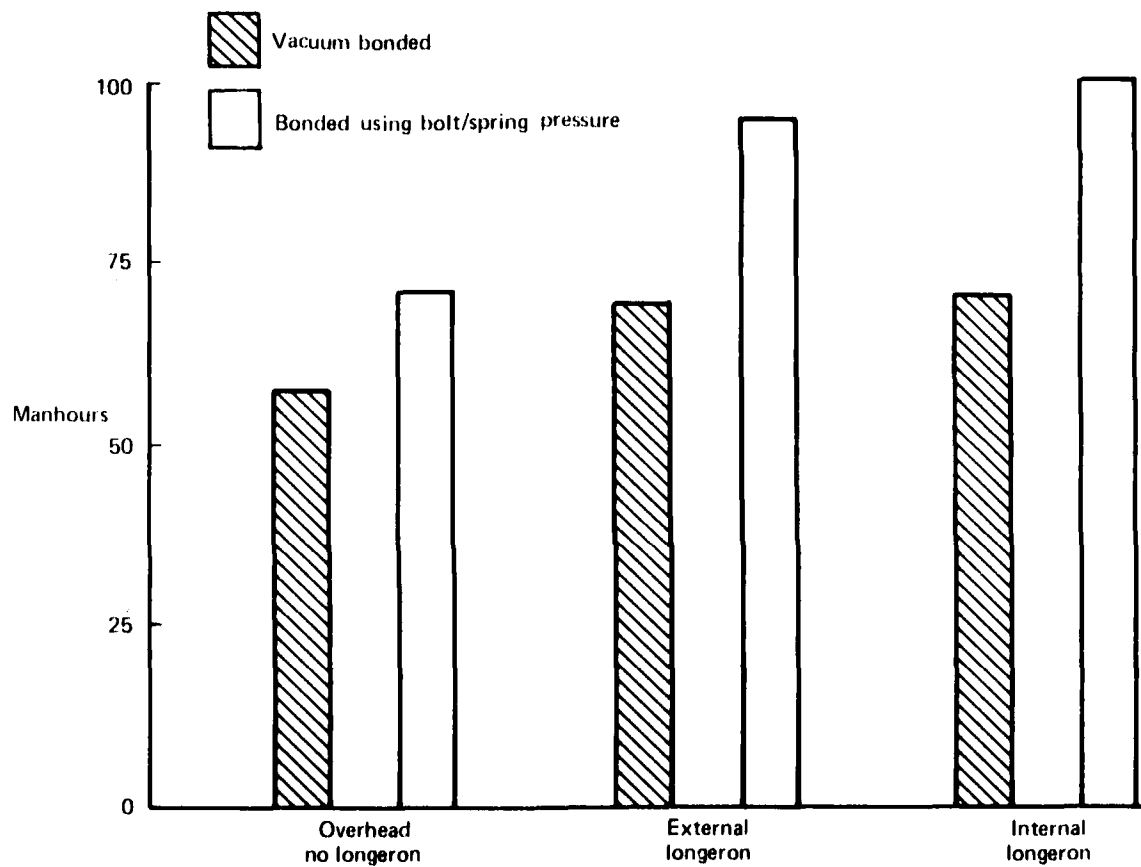


Figure 92.—Comparative Man-hours Required for Repairs using Bolts/Springs for Pressure Application Versus Use of a Vacuum Bag

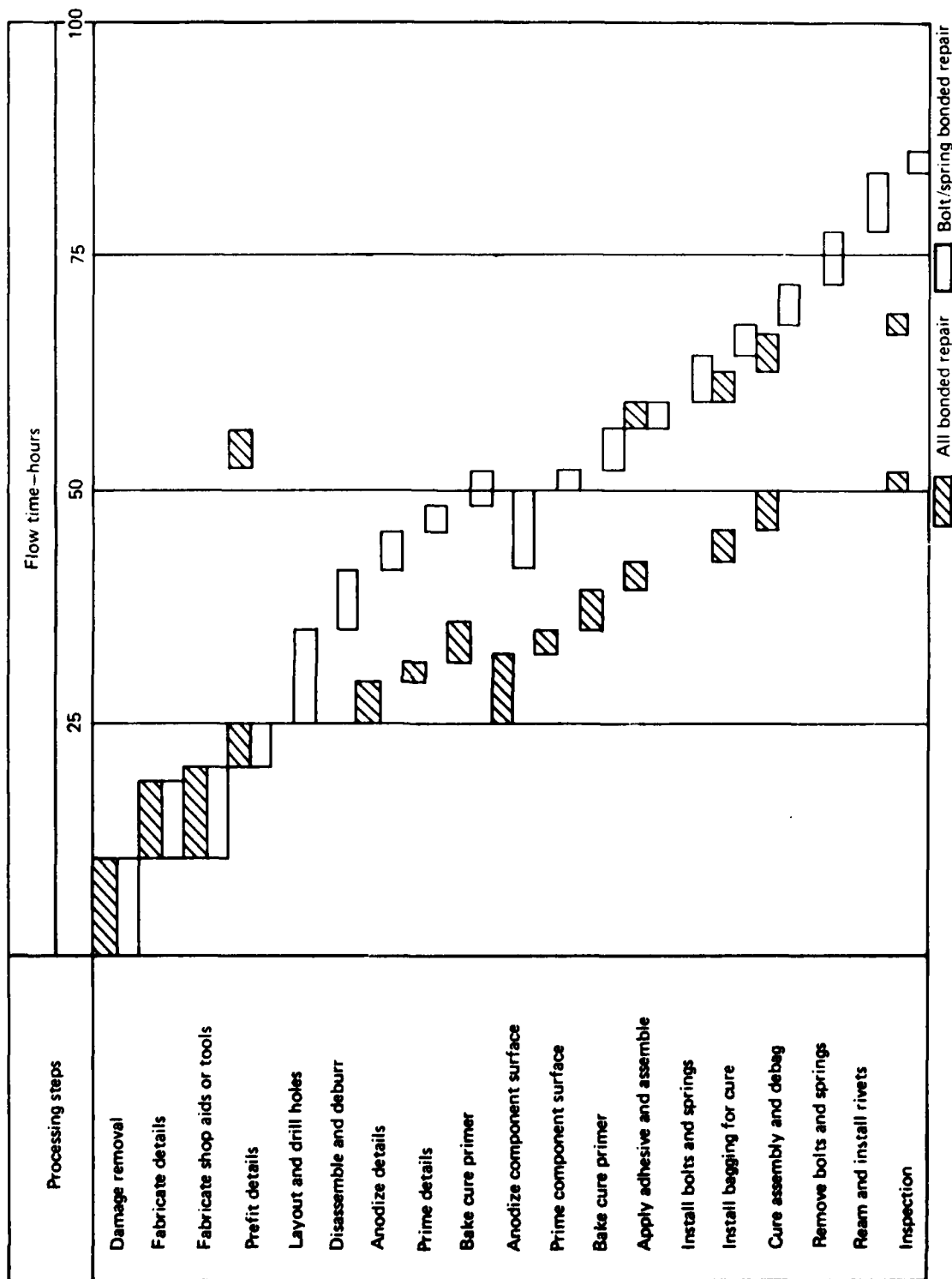


Figure 93.—Comparative Flow Time of Repair Methods, Internal Longeron

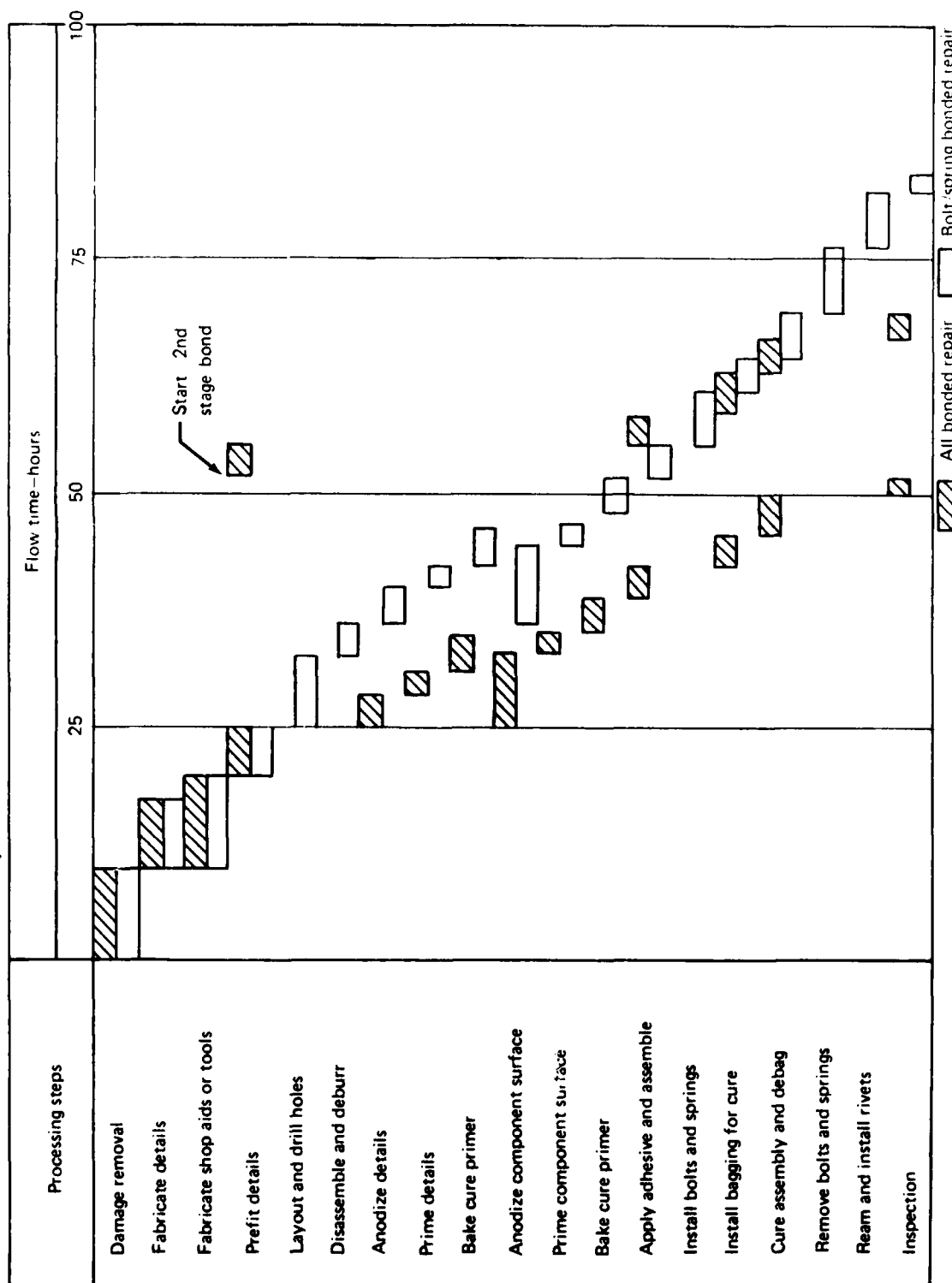


Figure 94. —Comparative Flow Time of Repair Methods, External Longeron

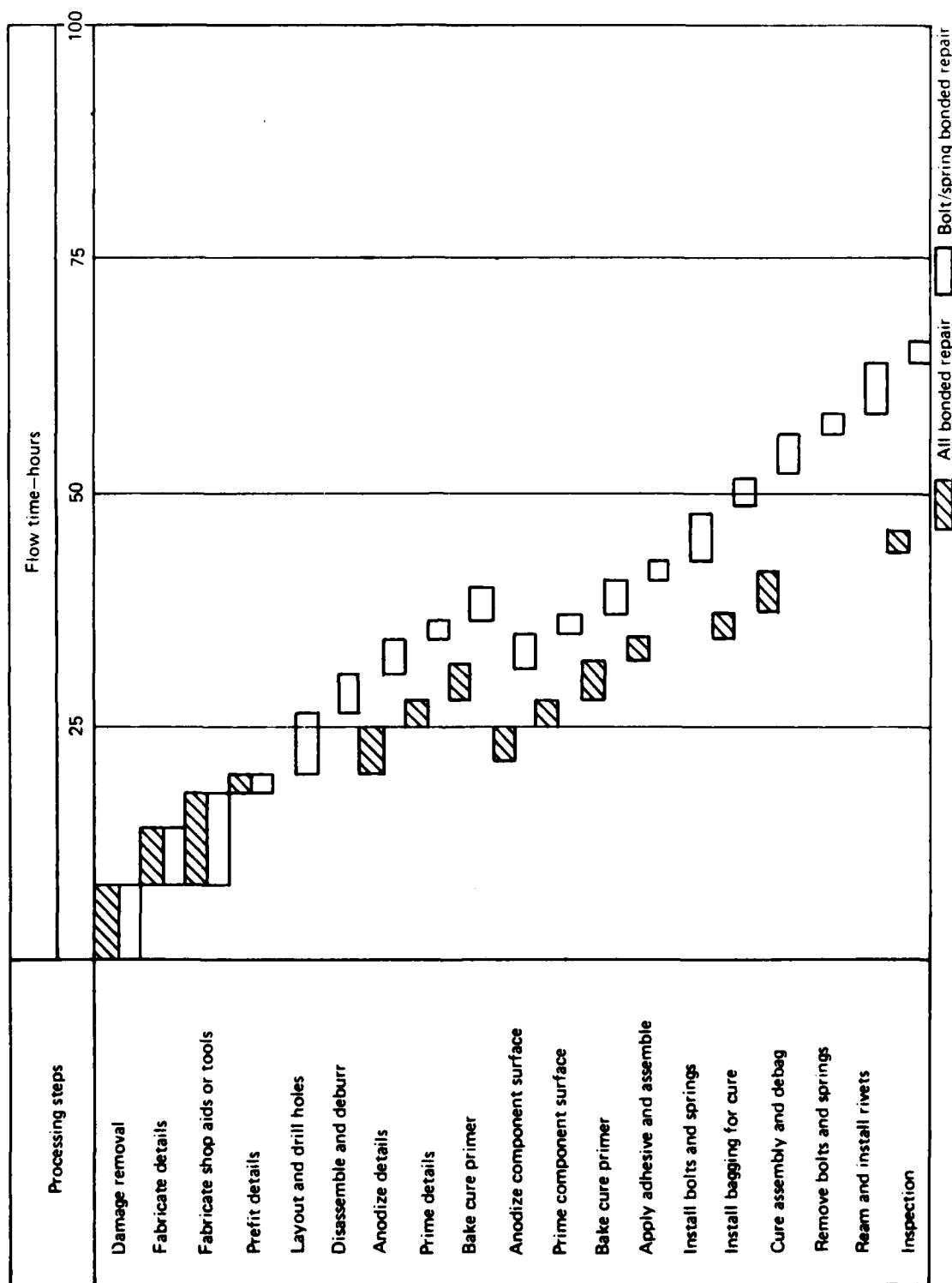


Figure 95. —Comparative Flow Time of Repair Methods, Overhead—No Longeron

6.0 DEFINITION OF FACILITY AND EQUIPMENT REQUIREMENTS

The purpose of this section is to define the facilities and equipment that will be required at the AFLC Air Logistics Centers or at the operational bases to effectively accomplish repairs on a PABST-type bonded aircraft fuselage. This information is supplemental to similar information appearing in the last three chapters of the recently published standardized repair handbook for adhesively bonded structure (Ref. 9). The difference is that emphasis in the handbook is on the repair of honeycomb sandwich or simple laminate structure and it is generally assumed that the components can be removed from the aircraft. Consequently, they can be placed in a bonding tool for applying heat and pressure or cured using heating blankets or ovens and envelope vacuum bagging. By contrast, it is expected that repairs to a PABST-type fuselage will preferably be made without removing the damaged sections from the aircraft. This is because the tasks of removing and replacing the large bonded panels will in themselves be major efforts. In addition to the normal tasks, it will also probably be necessary to provide support for the fuselage until the panel is replaced.

It is expected that producing primary quality structural repairs under on-the-aircraft conditions will require many special considerations. In general, the repairs will be made in a hanger area and not in an area with a controlled environment. Care will need to be taken to minimize contamination of the cleaned surfaces prior to bonding.

Access to the damage may be difficult. It can be expected that damage will prefer to occur in the proximity of control cables, hydraulic lines and electrical wiring. These, as well as the complexity of the internal structure with its frames, stringers and clips, will make it difficult to locate and seal a vacuum bag or to position heating equipment.

A summary of the facilities and equipment that will be needed to accomplish these repairs is given in the following paragraphs.

1. **Damage Removal**- The equipment required will be the same as that used for current bonded repairs. This includes hand-held routers, saws, etc. This equipment is described in Chapter 8 of Reference 9.
2. **Fabrication of Metal Details**- This may be accomplished with standard metal working tools. Skin patches for single contour areas may be formed using standard rolling equipment. Small compound curved patches can be formed using the roto-peen tool described in Section 7.6 of the referenced handbook. Stretch form techniques may be used to fabricate larger compound curved skin pieces.

It is assumed that some of the more difficult to form sections such as the curved frame members will be purchased and stocked as spares. When required, fabrication of these members will be much the same as required for conventional riveted fuselage repair.

Some examples of this type of equipment are given in the following paragraphs. A buffalo form roll machine, especially adapted to form zee frames to fuselage contours, is shown in Figure 96. The metal strips are first power brake formed to the section shape, e.g., a zee, in a straight configuration. The part is then formed longitudinally

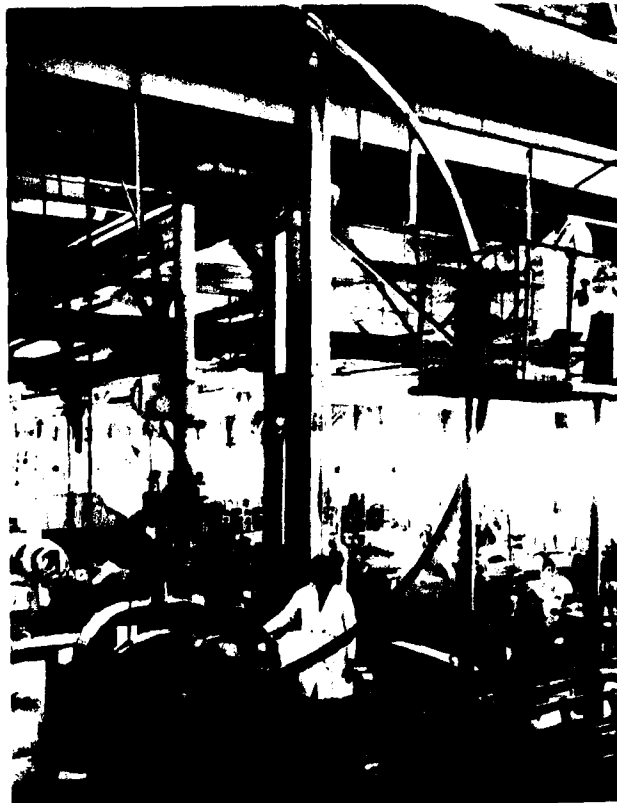


Figure 96. -- A Buffalo Roll Being Used to Form a Frame Section to Proper Radius

using a set of die rolls that are adjusted to produce a curvature appropriate for the selected fuselage diameter.

A second method illustrated in Figure 97 uses a Model M-3 Yoder progressive multiple form roll. This machine has seven roll stages. The part starts as a piece of flat coil stock and emerges in the desired section shape, e.g., as a zee section. This section then progresses through curving rolls which produce curvature to the desired radius.

A more preferred frame forming method is illustrated in Figure 98. This is a Sheridan stretch wrap forming machine. It has a special designed stretch form block with snake-type fillers. This machine holds all surfaces of the detail in tension. The jaws grip each end of the detail while it is extended in a straight line. The arms are then translated and rotated to curve the section to the stretch form block contour.

3. **Bond Surface Preparation** The importance of utilizing high-quality surface preparation procedures to obtain acceptable bond durability has been adequately demonstrated by several programs. Likewise the superiority of the phosphoric acid anodizing process has been verified (Ref. 10). It is, therefore, highly preferable that, at the ALC's, surface preparation of aluminum be accomplished in phosphoric acid anodizing tanks. Consideration should also be given to installing small tank systems at selected bases.

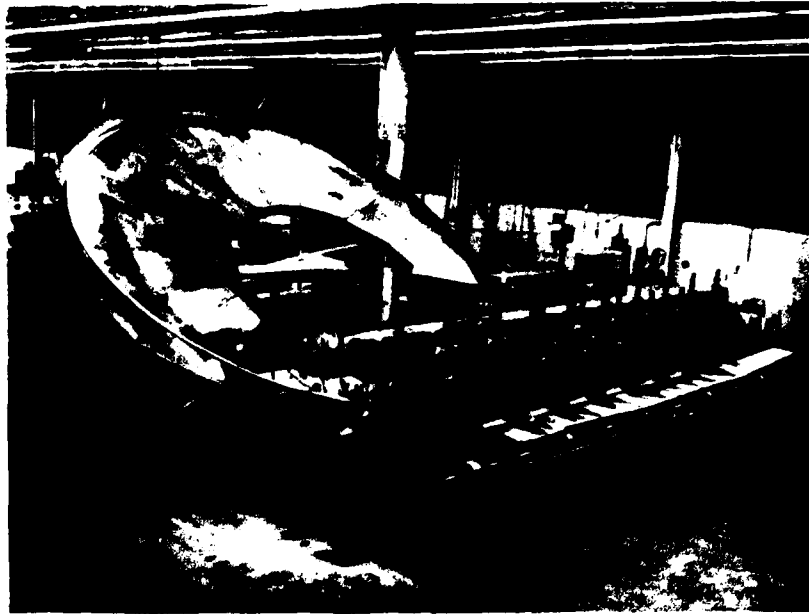


Figure 97.—Use of a Model M-3 Yoder Progressive Multiple Form Roll with a Special Curve-Forming Attachment

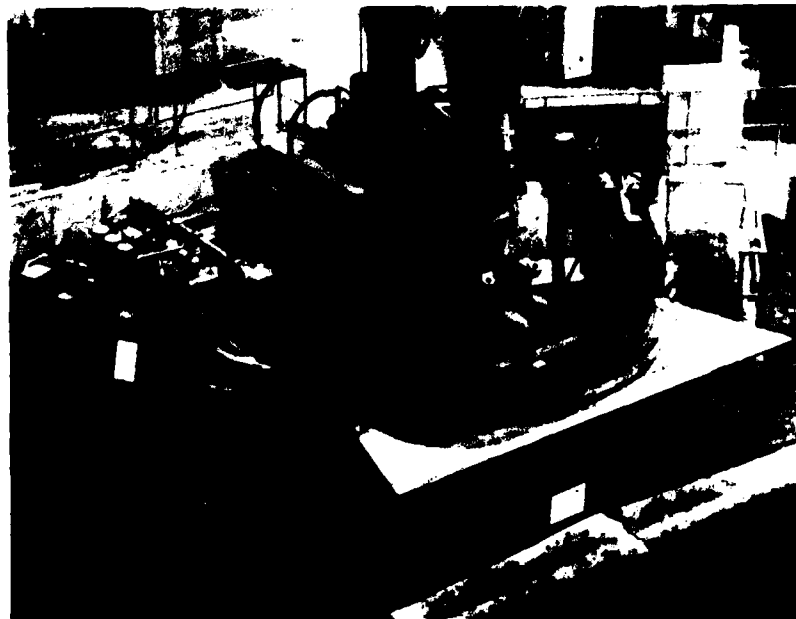


Figure 98.—A Sheridan Model A-15 Stretch-Wrap Forming Machine

Portable equipment will be used to hand anodize aluminum surfaces on the aircraft or on detached components that cannot be placed in the tanks. The main requirement is a dc power supply. A suitable instrument was shown previously in Figure 69. This is a Regal Line Model R2518, unfiltered, R series bench model. The capacity of this particular unit is 0 to 15 volts and 0 to 25 amps. The input power is 120 volts ac.

4. **Cure of the Adhesive** Pressure for the cure may be supplied using standard vacuum bagging materials and a vacuum source. Heating for the large repairs made in this program was quite satisfactorily accomplished using the hot air heater shown in Figure 99. The unit has a 20 KW heater with a 440 volt ac, 30 ampere, 3-phase power supply. It is capable of supplying filtered shop air at 250 CFM and 500°F. All electrical equipment and connections are contained in sealed explosion proof housings.

The heater is operated by constructing a shroud of plastic film around the area to be heated. An inserted hose from the heater supplies sufficient pressure to maintain the shroud in an inflated plenum shape. Typically, a baffle is installed at the hose entrance to prevent occurrence of a local hot spot. The cure temperature is regulated by thermocouples on the part transmitting temperatures to the heater controller.



Figure 99.—A Portable Compressed Hot Air Heater Used for Bond Curing

5. **Nondestructive Inspection** The use of an instrument such as the Fokker Bond Tester or the NDT-210 Bond Tester is considered a minimum level of inspection suitable for PABST type structure. These instruments are portable and especially adaptable to the inspection of bonded laminates. Of the two, the Fokker Unit is more widely used. The NDT-210 unit, however, has a wider selection of probe types that can give better access to difficult-to-inspect areas.

7.0 CONCLUSIONS

The accomplishment of this program has resulted in the following conclusions:

1. The analysis studies and component tests performed in this program have amply verified that bonded repairs can be used to restore a damaged PABST-type bonded fuselage to its initial condition of static and fatigue strength and crack growth damage tolerance.
2. Two practical methods of applying the curing pressure were shown to be satisfactory for the repair bond. These were the use of vacuum pressure and the use of a combination bolt/spring pressurizing procedure. Of these two, the vacuum method was concluded to be less costly and to require less time to accomplish.
3. For the repair design to be satisfactory, it was necessary that the repair splices be adhesively bonded and that the load transfer in splices be accomplished entirely by the adhesive, i.e., any mechanical fasteners present were considered nonload transferring. The fatigue analysis indicated that a repair design using mechanical fasteners for load transfer did not meet the fatigue requirements of the baseline structure.
4. Either of the elevated temperature curing adhesives evaluated in this program, i.e., FM73 or EA9628, could be used to accomplish satisfactory repairs for the PABST fuselage. The room temperature curing adhesive that was evaluated was not satisfactory. It was concluded from this and past work (Ref. 7) that this unacceptability applies to ambient temperature curing adhesives in general.
5. It can be expected that the adhesive cured using vacuum pressure will have slightly lower strength and stressed environmental durability than the same adhesive cured in an autoclave, i.e., under production conditions. This presents no problem in designing a repair having the same strength and durability as the baseline structure. Stresses in the bondline can readily be adjusted by varying the lap length of splices, widening the base of bonded stiffeners, increasing taper ratios, etc.
6. In general, it has been proven that the phosphoric acid non-tank anodize procedure provides a superior, repair compatible, surface preparation method for bonding aluminum (Refs. 7 and 11). The use of this procedure for accomplishing rather large complex repairs was demonstrated in this program.

Concern still remains over some difficulties that were encountered in anodizing the large panel surfaces. This is relative to the adhesive failures, i.e., rather than cohesive, that occurred in six wedge specimens used for post repair evaluations.

Although the marginal or unsatisfactory areas represented by these specimens were only a small percentage of the total area anodized, the fact that they occurred must be given serious consideration. They serve to emphasize the need for special attention to all procedural details during the anodizing process. Items that are especially essential are:

- a. Maintenance of intimate contact of the metal surface and the anodizing materials. This is especially critical when working in the overhead position.
- b. Expeditious removal of the anodizing materials when the process is complete and immediate thorough rinsing to remove all acid from the anodized surface.
- c. Maintenance of an adequate current-density level, i.e., amps/sq ft, during the anodizing process.